Dr. Rolf M. Schwiete Center for Limbal Stem Cell and Congenital Aniridia Research
Saarland University, Homburg/Saar
Chair: Prof. Dr. Nóra Szentmáry

**Effect of Rose Bengal photodynamic therapy (RB-PDT) on human corneal
epithelial and stromal cells**

**Cumulative Dissertation for the Degree of
Doctor of Medicine and Natural Sciences (MD/PhD)
Faculty of Medicine**

SAARLAND UNIVERSITY

2024

Submitted by Ning Chai
Born on August 30,1994 in Hefei, P.R. China

Aus der Dr. Rolf M. Schwiete Zentrum für Limbusstammzellforschung und kongenitale Aniridie
Universität des Saarlandes, Homburg/Saar
Direktor: Prof. Dr. Nóra Szentmáry

Auswirkungen der Rose-Bengal-photodynamischen Therapie (RB-PDT) auf humane Hornhautepithel- und Stromazellen

Kumulative Dissertation zur Erlangung des Grades eines
Doktor der Medizin und der Naturwissenschaften (MD/PhD)
der Medizinischen Fakultät

UNIVERSITÄT DES SAARLANDES

2024

vorgelegt von: Ning Chai

geb. am: 30.08.1994 in Hefei, China

Tag der mündlichen Prüfung: 12.08.2024

Dekan: Univ.-Prof. Dr. med. Michael D. Menger

1. Berichterstatter: Prof. Dr. Nóra Szentmáry

2. Berichterstatter: Prof. Dr. Thomas Vogt

Table of contents

1. Zusammenfassung

Auswirkungen der Rose-Bengal-photodynamischen Therapie (RB-PDT) auf humane

Hornhautepithel- und Stromazellen

Die Rose-Bengal-Photodynamische Therapie (RB-PDT) nutzt Rose-Bengal-Farbstoff als Photosensibilisator, der durch 500-570 nm grünes Licht aktiviert wird. Dies erzeugt reaktive Sauerstoffspezies (ROS), beseitigt Bakterien, moduliert Wachstumsfaktoren und vernetzt Kollagen, was die Gewebesteifigkeit erhöht. Ihre Wirkung auf menschliche Hornhautzellen wurde jedoch noch nicht untersucht. *Im ersten Teil* der Studie der Studie untersuchten wir die Auswirkungen von RB-PDT auf verschiedene menschliche Hornhautzelltypen, einschließlich einer Hornhautepithelzelllinie (HCE-T), limbaler Epithelstammzellen (T-LSC), primärer Hornhautfibroblasten (HCF), Keratokonusfibroblasten (KC-HCF) und limbaler Fibroblasten (LFC). Nach RB-PDT nahm die Viabilität jedoch bei 0,17 J/cm² in HCF und KC-HCF sowie bei 0,35 J/cm² in T-LSC, HCE-T und LFC signifikant ab. *Im zweiten Teil* der Studie untersuchten wir die Auswirkungen von RB-PDT auf die Zellmigration und Interaktionen zwischen Epithel- und Stromazellen. RB-PDT die Migration von HCE-T, HCF und KC-HCF signifikant hemmte. Konditioniertes Medium (CM) von RB-PDT-behandelten HCE-T-Zellen förderte die Migration von HCF, während CM von RB-PDT-behandelten HCF die Migration von HCE-T unterstützte. *Im dritten Abschnitt* der Studie untersuchten wir den Einfluss von RB-PDT auf die Expression Gene und Proteine in HCF und KC-HCF, darunter Kollagen I und V, NF-κB p65, LOX und TGFβ. Die TGFβ-mRNA-Spiegel in HCF sanken, in KC-HCF nahmen die mRNA-Spiegel von Kollagen I und V ab. LOX und NF-κB p65 wurden durch RB-PDT nicht beeinflusst. Weitere Forschungen sind erforderlich, um die Auswirkungen von RB-PDT auf menschliche Hornhautzellen besser zu verstehen, insbesondere durch Studien in Tiermodellen für Keratitis, um die klinische Anwendung zu verbessern.

2. Summary

Effect of Rose Bengal photodynamic therapy (RB-PDT) on human corneal epithelial and stromal cells

Rose Bengal photodynamic therapy (RB-PDT) uses rose bengal dye as a photosensitizer, activated by 500-570 nm green light. This activation induces various biological effects, including reactive oxygen species (ROS) generation, cytotoxicity, bacterial eradication, growth factor secretion modulation, and collagen crosslinking, leading to increased tissue rigidity. Despite its clinical use, RB-PDT's impact on human corneal cells is not analysed, yet. *In the first part* of the study, we examined the effects of RB-PDT on various human corneal cell types, including a corneal epithelial cell line (HCE-T), limbal epithelial stem cells (T-LSC), primary corneal fibroblasts (HCF), keratoconus fibroblasts (KC-HCF), and limbal fibroblasts (LFC). After RB-PDT, viability significantly decreased at a fluence of 0.17 J/cm² in HCF and KC-HCF, and at 0.35 J/cm² in T-LSC, HCE-T, and LFC. *In the second part* of the study, we examined the impact of RB-PDT on cell migration and epithelial-stromal interactions in human corneal cells. RB-PDT significantly inhibited the migration of HCE-T, HCF, and KC-HCF. Conditioned medium (CM) from RB-PDT treated HCE-T cells enhanced HCF migration in scratched cultures, and CM from RB-PDT treated HCF promoted HCE-T migration. *In the third segment* of the study, we examined the influence of RB-PDT on the expression of genes and proteins in HCF and KC-HCF, including collagen I and V, NF-κB p65, LOX and TGF-β. In HCF, TGF-β mRNA levels decreased in KC-HCF, mRNA levels of collagen I and V decreased, LOX and NF-κB p65 were unaffected by RB-PDT. Further research is necessary to better understand RB-PDT's impact on human corneal cells, such as studying its effects on corneal cells in an animal keratitis model, optimizing its clinical use.

3. Introduction and motivation

In recent decades, human medicine has undergone continuous evolution and improvement. Numerous diseases have been discovered, researched, and effectively treated. However, the conventional approach, which involves a combination of drugs and surgical interventions, has its limitations. The ongoing development of antibiotic resistance, for instance, poses challenges to antimicrobial treatments. Moreover, for certain specific pathogenic conditions, there is a growing need to explore more convenient and efficient therapeutic procedures that can circumvent surgeries and alleviate both the physiological and economic burdens on patients. In this context, photodynamic therapy (PDT) has captured the attention of researchers.

PDT is a technique that involves combining a photosensitizer (PS) with light of an appropriate wavelength. Due to its photochemical properties, this technique can be applied to various tissues within the human body, leading to diverse therapeutic effects based on the administered dosage [43].

Upon exposure to light of the appropriate wavelength, the PS initially absorbs the light energy, causing the excitation of an electron within the PS and its transition to a higher energy level. This transition signifies the conversion of the PS from its ground state (S_0) to a singlet excited state (S_1). Subsequently, S_1 may revert to S_0 through processes such as fluorescence emission. Alternatively, it may undergo intersystem crossing (ISC), leading to further transformation into a triplet excited state (T_1). The T_1 state of the PS is more stable than the S_1 state, providing the PS with increased opportunities to react with surrounding molecules [21,39,50]. Therefore, the T_1 state of the photosensitizer serves as the primary source of photosensitive reactions during the PDT process [50]. The energy transition between the ground state and the T_1 state of the photosensitizer is depicted in the Jablonski diagram (**Figure 1**).

In the literature, researchers have outlined two primary types of photosensitive reactions, namely Type I and Type II. Both of these reactions are based on the T_1 state of the photosensitizer [39]. However, their distinction lies in the fact that Type II reactions are oxygen (O_2) dependent, mediating the direct interaction between the T_1 state of the photosensitizer and an O_2 molecule. In this interaction, energy and electrons are directly transferred from the photosensitizer to O_2 molecules, leading to the generation of singlet oxygen ($^1O_2$), one of the reactive oxygen species (ROS) molecules. When oxygen becomes depleted, Type I photosensitive reactions occur, involving the transfer of electrons or hydrogen from the photosensitizer to its reaction substrates (i.e., cell membranes and organelles)[42]. This leads to the production of other reactive oxygen species (ROS) as well, such as superoxide anion (O_2^-), hydroxyl radicals (OH^-), or hydrogen peroxide (H_2O_2) [27]. Currently, it is acknowledged that the $^1O_2$ generated in Type II reactions serves as the primary mediator of the biological effects in PDT [19]. Therefore, the adequate supply of oxygen is crucial in the PDT treatment process.
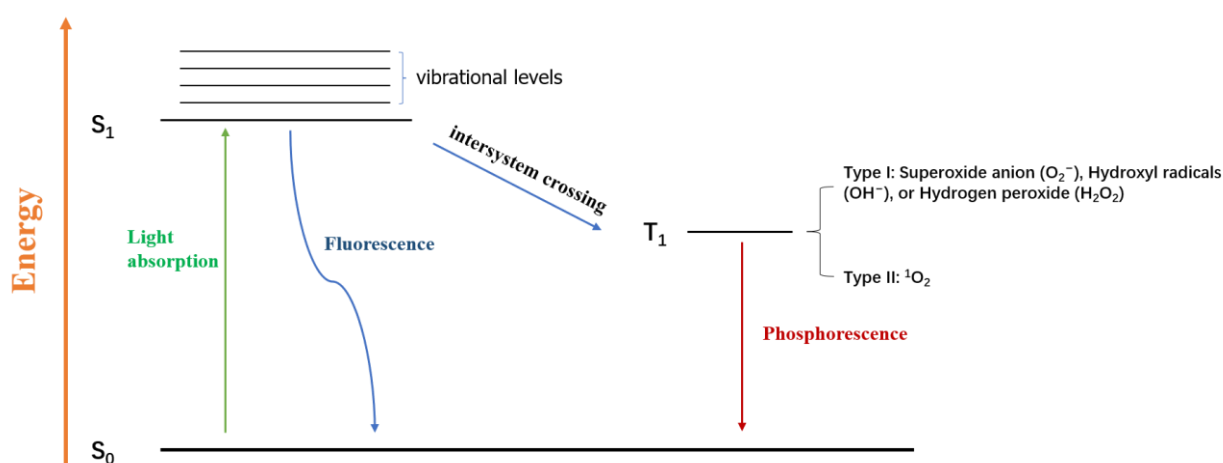

Figure 1. A simplified form of the *Jablonski* diagram is illustrated in the diagram. Once the photosensitizer (PS) absorbs a sufficient amount of energy in the form of electromagnetic radiation, such as light, it can transition from the ground state (S_0) to the electronic singlet state

(S_1). Subsequently, the PS in the S_1 state can undergo intersystem crossing to become the triplet state (T_1). These changes are associated with the electron spin direction of the PS molecule. (Image source: own presentation).

The biological effects mediated by PDT are influenced by various factors. These factors include the type of photosensitizer, tissue absorption efficiency, and the wavelength and penetrative capability of the light. Additionally, within cellular environments, a variety of proteins constitute protective mechanisms against reactive oxygen species (ROS). A series of enzymes, including superoxide dismutase (SOD), catalase (CAT), and glutathione peroxidase (GPx), are responsible for eliminating excess ROS to maintain cellular homeostasis [5, 47]. Consequently, these factors collectively impact the efficacy of PDT when applied in the human body. The PS is one of the key factors influencing the photosensitive process in PDT. Rose Bengal (RB) has been approved by the U.S. Food and Drug Administration as a diagnostic ocular surface dye [29]. In subsequent developments, the photosensitive properties of RB were discovered. Rose Bengal photodynamic therapy (RB-PDT) requires green light for excitation, with its peak absorption occurring at around 550 nm [1]. Furthermore, RB exhibits a high quantum yield, indicating the efficiency of photon utilization in photochemical reactions. The quantum yield of RB from the S_1 to the T_1 state is approximately 0.9, while the quantum yield of its singlet oxygen production ($\Phi\Delta$) is around 0.7 [43]. It is also important to note that RB can tightly bind to collagen molecules in the extracellular matrix (ECM), influencing its penetration depth within tissues [43]. Research indicates that the infiltration depth of RB within the corneal stroma is approximately 100-120 μm, whereas another photosensitizer, riboflavin, can reach a depth of about 400 μm [25]. Beyond mediating cytotoxic effects through the release of reactive oxygen species (ROS), RB-PDT has been found to enhance tissue hardness. This is attributed to RB's ability to mediate the insertion of covalent bonds into collagen molecules (crosslinking),

thereby increasing the stiffness of the tissue. Based on these properties, RB-PDT has been explored in treatment research for various diseases, including tumors [4, 38], supporting wound healing [17, 29], and treatment of infectious diseases (e.g., keratitis) [2, 12]. Moreover, researchers have successfully employed RB-PDT to induce stiffening of the cornea, showing promise in slowing down or halting the progression of keratoconus [9, 19].

The cornea, positioned as the outermost layer of the eye, possesses the highest refractive power in the human eye. Histologically, the cornea exhibits a multilayered structure, comprising the corneal epithelial layer, Bowman's layer, the stromal layer, Descemet's membrane (stromal basement membrane), and the endothelial layer [13]. The corneal epithelial layer serves to protect against the entry of foreign substances and abrasions. The stromal layer, representing approximately 90% of the corneal thickness, consists of keratocytes as resident cells, which are capable of secreting various ECM substances, such as Type I collagen and Type V collagen, among others. These ECM molecules are highly organized to maintain the clarity of the cornea. Corneal endothelial cells play a pivotal role in maintaining the dehydration state of the corneal stroma to prevent swelling and edema [8]. All the aforementioned corneal tissue structures collaboratively form a transparent, avascular, and optically clear tissue, ensuring the smooth passage of light into the eye and ultimately resulting in clear vision.

Keratoconus is a progressively developing corneal ectasia. Typically detected during adolescence, this condition involves a gradual thinning of the bilateral corneal stroma over time, resulting in a conical protrusion [33 ,50]. In severe cases, keratoconus can lead to corneal stromal edema, opacification, and potential vision decline. Therefore, it is crucial to find ways to slow down the ectasia progression. Before the emergence of PDT-mediated crosslinking, the primary approach involved the use of rigid gas-permeable contact lenses to mitigate the progression of the disease [14]. For advanced stages of keratoconus or acute cases, corneal

transplantation may be necessary. Although corneal transplantation techniques are relatively mature and have a high success rate, this undoubtedly requires a well-established corneal bank and economic support.

In 1998, Spoerl and colleagues first reported the use of riboflavin-ultraviolet A (UVA) PDT to mediate crosslinking and enhance the stiffness of the cornea [49]. This technique was subsequently applied in the treatment of keratoconus, proving highly successful in reducing the need for corneal transplantation [41, 43, 44]. Currently, riboflavin-UVA PDT-mediated crosslinking is widely implemented in clinical practice and stands as one of the standard treatment procedures for keratoconus [40]. However, a limitation of riboflavin lies in its penetration depth, as its penetration is relatively deep (~400 μm) [38]. If the corneal thickness is less than 400 μm, riboflavin may exceed the corneal stromal layer and reach the endothelial cell layer, causing potential damage to non-regenerative endothelial cells during the treatment process. Additionally, because riboflavin requires UVA for illumination, this may pose a risk of damage to the cornea and deeper ocular structures [13, 45]. In the literature, several studies have described postoperative complications following riboflavin-UVA PDT [3, 7, 21].

In 2013, Cherfan et al. reported that RB-PDT-mediated crosslinking can similarly increase corneal stiffness to riboflavin-UVA-PDT, a finding that has been validated in animal models [12]. Moreover, it is noteworthy that, besides its role in mediating crosslinking, RB-PDT has gained recognition as a promising antimicrobial therapy, and its clinical efficacy has been reported by various institutions [2, 15, 31, 32]. These two methods, RB-PDT and riboflavin-UVA-PDT, have been compared by numerous research groups [22, 30, 44]. Due to the insufficient clinical evidence regarding the therapeutic efficacy of RB-PDT in human keratoconus disease, definitive conclusions are still awaited. However, due to the shallower penetration depth of RB-PDT and the use of green light for excitation, its postoperative

complications have not been reported, yet. Therefore, as an "updated" PDT technique, additional data from experimental models utilizing primary human corneal cells are necessary to gain a more comprehensive understanding of the impact of RB-PDT. This will aid in optimizing the utilization of this method.

This study was approved by the Ethics Committee of Saarland/Germany (Nr. 217/18). All human tissues were handled according to the Declaration of Helsinki Principles.

Assessment of Rose Bengal Photodynamic Therapy on Viability and Proliferation of Human Keratolimbal Epithelial and Stromal Cells *In Vitro* (Publication 1) [9]

In the context of conducting *in vitro* cell experiments using RB-PDT, the primary consideration is determining the optimal dosage for the treatment. In this study, various human corneal cell types were investigated, including a corneal epithelial cell line (HCE-T), primary corneal fibroblasts (HCF), keratoconus fibroblasts (KC-HCF), limbal fibroblasts (LFC), and limbal epithelial stem cell line (T-LSC). Following the application of RB-PDT to these cell cultures, we elucidated the impact of RB-PDT on the viability and proliferation of these cell types.

When RB or green light illumination was applied alone, there was no significant impact on cell viability or proliferation across all cell types. However, 24 hours following RB-PDT, a significant decrease in viability was observed at a fluence of 0.17 J/cm^2 in HCF and KC-HCF, and at a fluence of 0.35 J/cm^2 in T-LSC, HCE-T, and LFCs. Furthermore, cell proliferation exhibited a significant reduction at a fluence of 0.14 J/cm^2 in T-LSC, HCE-T, and KC-HCF, and at a fluence of 0.17 J/cm^2 in HCF.

This foundational research provides essential insights for subsequent experiments, laying the groundwork for further investigations.

Human corneal epithelial cell and fibroblast migration and growth factor secretion after rose bengal photodynamic therapy (RB-PDT) and the effect of conditioned medium (Publication 2) [10]

The use of RB-PDT as a therapeutic technique for treating corneal diseases has been implemented in clinical practice. However, the impact of RB-PDT on corneal wound healing remains unclear. Therefore, our objective is to investigate the influence of RB-PDT on the migration ability of HCE-T, HCF and KC-HCF, and the potential reasons behind.

The existing literature highlights the interconnectedness of corneal epithelial cells and stromal cells during the wound healing process [23, 25, 28]. Corneal epithelial damage, such as external stimuli or scratches, initially induces apoptosis of stromal cells [51]. Subsequently, stromal cells can modulate the wound healing of epithelial cells, including cell migration and proliferation, through a paracrine pattern. Therefore, we further investigated the regulation of RB-PDT on several essential growth factors in the cornea, including Epidermal Growth Factor (EGF), Hepatocyte Growth Factor (HGF), Keratinocyte Growth Factor (KGF), Fibroblast Growth Factor basic (FGFb), and Transforming Growth Factor beta (TGFβ).

Furthermore, we collected culture medium from RB-PDT-treated HCE-T to produce conditioned medium (CM), which was then introduced into scratched HCF cultures. Similarly, culture medium from RB-PDT-treated HCF was collected and added to scratched HCE-T cultures. The growth factor concentration in the conditioned medium was also analyzed. This approach allowed us to observe how corneal epithelial cells and stromal cells interacted with each other following RB-PDT.

Through a scratch assay, we discovered that RB-PDT significantly inhibits the migration of HCE-T, HCF, and KC-HCF. However, after RB-PDT treatment, the collected CM can significantly enhance the migration the other cell type (HCF or HCE-T). For instance, CM

collected from RB-PDT-treated HCE-T markedly promotes HCF migration, and similarly, CM produced from RB-PDT-treated HCF significantly upregulates HCE-T migration. However, there is no such positive interaction between HCE-T and KC-HCF.

ELISA results provided further evidence of the reasons behind these observations. In scratched HCF and KC-HCF, RB-PDT notably reduces KGF levels. In HCE-T CM, RB-PDT increases HGF and FGFb levels while decreasing TGFβ levels. In HCF CM, RB-PDT elevates FGFb levels and decreases TGFβ levels. In KC-HCF CM, RB-PDT not only increases FGFb levels and decreases TGFβ levels but also reduces EGF and HGF levels.

In the cornea, EGF can be synthesized by epithelial cells or by fibroblasts, which exert a paracrine effect on epithelial cells to stimulate their proliferation [20, 51]. HGF, KGF, FGFb, and TGFβ are classical regulatory factors involved in the epithelial-stromal interactions of the cornea. HGF, KGF, and FGFb can be produced in keratocytes and act on corneal epithelial cells, promoting their migration and proliferation [6, 25, 28, 42]. TGFβ can be generated in corneal epithelial cells and reaches the stromal layer through the epithelial basement membrane, thereby regulating migration and differentiation of fibroblasts. Excessive TGFβ signaling can lead to the formation of corneal fibrosis, and result in corneal haze [27, 34, 49].

Furthermore, we investigated the soluble E-cadherin (SE-Cad) levels in the HCE-T cell culture supernatant and soluble N-cadherin (SN-Cad) levels in the HCF culture supernatant. The results revealed that after RB-PDT, SN-Cad levels in HCF cell culture significantly decreased. Additionally, an increase in SN-Cad level was observed when using CM collected from RB-PDT treated HCE-T, which was accompanied by an enhanced migration. In the literature, N-cadherin is recognized as a transmembrane protein, which can undergo cleavage by proteases and leads to the release of its soluble form into the supernatant [17]. The increase of SN-Cad

level suggests a reduction in cell adhesion, which may further promote cell migration. Therefore,

RB-PDT may influence cell migration by modulating Cadherin expression in HCF.

Short-Term Effect of Rose Bengal Photodynamic Therapy (RB-PDT) on Collagen I, Collagen V, NF-κB, LOX, TGF-β and IL-6 Expression of Human Corneal Fibroblasts, *in vitro* (Publication 3) [11]

Based on previous research, we know that RB-PDT can enhance corneal stiffness by promoting the generation of covalent bonds between corneal collagen molecules, offering a potential therapeutic approach for ectatic corneal diseases such as keratoconus. However, the specific impact of RB-PDT on several essential proteins and genes expressed by corneal fibroblasts was still unknown. These include collagen I and collagen V—the two primary collagen subtypes in the cornea. Additionally, lysyl oxidase (LOX), an enzyme facilitating the formation of covalent bonds between corneal collagens, plays a pivotal role in physiologically regulating corneal hardness. Transforming growth factor β (TGFβ) serves as a crucial growth factor essential for maintaining the dynamic balance of the extracellular matrix. Following corneal damage or stimulation, the TGFβ increase could promote collagen secretion, facilitating the healing process. Excessive TGFβ production, however, may lead to corneal scarring or haze, impacting visual acuity. Nuclear factor kappa-light-chain-enhancer of activated B cells (NFκB) and interleukin-6 (IL-6) are closely associated with inflammation levels. Elevated levels in the cornea often indicate an upregulation of inflammatory processes. Understanding the intricate interplay between RB-PDT and the expression of these genes and proteins in corneal fibroblasts is important for comprehension of RB-PDT therapeutic potential.

In this study, primary fibroblasts derived from healthy corneas (HCF, n=5) and keratoconus corneas (KC-HCF, n=5) were subjected to *in vitro* culture. Following a 24-hour period after RB-PDT, the cells were harvested, and RNA and protein were extracted. The RNA and protein levels in control and treated groups were quantified using qPCR and Western Blot. The results revealed that RB-PDT led to a reduction in collagen I, collagen V, and TGFβ1 mRNA

expression in KC-HCF, concurrently increasing IL-6 mRNA and protein expression. In HCF, RB-PDT resulted in a decrease in TGFβ1 mRNA expression while causing an increase in TGFβ1 and IL-6 protein levels. This indicates that RB-PDT has upregulated the inflammation level in both cell types. Although TGFβ1 mRNA levels have decreased in both cell types, there was a discrepancy between TGFβ mRNA and protein results. In HCF, TGFβ protein expression is upregulated, while in KC-HCF, the TGFβ content remains unchanged. This disparity may be attributed to mRNA stability and post-transcriptional regulation of protein expression. It is noteworthy that the decrease in TGFβ1 mRNA levels in both cell types aligns with the ELISA results from Figure 6 in Publication 2, indicating that RB-PDT can modulate TGFβ levels in both HCF and KC-HCF.

4. Publication 1

Thieme

Assessment of Rose Bengal Photodynamic Therapy on Viability and Proliferation of Human Keratolimbal Epithelial and Stromal Cells *In Vitro*

Untersuchung der photodynamischen Bengalrosa-Therapie auf die Viabilität und Proliferation humaner keratolimbaler Epithel- und Stromazellen in vitro

Authors

Ning Chai[1], Tanja Stachon[1], Mahsa Nastaranpour[1], Zhen Li[1], Berthold Seitz[2], Myriam Ulrich[1], Achim Langenbucher[3], Nóra Szentmáry[1,4]

Affiliations

1 Dr. Rolf M. Schwiete Center for Limbal Stem Cell and Aniridia Research, Saarland University, Homburg/Saar, Germany
2 Department of Ophthalmology, Saarland University Hospital and Saarland University, Faculty of Medicine, Homburg/Saar, Germany
3 Institute of Experimental Ophthalmology, Saarland University, Homburg/Saar, Germany
4 Department of Ophthalmology, Semmelweis University, Budapest, Hungary

Correspondence

Ning Chai
Dr. Rolf M. Schwiete Center for Limbal Stem Cell and Aniridia Research, Saarland University
Kirrberger Strasse 100 Geb. 22, 66424 Homburg/Saar, Germany
Phone: + 49(0)6 841 162 12 17, Fax: + 49(0)6 841 16 123 10
ning.chai@uks.eu

Supplementary material is available under
https://doi.org/10.1055/a-2038-8899

ABSTRACT

Purpose To investigate the effect of Rose Bengal photodynamic therapy (RB-PDT) on viability and proliferation of human limbal epithelial stem cells (T-LSCs), human corneal epithelial cells (HCE-T), human limbal fibroblasts (LFCs), and human normal and keratoconus fibroblasts (HCFs and KC-HCFs) *in vitro*.

Methods T-LSCs and HCE-T cell lines were used in this research. LFCs were isolated from healthy donor corneal limbi (n = 5), HCFs from healthy human donor corneas (n = 5), and KC-HCFs from penetrating keratoplasties of keratoconus patients (n = 5). After cell culture, RB-PDT was performed using 0.001 % RB concentration and 565 nm wavelength illumination with 0.14 to 0.7 J/cm² fluence. The XTT and the BrdU assays were used to assess cell viability and proliferation 24 h after RB-PDT.

Results RB or illumination alone did not change cell viability or proliferation in any of the cell types (p ≥ 0.1). However, following RB-PDT, viability decreased significantly from 0.17 J/cm² fluence in HCFs (p < 0.001) and KC-HCFs (p < 0.0001), and from 0.35 J/cm² fluence in T-LSCs (p < 0.001), HCE-T (p < 0.05), and LFCs ((p < 0.0001). Cell proliferation decreased significantly from 0.14 J/cm² fluence in T-LSCs (p < 0.0001), HCE-T (p < 0.05), and KC-HCFs (p < 0.001) and from 0.17 J/cm² fluence in HCFs (p < 0.05). Regarding LFCs proliferation, no values could be determined by the BrdU assay.

Conclusions Though RB-PDT seems to be a safe and effective treatment method *in vivo*, its dose-dependent phototoxicity on corneal epithelial and stromal cells has to be respected. The data and experimental parameters applied in this study may provide a reliable reference for future investigations.

(C.I. 45440, Carl Roth, Karlsruhe, Germany); trypan blue solution (Sigma-Aldrich, Irvine, UK).

Cell isolation and cell culture

Human telomerase-immortalized limbal epithelial stem cells

The human telomerase-immortalized limbal epithelial stem cells (T-LSCs) were generously provided by the research group of Daniel Aberdam [20]. T-LSCs were cultured in T25 flasks with KSFM, supplemented with 25 µg/mL BPE, 0.2 ng/mL EGF, 0.4 mM $CaCl_2$, 2 mM glutamine, and 100 U/mL penicillin/streptomycin. The medium was changed every 3–4 days until the cells reached 90% confluence.

Human corneal epithelial cell line

The human corneal epithelial cell line (HCE-T) was provided by the RIKEN cell bank (RCB 2280, Ibaraki, Japan). Cells were cultured in DMEM/F12 medium supplemented with 5% FCS, 1% P/S, 10 ng/mL EGF and 1% insulin, transferrin, and selenium (ITS) (HCE-T medium). When cells reached 80% confluence, they were seeded into a 96-well plate for further experiments.

Primary human limbal fibroblasts

Primary human limbal fibroblasts (LFCs) were collected from the limbal tissue of five healthy donors. In brief, the limbal area of the cornea was punched using 1.5 mm biopsy punches. The tissue flaps were digested by collagenase A at 37 °C for 24 h. CellTrics filters (Sysmax, Norderstedt, Germany) were then used to separate the limbal epithelial cells and the LFCs, flushing the filter with PBS. The LFCs were collected from the flowthrough solution. After a centrifugation step, the LFCs were stored in liquid nitrogen until use. Before measurements, LFCs were cultured in DMEM/F12, supplemented by 5% FCS and 1% P/S.

Primary human corneal fibroblasts

Five normal human corneal samples, which did not match corneal transplantation criteria (< 1800 endothelial cells/cm²) were obtained from the Klaus Faber Center for Corneal Diseases, including Lions Eye Bank. Five human keratoconus cornea samples were obtained from elective penetrating keratoplasties. None of these samples underwent previous ocular surgery and all patients signed an informed consent before surgery.

To isolate keratocytes or keratoconus keratocytes, corneoscleral or corneal buttons were first rinsed with PBS under sterile conditions. Then, tissues were cut into pieces using a surgical scalpel and were subsequently put into a 1.5-mL tube containing 1.0 mg/mL collagenase A with DMEM/F12 medium, 5% FCS, and 1% P/S (the combination of DMEM/F12 medium, 5% FCS, and 1% P/S is defined as "basic medium" in the following text). After incubating the tissue pieces in collagenase-containing solution at 37 °C overnight, the tube was centrifuged at 1500 rpm for 5 minutes, and the supernatant was discarded. Thereafter, the cell sediment was resuspended in 1 mL basic medium and was put into a T75 flask containing 13 mL basic medium. The cell-containing flasks were subsequently stored at 37 °C using 5% CO_2 and 95% relative humidity in the incubator. The medium was changed every 4 days. As soon as cells reached 90% confluence, they were harvested by trypsin EDTA and were passaged to 8 new T75 flasks. Thereafter,

reaching 90% confluence, the cells were trypsinized again and were kept in liquid nitrogen for the subsequent experiments.

During incubation, human keratocytes differentiate into human corneal fibroblasts using FCS in the culture medium. In the following text, we will use the abbreviation HCFs for normal human corneal fibroblasts and KC-HCFs for keratoconus human corneal fibroblasts.

Rose Bengal photodynamic therapy

T-LSCs, HCE-T, LFCs, HCFs, and KC-HCFs were seeded into 96 wells using 15 000 cells/cm² and 100 µL/well supplemented with KSFM for T-LSCs, 100 µL/well HCE-T medium for HCE-T cells, and 100 µL/well basic medium for LFCs, HCFs, and KC-HCFs. When cells reached 80% confluence, the RB-PDT treatment was performed.

As the first step, the 0.001% (m/v) RB solution was prepared by dissolving the RB stock powder in the basic medium. After sterilization by a 0.20-µm sterilizing filter, the RB solution was stored at 4 °C in darkness for up to 1 month.

The illumination system, with 565 nm wavelength illumination, was built and calibrated by the Experimental Ophthalmology of Saarland University, Homburg/Saar, Germany. Using a controller, the LED power and the time of illumination could be adjusted according to the required light fluence. In the present study, the illumination time was fixed to 600 s, and the power ranged from 0.23 mW/cm² to 1.17 mW/cm² (with 0.14 to 0.7 J/cm² fluence).
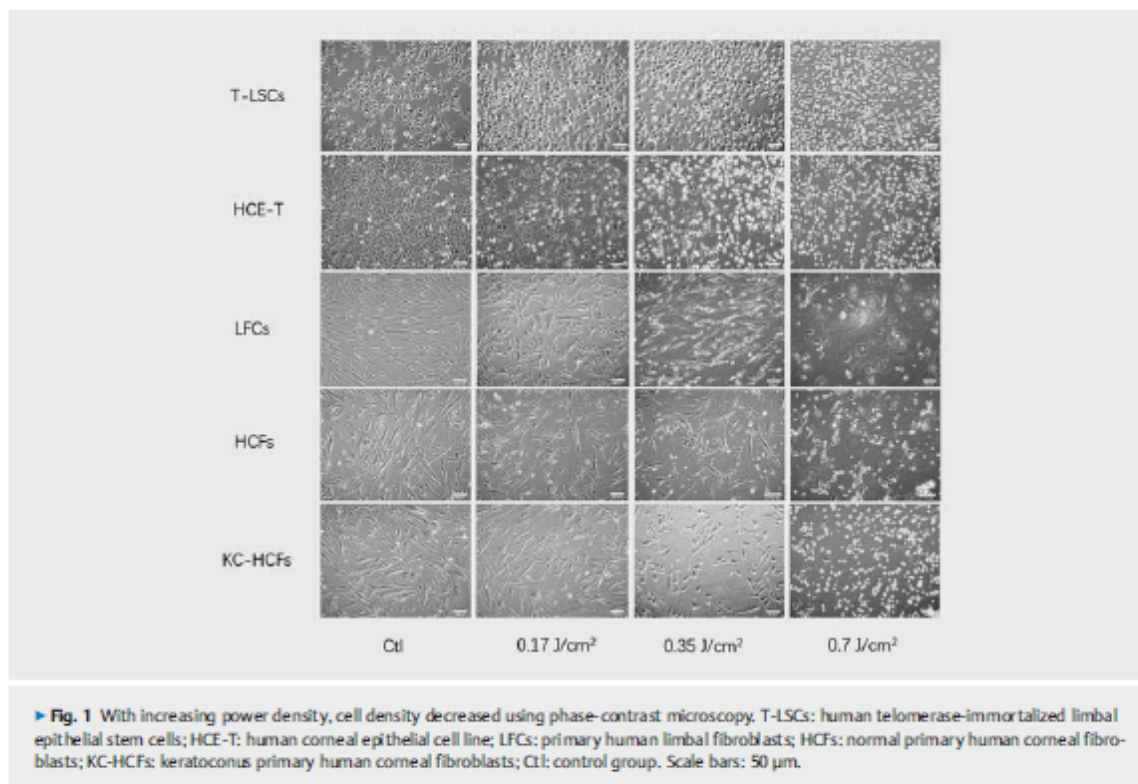
The cells were divided into various groups according to the used energy settings.

1. The control group (Ctl) was rinsed with PBS three times without the use of RB or illumination.
2. The cells in the "RB only" group were allowed to absorb the 0.001% RB solution for 30 minutes at 37 °C without illumination, which was followed by rinsing with PBS three times. Then, another 100 µL medium were added to each well.
3. The cells in the "illumination only" group were rinsed with 100 µL PBS two times and subsequently underwent 0.14 J/cm², 0.17 J/cm², 0.25 J/cm², 0.35 J/cm², or 0.7 J/cm² illumination in another 100 µL PBS, without adding RB. Thereafter, PBS was replaced by 100 µL medium.
4. The RB-PDT group was allowed to absorb the 0.001% RB solution for 30 minutes at 37 °C, which was followed by rinsing with PBS twice. Then, another 100 µL PBS were added to each well and the plates were positioned at the illumination box. Thereafter, the plates underwent 0.14 J/cm2, 0.17 J/cm², 0.25 J/cm², 0.35 J/cm², or 0.7 J/cm² illumination. The cells were subsequently rinsed with 100 µL PBS, which was then replaced by 100 µL medium.

In all groups, cells were further incubated at 37 °C for 24 h and then were used for analysis.

XTT, trypan blue and BrdU assays

The XTT assay was performed according to the manufacturer's protocol to determine the viability of the cells. For a 96-well plate, a clear mixture of 5 mL XTT labeling solution and 0.1 mL electron coupling reagent were used. The labeling solution and the coupling reagent had to be thawed and mixed directly before use.

▶ **Fig. 1** With increasing power density, cell density decreased using phase-contrast microscopy. T-LSCs: human telomerase-immortalized limbal epithelial stem cells; HCE-T: human corneal epithelial cell line; LFCs: primary human limbal fibroblasts; HCFs: normal primary human corneal fibroblasts; KC-HCFs: keratoconus primary human corneal fibroblasts; Ctl: control group. Scale bars: 50 μm.

After adding 50 μL of the mixture to each well, the culture plates were placed for 3 h in the 37 °C incubator. Thereafter, a Tecan Infinite F50 Absorbance Microplate Reader (Tecan Infinite Reader, TECAN Deutschland GmbH, Crailsheim, Germany) was used at 450 nm wavelength (reference wavelength: 690 nm) to measure the optical density.

We further used the trypan blue assay to analyze the ratio of dead and live cells following 0.7 J/cm^2 RB-PDT of LFCs (n = 3). In general, LFCs were cultured in 12-well plates until reaching 80 % confluence, then RB-PDT was performed. Twenty-four hours after treatment, LFCs were harvested using trypsin EDTA and were centrifuged at 2000 rpm for 4 minutes. Thereafter, we removed the supernatant and added 30 μL basic medium and 30 μL trypan blue solution. Then, 10 μL basic medium were added in order to resuspend the cells and to calculate the percentage of dead cells in a hemocytometer (WQ-0344, Neolab, Heidelberg, Germany).

The BrdU assay was used to evaluate the proliferation of the cells. In brief, cells were firstly incubated with 10 μL BrdU labeling solution for 3 h at 37 °C. Then, the BrdU labeling solution was replaced by 200 μL FixDenat solution in each well for 30 min. The mixture of anti-BrdU-POD and antibody dilution solution were subsequently added, which was followed by rinsing the cells with 200 μL PBS, three times. The color changes could be observed immediately after adding the stop solution to the substrate solution. The Tecan microplate reader mentioned above was used to gather the optical density value from each plate.

Statistical analysis

GraphPad Prism 9.2 was used for statistical analysis of the data. Data are presented as the mean ± SD (minimum-maximum). For analysis of the results of the XTT and BrdU assays, one-way ANOVA followed by Dunnett's multiple comparison test was used. Paired t-test was used to analyze the trypan blue assay results. A p value below 0.05 was considered statistically significant.
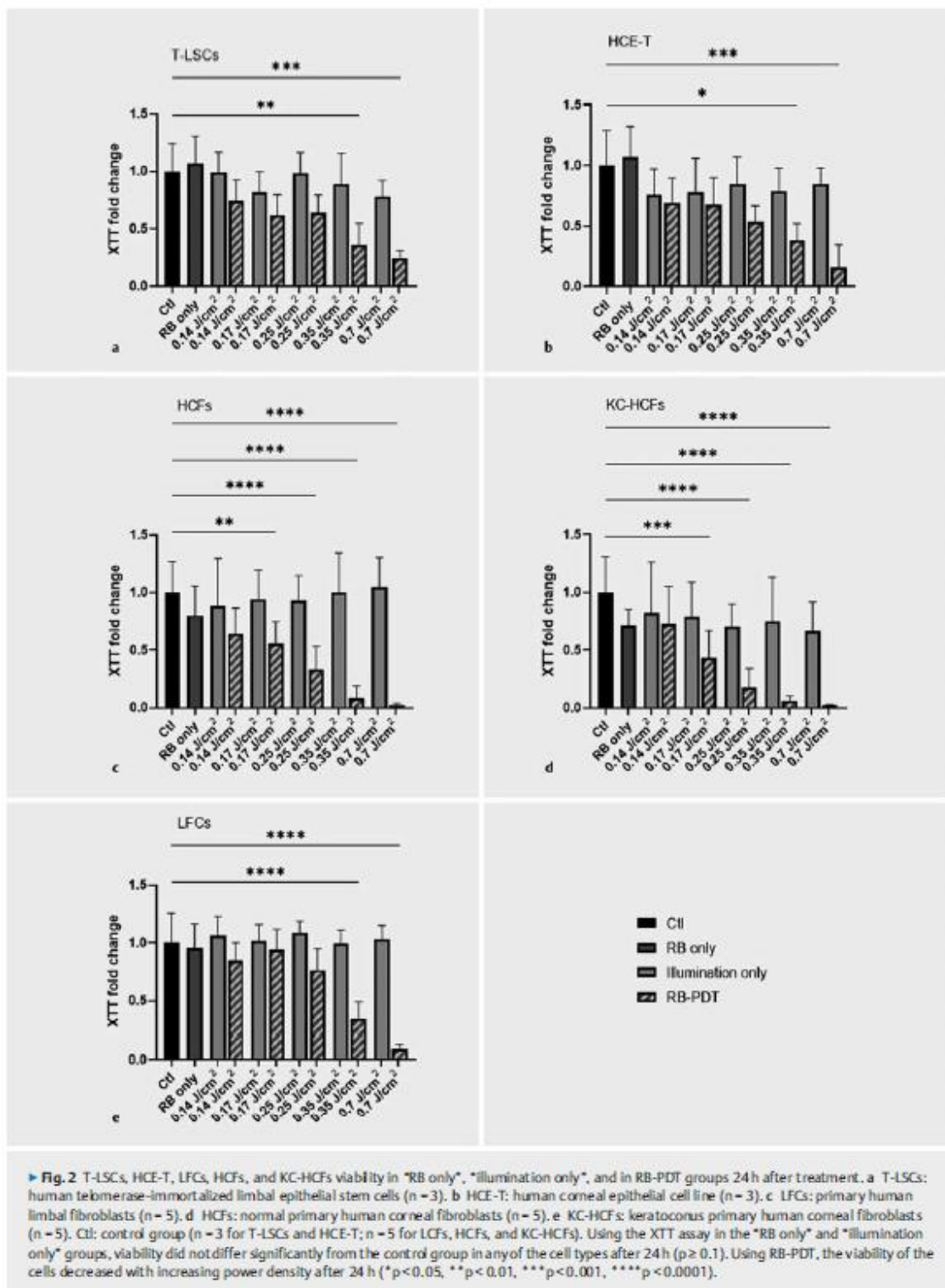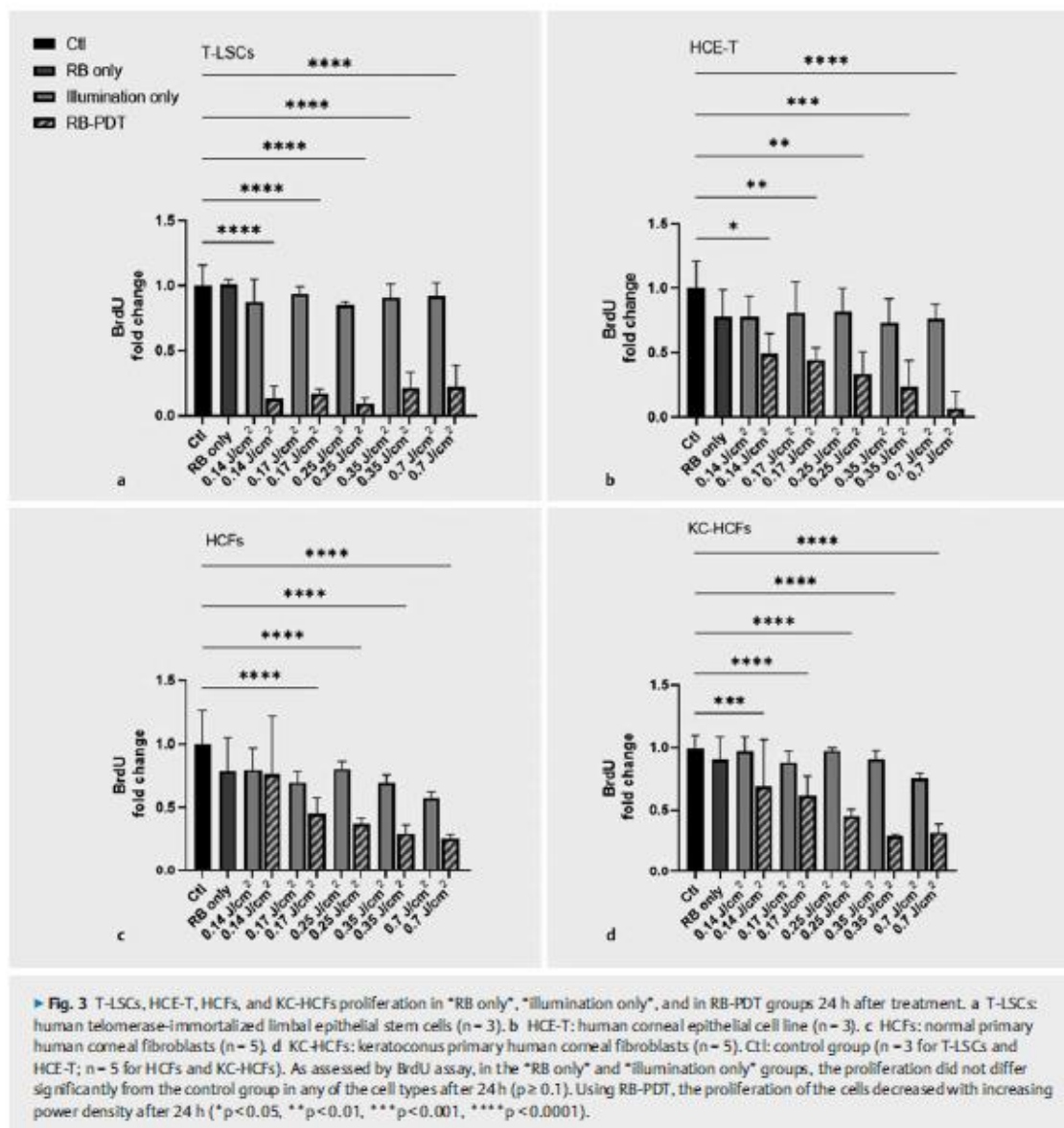
Results

Cell viability

T-LSCs, HCE-T, LFCs, HCFs, and KC-HCFs morphology 24 h following RB-PDT with 0.17 J/cm^2, 0.35 J/cm^2, and 0.7 J/cm^2 fluence is shown in ▶ **Fig. 1**, and cell viability 24 h after RB-PDT in ▶ **Fig. 2**.

In the "RB only" and "illumination only" groups, viability did not differ significantly from the control group in any of the cell types after 24 h ($p \geq 0.1$).

Using RB-PDT, the viability of the cells decreased with increasing fluence. In the RB-PDT group, viability was significantly lower than in the control group from 0.17 J/cm^2 fluence in HCFs ($p < 0.001$) and KC-HCFs ($p < 0.0001$), and from 0.35 J/cm^2 fluence in T-LSCs ($p < 0.001$), HCE-T ($p < 0.05$), and LFCs ($p < 0.0001$). Using 0.35 J/cm^2 fluence for RB-PDT, HCFs, and KC-HCFs, viability was less than 10% of those in the control group of the same cell type. Using 0.7 J/cm^2 fluence for RB-PDT, T-LSCs viability was ap-

► **Fig. 2** T-LSCs, HCE-T, LFCs, HCFs, and KC-HCFs viability in "RB only", "illumination only", and in RB-PDT groups 24 h after treatment. **a** T-LSCs: human telomerase-immortalized limbal epithelial stem cells (n = 3). **b** HCE-T: human corneal epithelial cell line (n = 3). **c** LFCs: primary human limbal fibroblasts (n = 5). **d** HCFs: normal primary human corneal fibroblasts (n = 5). **e** KC-HCFs: keratoconus primary human corneal fibroblasts (n = 5). Ctl: control group (n = 3 for T-LSCs and HCE-T; n = 5 for LCFs, HCFs, and KC-HCFs). Using the XTT assay in the "RB only" and "illumination only" groups, viability did not differ significantly from the control group in any of the cell types after 24 h (p ≥ 0.1). Using RB-PDT, the viability of the cells decreased with increasing power density after 24 h (*p < 0.05, **p < 0.01, ***p < 0.001, ****p < 0.0001).

► **Fig. 3** T-LSCs, HCE-T, HCFs, and KC-HCFs proliferation in "RB only", "illumination only", and in RB-PDT groups 24 h after treatment. **a** T-LSCs: human telomerase-immortalized limbal epithelial stem cells (n = 3). **b** HCE-T: human corneal epithelial cell line (n = 3). **c** HCFs: normal primary human corneal fibroblasts (n = 5). **d** KC-HCFs: keratoconus primary human corneal fibroblasts (n = 5). Ctl: control group (n = 3 for T-LSCs and HCE-T; n = 5 for HCFs and KC-HCFs). As assessed by BrdU assay, in the "RB only" and "illumination only" groups, the proliferation did not differ significantly from the control group in any of the cell types after 24 h (p ≥ 0.1). Using RB-PDT, the proliferation of the cells decreased with increasing power density after 24 h (*p < 0.05, **p < 0.01, ***p < 0.001, ****p < 0.0001).

proximately 24 %, HCE-T viability 16 %, and LFCs viability 10 % of those in the control group.

Based on the viability assay, the half-maximal inhibitory concentration (IC_{50}) of RB-PDT was $0.318\,J/cm^2$ for HCE-T ($R^2 = 0.65$), $0.317\,J/cm^2$ for LFCs ($R^2 = 0.905$), $0.315\,J/cm^2$ for T-LSCs ($R^2 = 0.637$), $0.217\,J/cm^2$ for HCFs ($R^2 = 0.73$), and $0.185\,J/cm^2$ for KC-HCFs ($R^2 = 0.702$).

Cell proliferation

Results of the BrdU assay showing cells in the S phase of the cell cycle are displayed in ► **Fig. 3**.

In the "RB only" and "illumination only" groups, proliferation did not differ significantly from the control group in any of the cell types after 24 h (p ≥ 0.1).

In the RB-PDT group, proliferation was significantly lower than in the control group from $0.14\,J/cm^2$ fluence in T-LSCs (p < 0.0001), HCE-T (p < 0.05), and KC-HCFs (p < 0.001), and from $0.17\,J/cm^2$ fluence in HCFs (p < 0.05). Using $0.14\,J/cm^2$ fluence for RB-PDT, T-LSCs proliferation was 13 % of those in the control group of the same cell type. Using $0.7\,J/cm^2$ fluence for RB-PDT, HCE-T, HCFs, and KC-HCFs proliferation was 6, 25, and 30 % of the controls, respectively.

Using the BrdU assay for LFCs, we did not get reliable measurement results. There were no changes in LFCs proliferation following RB-PDT, even with the highest fluence ($0.7 \, J/cm^2$, $p > 0.9$, data not shown). However, at the same time, LFCs density decreased following treatment (► **Fig. 1**).

The authors hypothesized that due to an altered cell structure of the LFCs, the thymidine analog 5-bromo-2-deoxyuridine (BrdU) could not be inserted into the DNA, and thus could not be detected with the anti-BrdU-antibodies used in this assay.

Therefore, as an additional measurement, we performed a trypan blue assay of LFCs. Using the trypan blue assay, there were 61.3% dead LFCs 24h after RB-PDT and 6.2% in controls ($p < 0.001$, Supplement **Fig. S1**).

Discussion

Photodynamic therapy was first introduced as keratoconus treatment in 1998 in the form of riboflavin-UVA PDT/cross-linking (CXL) [21]. The riboflavin-UVA PDT is based on photo-induced CXL through the creation of new covalent bonds between the collagens and the proteoglycans, establishing a rigid corneal stroma with the participation of oxygen [22].

Besides riboflavin, RB is also used in CXL procedures, including skin/nerve graft fixation, and tendon repair, etc. [23–27]. Some researchers reported that based on their animal experiments, the RB-induced CXL had an equal or even better effect on corneal stiffness, with less cellular damage and a shorter healing time compared to riboflavin-UVA CXL [27–29].

The mechanisms behind both PDTs are similar, but there are several differences that should not be neglected. First, in contrast to riboflavin, RB has a special affinity to collagens, which are the main components of stroma [8,30]. Therefore, the penetration of RB is limited to the superficial 100 µm stromal layer, while the riboflavin penetration depth is nearly 400 µm [31]. Furthermore, the fluence used for RB-PDT and riboflavin-UVA-CXL differs as well. During RB-PDT, $150 \, J/cm^2$ and during riboflavin-UVA-CXL $5.4 \, J/cm^2$ fluence should be used to support collagen bond formation [32,33].

A variety of studies reported that riboflavin-UVA CXL damages keratocytes [33–35]; however, only a few studies reported on the cytotoxicity of RB-PDT using animal models [28,36]. The effect of RB-PDT on human corneal cells, in cell culture experiments, has not previously been analyzed.

In the current study, we proved that viability and proliferation of HCFs and KC-HCFs are strongly affected by the combination of RB and green light in a fluence-dependent manner. Our results showed that the viability of primary HCFs and KC-HCFs started to decrease from $0.17 \, J/cm^2$, which is much lower than the applied energy setting of RB-PDT in animal models ($150 \, J/cm^2$) [8,37], and also much lower than the $5.4 \, J/cm^2$ fluence during clinical application of RB antimicrobial therapy [38]. Through increasing the fluence to $0.7 \, J/cm^2$, nearly all cells lost their viability in culture. Furthermore, the RB concentration applied in the present study was 0.001% (m/v), in contrast to the 0.1% (m/v) clinically used concentration.

Following RB-PDT, HCFs proliferation was in line with changes in viability, with a significant decrease from $0.17 \, J/cm^2$. However,

in KC-HCFs, proliferation was already significantly reduced using a lower ($0.14 \, J/cm^2$) fluence. Our results indicated that KC-HCFs are more sensible to RB-PDT than HCFs. This is similar to the effect of riboflavin-UVA-PDT *in vitro* [39]. A previous study found that KC-HCFs failed to synthesize as much nitric oxide synthase (iNOS) as HCFs under hypoxic conditions [40]. iNOS supports nitric oxide (NO) synthesis, which has been reported to have multiple functions in cellular homeostasis, proliferation, and migration [41]. High NO concentration (higher than 1 µM) reduces cell viability through an inflammatory response [42]. However, a low NO concentration may act as an essential molecule in pro-survival/proliferation reactions within the cells after PDT [43]. Bazak et al. reported that the growth/invasion of multiple types of tumor cells was elicited by iNOS/NO, which was secreted by the tumor cells after PDT [44]. KC-HCFs may also be highly sensitive to RB-PDT due to the decreased iNOS production during the hypoxic PDT conditions. The explicit mechanisms still need to be elucidated.

LFCs viability was not affected by RB-PDT until $0.35 \, J/cm^2$ fluence, which is nearly 2-fold higher than the damaging density in HCFs. Although LFCs and HCFs' morphology was similar after RB-PDT (► **Fig. 1**), both responded with different cell survival to the same treatment. Ainscough et al. reported that the limbal fibroblasts could significantly stimulate the growth of limbal epithelial progenitors and could also secret more keratinocyte growth factor (KGF) compared to the central corneal equivalents [45]. KGF is one of the members of the fibroblast growth factor family and can be secreted by fibroblasts. Interestingly, Teranishi et al. found that KGF could protect corneal epithelial cells from all hypoxia-induced detrimental effects [46]. Similarly, Cai et al. reported that KGF protected the intestinal epithelial cells from hypoxia-induced apoptosis [47]. Based on these data, KGF may also participate in the regulation of cell survival in LFCs during PDT and hypoxia; however, this has to be proven in future experiments.

The BrdU assay is used to identify proliferating cells from quiescent cells in a variety of tissues [48,49], but it failed to accurately capture the growth of LFCs in our study. Our hypothesis is that there is an unspecific binding between the BrdU labeling reagent and the limbal fibroblasts. Although the authors also tried to apply a lower BrdU concentration (12.5%), 1/3 labeling duration, 1/3 fixation time, and repeat rinsing steps, all these changes did not have a significant effect on the measured value. As the BrdU assay worked well in all other cell types, we hypothesized that through special properties of LFCs, the assay did not have an appropriate outcome in these cells. Other methods should be utilized in the future in order to study LFCs proliferation, i.e., the detection of Ki-67 protein, a biomarker tightly related to cell cycle progression, may act as a proper metric to represent cell mitosis [50,51].

Limbal epithelial stem cells (LESCs) participate in corneal epithelial renewal. Therefore, LESCs are resources of the corneal epithelium and are crucial in the maintenance of corneal homeostasis [52]. In order to protect the limbus and LESCs, clinicians always choose a proper sized shield covering the corneoscleral area before RB use [16]. To the best of the authors' knowledge, there is no report focusing on the phototoxicity of RB-PDT on human LESCs and corneal epithelial cells *in vitro*.

In our present study, we used the T-LSCs (limbal epithelial stem cell line) and HCE-T (differentiated epithelial cell line) cell lines as

our experimental models [53, 54]. After RB-PDT, T-LSC and HCE-T viability decreased from $0.35 \, J/cm^2$. Furthermore, when the fluence reached $0.7 \, J/cm^2$, the viability of T-LSCs and HCE-T was higher than in the analyzed other cell types. From this perspective, RB-induced phototoxicity was lower on both corneal epithelial cell types.

Concerning cell proliferation, limbal epithelial stem cells seem to be highly sensitive to RB-PDT, since DNA synthesis activity was significantly reduced from $0.14 \, J/cm^2$ fluence ($p < 0.0001$). The proliferation of HCE-T cells also decreased significantly from $0.14 \, J/cm^2$ fluence ($p < 0.05$) and there was a clear gradient declination in an energy-dependent manner. In the literature, Bath et al. reported that hypoxic conditions could help to maintain a low proliferative rate in limbal epithelial stem cells [55] and, more importantly, hypoxic conditions could facilitate the maintenance of stemness in LESCs [55,56]. This suggests that the differentiation ability of limbal epithelial stem cells may persist after PDT, which is also an oxygen-lacking condition [57]. However, whether the differentiation ability of LESCs could be influenced through RB-PDT still needs to be further investigated.

Our study has several limitations. Although we tested the phototoxicity of RB-PDT in various types of human corneal cells, the detailed mechanisms behind these phenomena are still lacking. In addition, we used immortalized cell lines as cell models for limbal epithelial stem cells and corneal epithelial cells, which may also introduce disparities.

CONCLUSIONS

Already known:

- RB-PDT may be a potential treatment method of infectious keratitis and an effective corneal stiffening procedure.
- In animal models, corneal RB-PDT was a safe treatment procedure. However, there is no previous report focusing on the cytotoxicity of RB-PDT on human corneal cells *in vitro*.
- The effect of RB-PDT on viability and proliferation of corneal epithelial and stromal cells should be evaluated *in vitro* to provide a practical experimental model for future analysis.

Newly described:

- The fluence-dependent phototoxicity of RB-PDT on human corneal epithelial and stromal cells should be kept in mind.
- The data and the experimental parameters applied in this study provide a reliable reference for future investigations.

Acknowledgement

Conflict of Interest

The authors declare that there is no conflict of interest.

References

[1] Bykhovskaya Y, Li X, Epifantseva I et al. Variation in the lysyl oxidase (LOX) gene is associated with keratoconus in family-based and case-control studies. Invest Ophthalmol Vis Sci 2012; 53: 4152–4157. doi:10.1167/iovs.11-9268

[2] McKay TB, Hjortdal J, Priyadarsini S et al. Acute hypoxia influences collagen and matrix metalloproteinase expression by human keratoconus cells *in vitro*. PLoS One 2017; 12: 1–13. doi:10.1371/journal.pone.0176017

[3] Bykhovskaya Y, Margines B, Rabinowitz YS. Genetics in Keratoconus: where are we? Eye Vis (Lond) 2016; 3: 1–10. doi:10.1186/s40662-016-0047-5

[4] Wollensak G, Spoerl E, Seiler T. Riboflavin/ultraviolet-a-induced collagen crosslinking for the treatment of keratoconus. Am J Ophthalmol 2003; 135: 620–627. doi:10.1016/s0002-9394(02)02220-1

[5] Hou Y, Le VNH, Clahsen T et al. Photodynamic Therapy Leads to Time-Dependent Regression of Pathologic Corneal (Lymph) Angiogenesis and Promotes High-Risk Corneal Allograft Survival. Invest Ophthalmol Vis Sci 2017; 58: 5862–5869. doi:10.1167/iovs.17-22904

[6] Manayath GJ, Narendran V, Ganesh A et al. Low-fluence photodynamic therapy for early onset choroidal neovascular membrane following laser *in situ* keratomileusis. Indian J Ophthalmol 2012; 60: 584–585

[7] Alarcon EI, Poblete H, Roh HG et al. Rose Bengal binding to collagen and tissue photobonding. ACS Omega 2017; 2: 6646–6657. doi:10.1021/acsomega.7b00675

[8] Cherfan D, Verter EE, Melki S et al. Collagen cross-linking using rose bengal and green light to increase corneal stiffness. Invest Ophthalmol Vis Sci 2013; 54: 3426–3433. doi:10.1167/iovs.12-11509

[9] Inguscio V, Panzarini E, Dini L. Autophagy Contributes to the Death/Survival Balance in Cancer PhotoDynamic Therapy. Cells 2012; 1: 464–491. doi:10.3390/cells1030464

[10] Dobson J, de Queiroz GF, Golding JP. Photodynamic therapy and diagnosis: Principles and comparative aspects. Vet J 2018; 233: 8–18. doi:10.1016/j.tvjl.2017.11.012

[11] Kessel D, Reiners JJ. Photodynamic therapy: autophagy and mitophagy, apoptosis and paraptosis. Autophagy 2020; 16: 2098–2101. doi:10.1080/15548627.2020.1783823

[12] Santhiago MR, Randleman JB. The biology of corneal cross-linking derived from ultraviolet light and riboflavin. Exp Eye Res 2021; 202: 108355. doi:10.1016/j.exer.2020.108355

[13] Fokam D, Hoskin D. Instrumental role for reactive oxygen species in the inflammatory response. Front Biosci (Landmark Ed) 2020; 25: 1110–1119. doi:10.2741/4848

[14] Moloney JN, Cotter TG. ROS signaling in the biology of cancer. Semin Cell Dev Biol 2018; 80: 50–64. doi:10.1016/j.semcdb.2017.05.023

[15] Korb DR, Herman JP, Finnemore VM et al. An evaluation of the efficacy of fluorescein, rose bengal, lissamine green, and a new dye mixture for ocular surface staining. Eye Contact Lens 2008; 34: 61–64. doi:10.1097/ICL.0b013e31811ead93

[16] Martinez JD, Arrieta E, Naranjo A et al. Rose Bengal Photodynamic Antimicrobial Therapy: A Pilot Safety Study. Cornea 2021; 40: 1036–1043. doi:10.1097/ICO.0000000000002717

[17] Martinez JD, Naranjo A, Amescua G et al. Human Corneal Changes After Rose Bengal Photodynamic Antimicrobial Therapy for Treatment of Fungal Keratitis. Cornea 2018; 37: e46. doi:10.1097/ICO.0000000000001701

[18] Wertheimer CM, Elhardt C, Kaminsky SM et al. Enhancing Rose Bengal-Photosensitized Protein Crosslinking in the Cornea. Invest Ophthalmol Vis Sci 2019; 60: 1845–1852. doi:10.1167/iovs.19-26604

[19] Germann JA, Martinez-Enriquez E, Martinez-Garcia MC et al. Corneal collagen ordering after in vivo Rose Bengal and riboflavin cross-linking. Invest Ophthalmol Vis Sci 2020; 61: 28. doi:10.1167/iovs.61.3.28

[20] Roux LN, Petit I, Domart R et al. Modeling of Aniridia-Related Keratopathy by CRISPR/Cas9 Genome Editing of Human Limbal Epithelial Cells and Rescue by Recombinant PAX6 Protein. Stem Cells 2018; 36: 1421–1429. doi:10.1002/stem.2858

[21] Spoerl E, Huhle M, Seiler T. Induction of cross-links in corneal tissue. Exp Eye Res 1998; 66: 97–103. doi:10.1006/exer.1997.0410

[22] Brummer G, Littlechild S, McCall S et al. The role of nonenzymatic glycation and carbonyls in collagen cross-linking for the treatment of keratoconus. Invest Ophthalmol Vis Sci 2011; 52: 6363–6369. doi:10.1167/iovs.11-7585

[23] Redmond RW, Kochevar IE. Medical Applications of Rose Bengal- and Riboflavin-Photosensitized Protein Crosslinking. Photochem Photobiol 2019; 95: 1097–1115. doi:10.1111/php.13126

[24] Ni T, Senthil-Kumar P, Dubbin K et al. A photoactivated nanofiber graft material for augmented Achilles tendon repair. Lasers Surg Med 2012; 44: 645–652. doi:10.1002/lsm.22066

[25] Chan BP, Kochevar IE, Redmond RW. Enhancement of porcine skin graft adherence using a light-activated process. J Surg Res 2002; 108: 77–84. doi:10.1006/jsre.2002.6516

[26] Fairbairn NG, Ng-Glazier J, Meppelink AM et al. Light-Activated Sealing of Nerve Graft Coaptation Sites Improves Outcome following Large Gap Peripheral Nerve Injury. Plast Reconstr Surg 2015; 136: 739–750. doi:10.1097/PRS.0000000000001617

[27] Bekesi N, Kochevar IE, Marcos S. Corneal biomechanical response following collagen cross-linking with Rose Bengal-green light and riboflavin-UVA. Invest Ophthalmol Vis Sci 2016; 57: 992–1001. doi:10.1167/iovs.15-18689

[28] Lorenzo-Martín E, Gallego-Muñoz P, Ibares-Frías L et al. Rose Bengal and Green Light Versus Riboflavin–UVA Cross-Linking: Corneal Wound Repair Response. Invest Ophthalmol Vis Sci 2018; 59: 4821–4830. doi:10.1167/iovs.18-24881

[29] Gallego-Muñoz P, Ibares-Frías L, Lorenzo E et al. Corneal Wound Repair After Rose Bengal and Green Light Crosslinking: Clinical and Histologic Study. Invest Ophthalmol Vis Sci 2017; 58: 3471–3480. doi:10.1167/iovs.16-21365

[30] Verter EE, Gisel TE, Yang P et al. Light-initiated bonding of amniotic membrane to cornea. Invest Ophthalmol Vis Sci 2011; 52: 9470–9477. doi:10.1167/iovs.11-7248

[31] Redmond RW, Kochevar IE. Medical Applications of Rose Bengal- and Riboflavin-Photosensitized Protein Crosslinking. Photochem Photobiol 2019; 95: 1097–1115. doi:10.1111/php.13126

[32] Zhu H, Alt C, Webb RH et al. Corneal Crosslinking With Rose Bengal and Green Light: Efficacy and Safety Evaluation. Cornea 2016; 35: 1234–1241. doi:10.1097/ICO.0000000000000916

[33] Wollensak G, Spoerl E, Wilsch M et al. Keratocyte apoptosis after corneal collagen cross-linking using riboflavin/UVA treatment. Cornea 2004; 23: 43–49. doi:10.1097/00003226-200401000-00008

[34] Spoerl E, Mrochen M, Sliney D et al. Safety of UVA-riboflavin cross-linking of the cornea. Cornea 2007; 26: 385–389. doi:10.1097/ICO.0b013e3180334f78

[35] Krüger A, Hovakimyan M, Ramirez Ojeda DF et al. Combined nonlinear and femtosecond confocal laser-scanning microscopy of rabbit corneas after photochemical cross-linking. Invest Ophthalmol Vis Sci 2011; 52: 4247–4255. doi:10.1167/iovs.10-7112

[36] Naranjo A, Pelaez D, Arrieta E et al. Cellular and molecular assessment of rose bengal photodynamic antimicrobial therapy on keratocytes, corneal endothelium and limbal stem cell niche. Exp Eye Res 2019; 188: 107808. doi:10.1016/j.exer.2019.107808

[37] Vanden Berghe T, Vanlangenakker N, Parthoens E et al. Necroptosis, necrosis and secondary necrosis converge on similar cellular disintegration features. Cell Death Differ 2010; 17: 922–930. doi:10.1038/cdd.2009.184

[38] Levine H, Sepulveda-Beltran PA, Amescua G. Rose Bengal Photodynamic Antimicrobial Therapy as potential adjuvant treatment for Serratia marcescens corneal ulcer. Am J Ophthalmol 2021; 231: e1–e2. doi:10.1016/j.ajo.2021.07.007

[39] Song X, Stachon T, Wang J et al. Viability, apoptosis, proliferation, activation, and cytokine secretion of human keratoconus keratocytes after cross-linking. Biomed Res Int 2015; 2015: 254237. doi:10.1155/2015/254237

[40] Stachon T, Latta L, Seitz B et al. Hypoxic stress increases NF-κB and iNOS mRNA expression in normal, but not in keratoconus corneal fibroblasts. Graefes Arch Clin Exp Ophthalmol 2021; 259: 449–458. doi:10.1007/s00417-020-04900-8

[41] Wink DA, Mitchell JB. Chemical biology of nitric oxide: Insights into regulatory, cytotoxic, and cytoprotective mechanisms of nitric oxide. Free Radic Biol Med 1998; 25: 434–456. doi:10.1016/s0891-5849(98)00092-6

[42] Ridnour LA, Thomas DD, Donzelli S et al. The biphasic nature of nitric oxide responses in tumor biology. Antioxid Redox Signal 2006; 8: 1329–1337. doi:10.1089/ars.2006.8.1329

[43] Rapozzi V, Della Pietra E, Bonavida B. Dual roles of nitric oxide in the regulation of tumor cell response and resistance to photodynamic therapy. Redox Biol 2015; 6: 311–317. doi:10.1016/j.redox.2015.07.015

[44] Bazak J, Korytowski W, Girotti AW. Bystander Effects of Nitric Oxide in Cellular Models of Anti-Tumor Photodynamic Therapy. Cancers (Basel) 2019; 11: 1674. doi:10.3390/cancers11111674

[45] Ainscough SL, Linn ML, Barnard Z et al. Effects of fibroblast origin and phenotype on the proliferative potential of limbal epithelial progenitor cells. Exp Eye Res 2011; 92: 10–19. doi:10.1016/j.exer.2010.10.004

[46] Teranishi S, Kimura K, Kawamoto K et al. Protection of human corneal epithelial cells from hypoxia-induced disruption of barrier function by keratinocyte growth factor. Invest Ophthalmol Vis Sci 2008; 49: 2432–2437. doi:10.1167/iovs.07-1464

[47] Cai Y, Wang W, Qiu Y et al. KGF inhibits hypoxia-induced intestinal epithelial cell apoptosis by upregulating AKT/ERK pathway-dependent E-cadherin expression. Biomed Pharmacother 2018; 105: 1318–1324. doi:10.1016/j.biopha.2018.06.091

[48] Crane AM, Bhattacharya SK. The use of bromodeoxyuridine incorporation assays to assess corneal stem cell proliferation. Methods Mol Biol 2013; 1014: 65–70. doi:10.1007/978-1-62703-432-6_4

[49] Chen SL, Cai SR, Zhang XH et al. Targeting CRMP-4 by lentivirus-mediated RNA interference inhibits SW480 cell proliferation and colorectal cancer growth. Exp Ther Med 2016; 12: 2003–2008. doi:10.3892/etm.2016.3588

[50] Masoud Y, Ramin S, Mahboobeh R et al. Effect of Lithium and Valproate on Proliferation and Migration of Limbal Epithelial Stem/Progenitor Cells. Curr Eye Res 2019; 44: 154–161. doi:10.1080/02713683.2018.1521978

[51] Sun X, Kaufman PD. Ki-67: more than a proliferation marker. Chromosoma 2018; 127: 175–186. doi:10.1007/s00412-018-0659-8

[52] Nakatsu MN, Ding Z, Ng MY et al. Wnt/β-catenin signaling regulates proliferation of human cornea epithelial stem/progenitor cells. Invest Ophthalmol Vis Sci 2011; 52: 4734–4741. doi:10.1167/iovs.10-6486

[53] Araki-Sasaki K, Ohashi Y, Sasabe T et al. An SV40-immortalized human corneal epithelial cell line and its characterization. Invest Ophthalmol Vis Sci 1995; 36: 614–621

[54] Rubelowski AK, Latta L, Katiyar P et al. HCE-T cell line lacks cornea-specific differentiation markers compared to primary limbal epithelial cells and differentiated corneal epithelium. Graefes Arch Clin Exp Ophthalmol 2020; 258: 565–575. doi:10.1007/s00417-019-04563-0

[55] Bath C, Yang S, Muttuvelu D et al. Hypoxia is a key regulator of limbal epithelial stem cell growth and differentiation. Stem Cell Res 2013; 10: 349–360. doi:10.1016/j.scr.2013.01.004

[56] Wang L, González S, Dai W et al. Effect of hypoxia-regulated polo-like kinase 3 (Plk3) on human limbal stem cell differentiation. J Biol Chem 2016; 291: 16519–16529. doi:10.1074/jbc.M116.725747

[57] Wertheimer CM, Mendes B, Pei Q et al. Arginine as an Enhancer in Rose Bengal Photosensitized Corneal Crosslinking. Transl Vis Sci Technol 2020; 9: 1–11. doi:10.1167/tvst.9.8.24

5. Publication 2

PLOS ONE

Human corneal epithelial cell and fibroblast migration and growth factor secretion after rose bengal photodynamic therapy (RB-PDT) and the effect of conditioned medium

Ning Chai[1]*, Tanja Stachon[1], Tim Berger[2], Zhen Li[1], Berthold Seitz[2], Achim Langenbucher[3], Nóra Szentmáry[1,4]

1 Dr. Rolf M. Schwiete Center for Limbal Stem Cell and Aniridia Research, Saarland University, Homburg, Saar, Germany, 2 Department of Ophthalmology, Saarland University Medical Center, Homburg, Saar, Germany, 3 Experimental Ophthalmology, Saarland University, Homburg, Germany, 4 Department of Ophthalmology, Semmelweis University, Budapest, Hungary

* ning.chai@uks.eu

Abstract

Purpose

To investigate human corneal epithelial cell and fibroblast migration and growth factor secretion after rose bengal photodynamic therapy (RB-PDT) and the effect of conditioned medium (CM).

Methods

A human corneal epithelial cell line (HCE-T), human corneal fibroblasts (HCF) and keratoconus fibroblasts (KC-HCF) have been used. Twenty-four hours after RB-PDT (0.001% RB concentration, 565 nm wavelength illumination, 0.17 J/cm^2 fluence) cell migration rate using scratch assay and growth factor concentrations in the cell culture supernatant using ELISA have been determined. In addition, the effect of CM has been observed.

Results

RB-PDT significantly reduced migration rate in all cell types, compared to controls ($p \leq 0.02$). Migration rate of HCE-T cultures without RB-PDT (untreated) was significantly higher using HCF CM after RB-PDT, than using HCF CM without RB-PDT ($p<0.01$). Similarly, untreated HCF displayed a significantly increased migration rate with HCE-T CM after RB-PDT, compared to HCE-T CM without treatment ($p<0.01$). Furthermore, illumination alone and RB-PDT significantly decreased keratinocyte growth factor (KGF) concentration in HCF and KC-HCF supernatant, and RB-PDT significantly decreased soluble N-Cadherin (SN-Cad) concentration in HCF supernatant, compared to controls ($p<0.01$ for all). In HCE-T CM, RB-PDT increased hepatocyte growth factor (HGF) and basic fibroblast growth factor (FGFb) concentration ($p \leq 0.02$), while decreasing transforming growth factor β (TGF-β) concentration ($p<0.01$). FGFb concentration increased ($p<0.0001$) and TGF-β concentration

decreased (p<0.0001) in HCF CM, by RB-PDT. Epidermal growth factor (EGF), HGF, and TGF-β concentration decreased (p≤0.03) and FGFb concentration increased (p<0.01) in KC-HCF CM, using RB-PDT.

Conclusions

HCE-T, HCF and KC-HCF migration rate is reduced 24 hours after RB-PDT. In contrast, HCE-T migration is enhanced using HCF CM after RB-PDT, and HCF migration rate is increased through HCE-T CM following RB-PDT. Modulation of EGF, KGF, HGF, FGFb, TGF-β and N-Cadherin secretion through RB-PDT may play an important role in corneal wound healing.

1. Introduction

Photodynamic therapy (PDT) became a potential treatment alternative in different types of diseases, in the last decades [1–3]. During PDT, different photosensitizers, such as riboflavin, Chlorin e6, rose bengal (RB) or 5-aminolevulinic acid and light of an appropriate wavelength are used [4–7].

Due to its superficial location and transparency, the corneal tissue may also undergo PDT. Crosslinking (CXL), as riboflavin-UVA-PDT was first introduced by Spoerl et al in 1998 [1]. CXL induces cross-links between the collagen fibers of the corneal tissue increasing corneal stiffness and stopping progression of keratoconus [8]. In addition, CXL also has promising applications in treatment of corneal melting, infectious keratitis, corneal ulcer and bullous keratopathy [9–13].

Rose bengal photodynamic therapy (RB-PDT), using green light (maximal absorption wavelength: 550–560 nm) may also be a promising treatment method in several ophthalmic pathologies [14, 15]. RB-PDT seemed to be an effective corneal stiffening procedure using animal models [16, 17]. Furthermore, using RB-PDT, some patients with infectious keratitis successfully healed [8, 15].

Although RB-PDT has already been used in patients with corneal pathologies, the effect of RB-PDT on corneal epithelial cells and fibroblasts has not been fully understood, yet. In the current study, our aim was to investigate human corneal epithelial cell and human corneal fibroblast migration and their growth factor secretion after RB-PDT, and the epithelial-stromal interaction through detecting the effects of conditioned medium (CM).

2. Materials and methods

This study was approved by the Ethics Committee of Saarland/Germany (Nr. 217/18). All human tissues were handled according to the Declaration of Helsinki principles.

2.1 Experimental reagents

Dulbecco's modified Eagle's medium (DMEM/F12) (Thermo Fisher Scientific, Waltham, MA, USA); 5% fetal calf serum **(FCS)** (Thermo Fisher Scientific, Waltham, MA, USA); 1% penicillin-streptomycin **(P/S)** (Sigma-Aldrich, St. Louis, USA); **Collagenase A** (Hoffmann-La Roche, Basel, Switzerland); **Trypsin EDTA** (Sigma-Aldrich, St. Louis, USA); **Epidermal Growth Factor** (EGF, Gibco, Paisley, UK); **Glutamine** (Sigma Aldrich, Germany); 1% **insulin, transferrin, and selenium (ITS)**; **PBS** (Merck, Sigma-Aldrich, Taufkirchen, Germany); **Rose**

Bengal B (C.I. 45440, Carl Roth, Karlsruhe, Germany); **RIPA buffer** (Thermo Fisher Scientific, Waltham, MA, USA).

2.2 Human corneal epithelial cell line (HCE-T)

The used human corneal epithelial cell line (HCE-T) was provided by the RIKEN cell bank (RCB 2280, Ibaraki, Japan). HCE-T cells were cultured in DMEM/F12 medium, supplemented by 5% FCS, 1% P/S, 10 ng/ml EGF and 1% ITS ("*HCE-T medium*"), using T75 flasks. After reaching 80% of confluence, HCE-T cells were detached using trypsin EDTA and were seeded into 6-well plates for the subsequent experiments.

2.3 Human corneal fibroblast (HCF) and human keratoconus corneal fibroblast (KC-HCF) isolation

Five healthy human corneoscleral buttons were provided by the Klaus Faber Center for Corneal Diseases, including Lions Eye Cornea Bank Saar-Lor-Lux, Trier/Westpfalz, in Homburg. These tissues didn't meet the requirements for corneal transplantation, due to low endothelial cell density (<1800 cell/cm^2). Five human keratoconus corneal samples were obtained from elective penetrating keratoplasties (all patients signed an informed consent, before surgery). The donor tissues / keratoconus samples were first rinsed by PBS, then were cut into small tissue pieces through a surgical scalpel (tissue diameter about 5 mm). Then, the small tissue pieces were put into a solution containing 1.0 mg/ml collagenase A, supplemented by DMEM/F12, 5% FCS, and 1% P/S. After incubation at 37°C overnight, centrifugation has been performed at 1500 rpm for 5 minutes, and the supernatant was discarded. Thereafter, the cell sediment was resuspended in 1 ml DMEM/F12, supplemented by 5% FCS and 1% P/S ("*basic medium*" in the following text) and was seeded into a T75 flask, containing 13 ml basic medium. The cell containing flasks were subsequently stored at 37°C, using 5% CO$_2$, and 95% relative humidity in the incubator. The medium was changed every 4 days. As soon as HCF and KC-HCF reached 80% confluence, these were harvested by trypsin EDTA and were passaged to 8 new T75 flasks. After reaching 80% confluence, HCF and KC-HCF were detached using trypsin EDTA and were seeded into 6-well plates for the subsequent experiments.

2.4 RB-PDT

The RB stock powder was stored in a dark environment until use. As the first step, the 0.001% (m/v) RB solution was prepared by dissolving the stock powder in *HCE-T* or *basic medium*. After sterilization by a 0.2 μm sterilizing filter, the RB solution was stored at 4°C in darkness, for up to 1 month.

The illumination box was built and calibrated at the Department of Experimental Ophthalmology, Saarland University, Homburg/Saar, Germany. In the present study, besides using 0.001% RB concentration, 565 nm wavelength illumination has been used and illumination time was always 600 s. During the present measurement series, we used 0.17 J/cm^2 fluence for all cell types. The used fluence values have been chosen based on our previous measurement series, which analyzed cell viability after RB-PDT *in vitro* [3]. The actually used fluence values were the lowest values, which already slightly affected cell viability.

When HCE-T, HCF or KC-HCF reached 80% confluence in the 6-well plates, treatment has been performed, using the following groups:

1. The cells in the control group (Ctrl) have been gently rinsed three times with 3 ml PBS, without the use of RB or illumination. Then, 2 ml DMEM/F12 supplemented by 1% ITS and 1% P/S has been added to each well.

2. The cells in the "RB only" group have been allowed to absorb the 0.001% RB solution for 30 minutes at 37°C without further light illumination, which has been followed by gentle rinsing three times with 3 ml PBS. Then, 2 ml DMEM/F12 supplemented by 1% ITS and 1% P/S has been added to each well.

3. The cells in the "illumination only" group have been rinsed two times with 3 ml PBS, then 3 ml PBS has been added to each well and the cells have been illuminated by green light using 0.17 J/cm^2 fluence, without adding RB. Thereafter, PBS was replaced by 2 ml DMEM/F12 supplemented by 1% ITS and 1% P/S.

4. The cells in the RB-PDT group have been allowed to absorb the 0.001% RB solution for 30 minutes at 37°C, which has been followed by rinsing with 3 ml PBS twice. Thereafter, 3 ml PBS has been added to each well and the cells have been subsequently illuminated using 0.17 J/cm^2 fluence. Then, PBS was replaced by 2 ml DMEM/F12 supplemented by 1% ITS and 1% P/S.

2.5 HCE-T, HCF and KC-HCF migration rate after treatment

As the first step, three parallel reference lines have been drawn at the bottom of the wells of the 6-well plates with 5 mm distance. Then, HCE-T, HCF or KC-HCF have been seeded, using 15000 cells/cm^2 and adding 3 ml HCE-T medium or basic medium. Reaching 80% confluence, one scratch has been generated in each well, perpendicular to the drawn bottom reference lines, using 100 μl pipette tips (Eppendorf AG, Hamburg, Germany). Then, treatment has been performed as described above (groups (1) to (4)).

Phase-contrast images have been taken directly after treatment (0 hour) and 24 hours afterwards. For each well, 4 different scratch areas have been photographically documented, along the previously drawn reference lines (S1 Fig), for subsequent analysis.

Images of 3 independent scratch assay experiments using HCE-T cell line and images of 5 independent scratch assay experiments using HCF (from 5 different donors) and KC-HCF (from 5 different keratoconus corneas) have been collected.

Phase contrast images have been analyzed using ImageJ (https://imagej.nih.gov/ij/). The Migration Rate (MR) has been calculated as follows:

MR = [Wound area (0 h)–Wound area (24 h)] / Wound area (0 h).

Schematic description of our experiments is shown at Fig 1.

2.6 HCE-T migration rate using HCF or KC-HCF conditioned medium

In order to observe epithelial cell (HCE-T) and stromal cell (HCF or KC-HCF) interactions after treatment, conditioned medium (CM) has been used. For these experiments, only in the "RB-PDT" chapter described "Ctrl" (1) and "RB-PDT" (4) groups have been included.

In brief, HCF and KC-HCF underwent treatment, as described above (only "Ctrl" (1) and "RB-PDT" (4) groups). As the last step of the treatment, 2 ml DMEM/F12 supplemented by 1% ITS and 1% P/S has been added to each well. After *48 hours* at 37°C, the HCF or KC-HCF supernatant has been collected from each well. Cell remnants have been removed from the supernatant using a centrifugation step (3000 rpm for 4 minutes) to get the subsequently used HCF or KC-HCF conditioned medium (HCF CM or KC-HCF CM).

HCE-T scratches have been performed as described above and HCE-T underwent treatment (only "Ctrl" or "RB-PDT" groups). However, instead of adding 2 ml DMEM/F12 supplemented by 1% ITS and 1% P/S as the last step of treatment, HCE-T cultures have been supplemented by the above described 2 ml HCF or KC-HCF CM and were incubated for 24
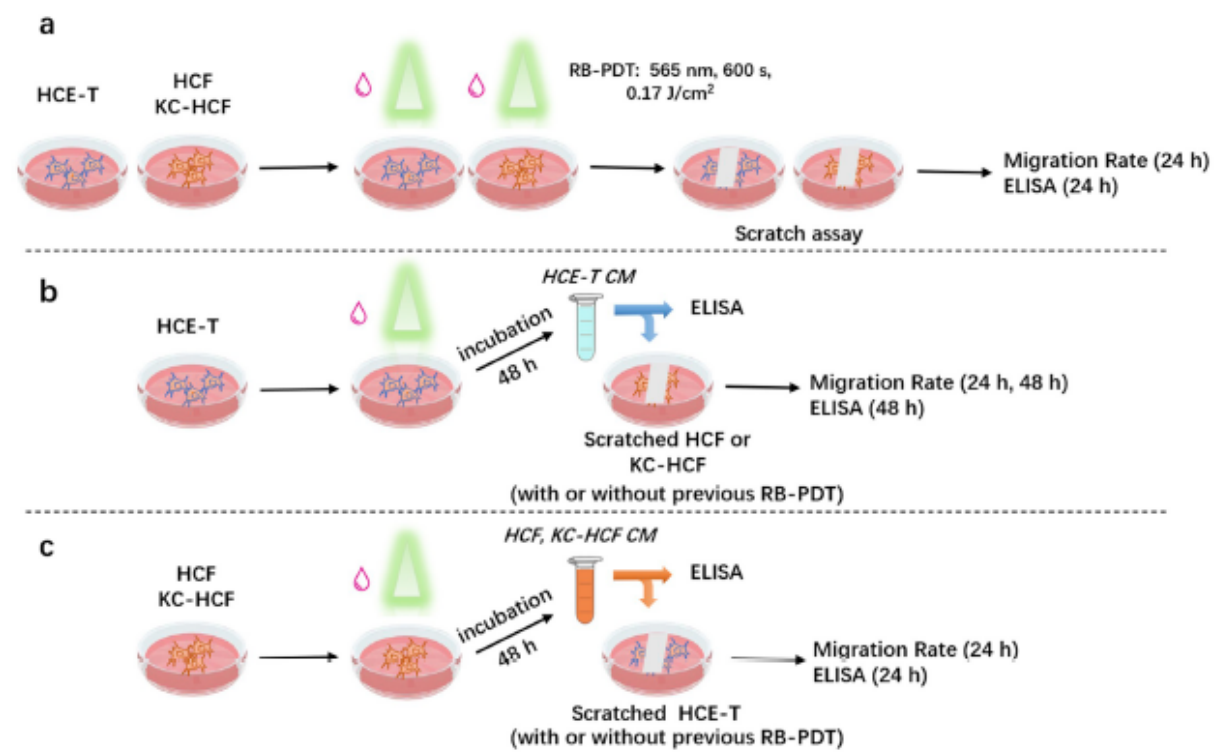
Fig 1. Schematic illustration of the experiments. (a) Human corneal epithelial cells (HCE-T), human corneal fibroblasts (HCF) and human keratoconus fibroblasts (KC-HCF) underwent rose bengal photodynamic therapy (RB-PDT; 0.001% RB concentration, 565 nm wavelength illumination, 17 J/cm^2 fluence), which was followed by scratch assay (migration rate measurement). Thereafter, the supernatant has been collected for the Enzyme-Linked Immunosorbent Assay (ELISA). (b) HCE-T underwent RB-PDT to generate HCE-T conditioned medium (CM). This CM has been added to scratched HCF and KC-HCF cultures to observe its effect on migration rate. The CM has also been collected for ELISA. (c) HCF and KC-HCF underwent RB-PDT to generate HCF or KC-HCF CM. This CM has been added to scratched HCE-T cultures to observe its effect on migration rate. The CM has also been collected for ELISA.

https://doi.org/10.1371/journal.pone.0296022.g001

hours at 37°C. Conditioned media have not been pooled, these have been used separately for each well.

Scratch assay images from each treatment group have been collected, as described above directly after treatment (0 hour) and after 24 hours.

2.7 HCF or KC-HCF migration rate using HCE-T conditioned medium

For these experiments, also only in the "RB-PDT" chapter described "Ctrl" (1) and "RB-PDT" (4) groups have been included.

In brief, HCE-T underwent treatment, as described above (only "Ctrl" (1) and "RB-PDT" (4) groups). As a last step of the treatment, 2 ml DMEM/F12 supplemented by 1% ITS and 1% P/S has been added to each well. After _48 hours_ at 37°C, the HCE-T supernatant has been collected from each well. Cell remnants have been removed from the supernatant using a centrifugation step (3000 rpm for 4 minutes) to get the subsequently used HCE-T conditioned medium (HCE-T CM).

HCF and KC-HCF scratches have been performed as described above and HCF and KC-HCF underwent treatment (only "Ctrl" or "RB-PDT" groups). However, instead of adding 2 ml DMEM/F12 supplemented by 1% ITS and 1% P/S as the last step of RB-PDT, HCF and KC-HCF cultures have been supplemented by the above described 2 ml HCE-T CM and were incubated for up to 48 hours at 37˚C. Conditioned media have not been pooled, these have been used separately from each well.

Scratch assay images from each treatment group have been collected, as described above directly after treatment (0 hour) and after 24 and 48 hours.

2.8 Enzyme linked immunosorbent assay (ELISA) of the cell culture supernatant

Epidermal growth factor (EGF), keratinocyte growth factor (KGF), hepatocyte growth factor (HGF), basic fibroblast growth factor (FGFb) and transforming growth factor β (TGF-β) concentrations in HCE-T, HCF and KC-HCF culture supernatant 24 hours after treatment and scratching have been measured using ELISA (Groups (1) to (4)). In addition, EGF, HGF and KGF concentration has been measured in 48-hours-conditioned HCE-T CM, HCF and KC-HCF CM (without scratch) and in the supernatant of scratched HCE-T, HCF and KC-HCF cultures, 24 or 48 hours after addition of different CM.

To perform the ELISA measurements, DuoSet® ELISA kits (Epidermal growth factor, EGF: DY251; Keratinocyte growth factor, KGF: DY251; Hepatocyte growth factor, HGF: DY294; Basic fibroblast growth factor, FGFb: DY233; Transforming growth factor β, TGF-β: DY240; E-Cadherin: DY648; N-Cadherin: DY1388-05) were purchased from R&D Systems (Minneapolis, USA). All measurements were performed in duplicate. The measurement was performed according to the manufacturer's protocol. In brief, 100 µl capture antibody was added to 96-well plates, and these were incubated overnight at room temperature. Thereafter, 100 µl supernatant was added to each well for 2 h. This step was followed by incubation with the detection antibody for another 2 h. The optical density (OD) value of the wells was detected using a Tecan Infinite F50 Absorbance Microplate Reader (Tecan Group AG, Männedorf, Switzerland) in order to assess growth factor concentration quantitatively. The possessed value was divided by the total protein concentration of the well to obtain the concentration in pictogram (pg) per milligram protein (mg). This value was used for statistical analysis.

2.9 Statistical analysis

Data have been analyzed using Graphpad Prism version 9.2 (GraphPad Software, San Diego, CA). Data were expressed as mean ± standard error of the mean (SEM). In order to compare multiple groups, one-way ANOVA followed by Dunnett's multiple comparison test was used and in order to compare two groups, the unpaired student's t-test was used. P values below 0.05 were considered statistically significant.

3. Results

3.1 HCE-T, HCF and KC-HCF migration rate after treatment

Fig 2 displays phase contrast images of HCE-T, HCF and KC-HCF cultures, directly after scratching (0 h) and 24 hours after treatments. Fig 3 shows migration rate in the same cultures, 24 hours after treatment. 0.17 J/cm^2 RB-PDT significantly decreased migration rate in all cell types, compared to Ctrl ($p \leq 0.02$). Nevertheless, using RB only, or illumination only, migration rate did not change in any of the cell types.
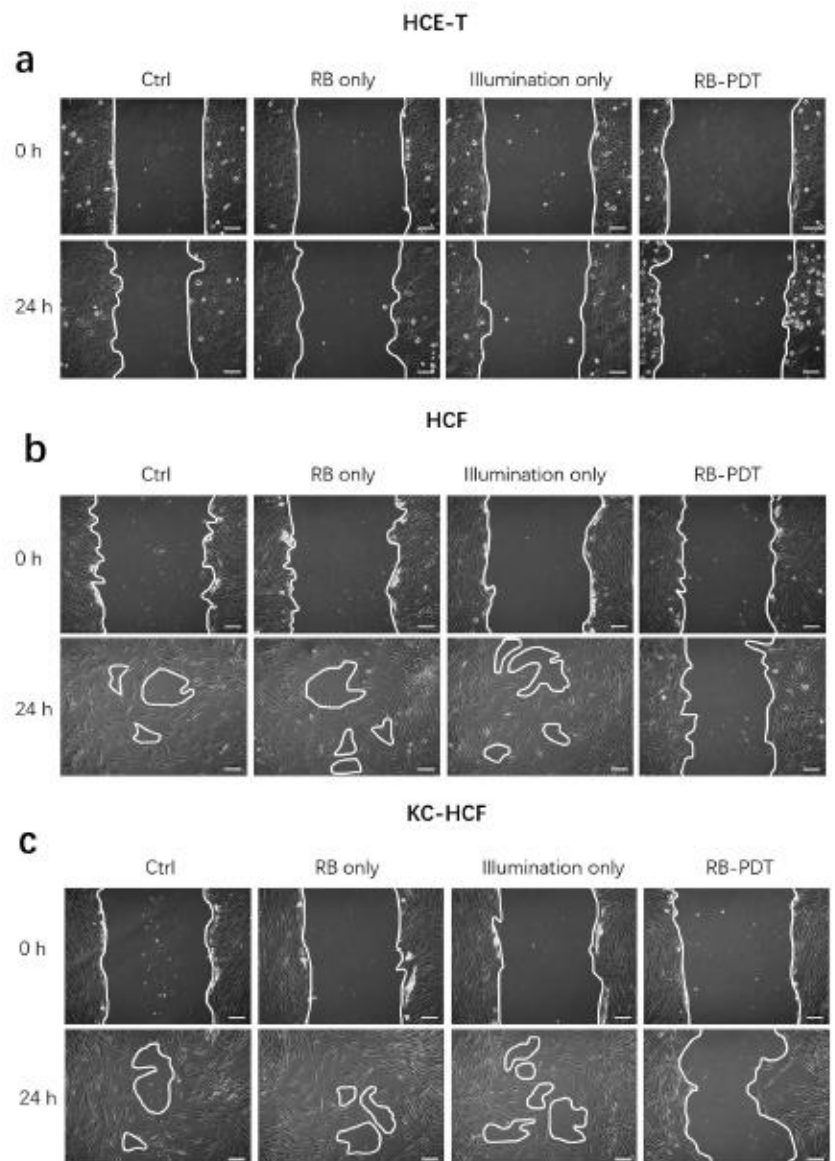
Fig 2. Representative phase contrast images of human cornea epithelial cell (HCE-T). (a), human corneal fibroblast (HCF) (b) and human keratoconus fibroblast (KC-HCF) (c) cultures directly after scratching (0 h) and 24 hours after treatment (Scale bar: 50 µm).
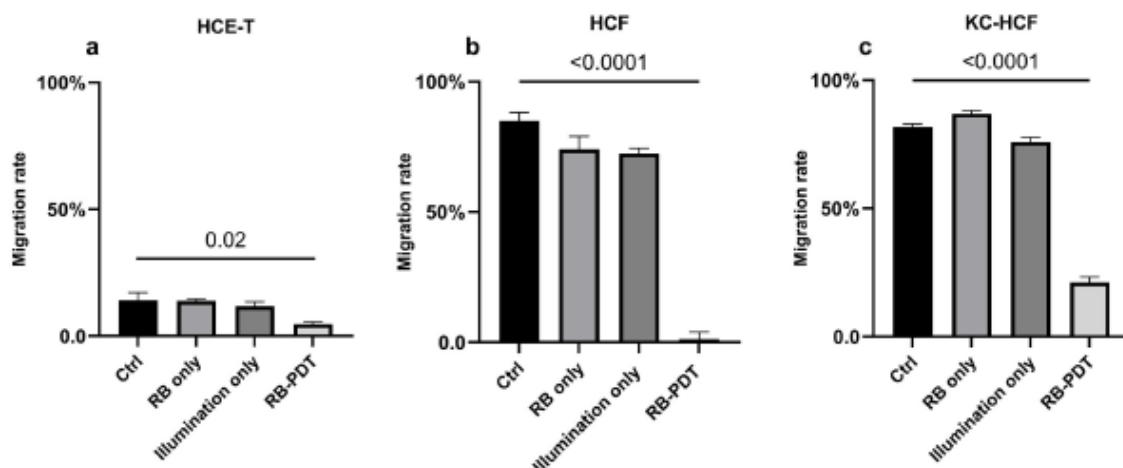
https://doi.org/10.1371/journal.pone.0296022.g002

Fig 3. Migration rate in human corneal epithelial cell line (HCE-T) (n = 3), human corneal fibroblast (HCF) (n = 5) and human keratoconus fibroblast (KC-HCF) (n = 5) cell cultures, 24 hours after treatment and scratching. Data are expressed as mean ± SEM. 0.17 J/cm² rose bengal photodynamic therapy (RB-PDT) significantly decreased migration rate in all cell types, compared to controls (Ctrl) (p≤0.02). The experiments using primary human corneal fibroblasts (HCF, KC-HCF) were repeated five times (from five different donors), while the experiments using a commercial corneal epithelial cell line (HCE-T) were repeated three times.

https://doi.org/10.1371/journal.pone.0296022.g003

3.2 Growth factor concentration in the cell culture supernatant, after treatment and scratching

Growth factor and soluble N-Cadherin (SN-Cad) concentrations in HCF and KC-HCF culture supernatant 24 hours after treatment and scratching are displayed at Fig 4. EGF, HGF and KGF concentration was not measurable in HCE-T cell culture supernatant 24 hours after
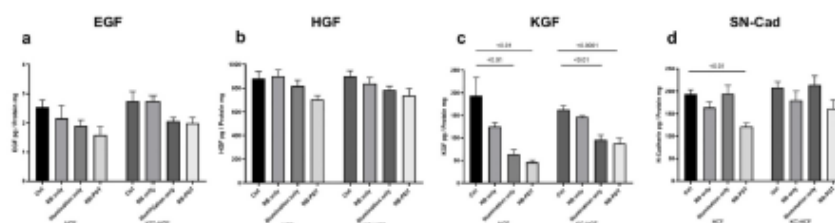

Fig 4. Epidermal growth factor (EGF), hepatocyte growth factor (HGF), keratinocyte growth factor (KGF), Soluble N-Cadherin (SN-Cad) concentration in human corneal fibroblast (HCF) and human keratoconus fibroblast (KC-HCF) cell culture supernatant 24 hours after treatment and scratching, as assessed by ELISA (n = 5). Data are expressed as mean ± SEM. 0.17 J/cm² illumination alone and 0.17 J/cm² rose bengal photodynamic therapy (RB-PDT) significantly decreased KGF concentration in both cell types, compared to controls (Ctrl) (p<0.01). In addition, 0.17 J/cm² RB-PDT, significantly decreased SN-Cad concentration in HCF cultures, compared to controls (p<0.01).

https://doi.org/10.1371/journal.pone.0296022.g004

32

treatment and scratching. FGFb and TGF-β concentrations were also not measurable in HCE-T, HCF and KC-HCF cell culture supernatant 24 hours after treatment and scratching. 0.17 J/cm^2 illumination alone and 0.17 J/cm^2 RB-PDT significantly decreased KGF concentration in HCF and KC-HCF cell culture supernatant, compared to controls (p<0.01) (Fig 4C). Nevertheless, EGF and HGF concentration, and KGF concentration in the RB only group did not differ significantly from other treatment groups 24 hours after treatment and scratching (Fig 4A–4C). Furthermore, 0.17 J/cm^2 RB-PDT, significantly decreased SN-Cad concentration in HCF cultures, compared to controls (p<0.01).

3.3 HCE-T migration rate using HCF or KC-HCF conditioned medium

HCE-T migration rate after 24 hours, using HCF or KC-HCF CM is displayed at Fig 5A and 5B.

Migration rate of untreated HCE-T cultures was significantly higher using RB-PDT treated HCF CM, than using HCF CM without RB-PDT (p<0.01) (Fig 5A. Migration rate of untreated HCE-T cultures was also significantly higher using HCF CM, than with KC-HCF CM (p<0.01). In addition, migration rate of untreated HCE-T cultures was also significantly higher using HCF CM after RB-PDT, than with KC-HCF CM after PDT (p<0.0001) (Fig 5A).

Migration rate of RB-PDT treated HCE-T cultures was significantly higher using HCF CM, than using KC-HCF CM (p = 0.03) (Fig 5B). In addition, migration rate in RB-PDT treated HCE-T cultures was significantly higher using KC-HCF CM after RB-PDT, than using KC-HCF CM without RB-PDT (p<0.01) (Fig 5B).

3.4 HCF and KC-HCF migration rate using HCE-T conditioned medium

HCF and KC-HCF migration rate after 24 and 48 hours, using HCE-T CM is displayed at Fig 5C–5F.

Migration rate was significantly higher in HCF, than in KC-HCF after 24 hours, using HCE-T CM (p<0.0001). Migration rate was also significantly higher in HCF, than in KC-HCF after 24 hours, using RB-PDT treated HCE-T CM (p<0.0001) (Fig 5C).

In RB-PDT treated KC-HCF cultures, migration rate after 24 hours was significantly higher using HCE-T CM without RB-PDT, than using HCE-T CM after PDT (p = 0.04) (Fig 5D).

Migration rate was significantly higher in HCF, than in KC-HCF, after 48 hours, using HCE-T CM (p<0.0001). Migration rate was also significantly higher in HCF, than in KC-HCF after 48 hours, using RB-PDT treated HCE-T CM (p<0.0001). In addition, in HCF cultures, migration rate after 48 hours, was significantly higher using HCE-T CM with RB-PDT, than using HCE-T CM without PDT (p<0.01) (Fig 5E).

3.5 Growth factor concentration in 48 hours conditioned medium, without scratching

Growth factor concentration in HCE-T CM (without scratching) and in HCF and KC-HCF CM (without scratching) is shown at Fig 6.

In HCE-T CM, RB only and illumination only significantly decreased EGF concentration (p<0.01; p = 0.04) (Fig 6A). RB-PDT significantly increased HGF and FGFb concentration (p = 0.02; p<0.0001) and significantly decreased TGF-β concentration (p<0.01), compared to controls (Fig 6B, 6D and 6E).

In HCF CM, RB-PDT significantly increased FGFb concentration (p<0.0001), and significantly decreased TGF-β concentration (p<0.0001) compared to controls (Fig 6I and 6J). In KC-HCF CM, RB-PDT significantly decreased EGF, HGF and TGF-β concentration (p<0.01; p = 0.03; p<0.0001) and increased FGFb concentration (p<0.01), compared to controls (Fig 6F, 6G, 6I and 6J).
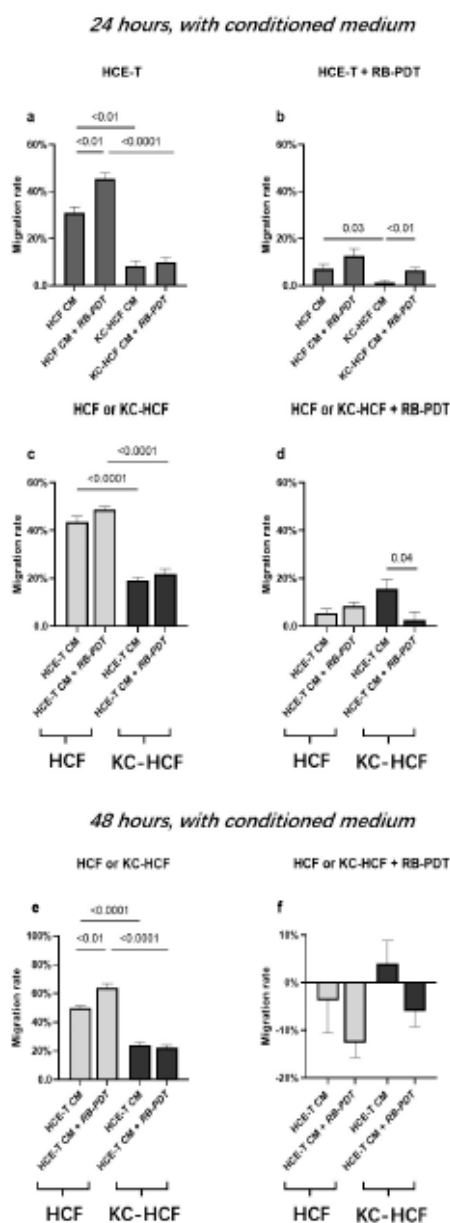
Fig 5. Migration rate in untreated and treated by rose-bengal photodynamic therapy (RB-PDT) human corneal epithelial cell (HCE-T) (n = 3), human corneal fibroblast (HCF) (n = 5) and human keratoconus fibroblast (KC-HCF) (n = 5) cell cultures after 24 and 48 hours, using conditioned medium (CM). Migration rate of untreated HCE-T cultures was significantly higher using HCF-CM after RB-PDT, than using HCF-CM without RB-PDT (p<0.01, 5a). Migration rate of untreated HCF was significantly higher using HCE-T CM after RB-PDT, than using HCE-T CM without RB-PDT (p<0.01, 5e). 48 hours after the use of CM, migration rate of RB-PDT treated HCF cultures using HCE-T CM with or without RB-PDT, and in KC-HCF cultures, using HCE-T CM after RB-PDT was in a negative range (although the wound area did not increase significantly compared to baseline) (5f). Data are expressed

as mean ± SEM. HCE-T CM: 48 hours conditioned HCE-T cell culture supernatant without or with previous rose bengal photodynamic therapy (RB-PDT), without scratch. HCF CM/KC-HCF CM: 48 hours conditioned HCF/ KC-HCF cell culture supernatant without or with previous rose bengal photodynamic therapy (RB-PDT), without scratch.

https://doi.org/10.1371/journal.pone.0296022.g005

3.6 Growth factor concentration in the supernatant of scratched cell cultures, 48 hours after addition of CM

Fig 7A–7P shows EGF, HGF and KGF concentration in HCE-T, HCF and KC-HCF culture supernatant (without or with RB-PDT of the scratched HCE-T, HCF or KC-HCF cultures), 24 or 48 hours after addition of different CM.

In the supernatant of the scratched HCE-T cultures, without RB-PDT, EGF concentration was significantly higher using HCF CM following RB-PDT, than using HCF CM without
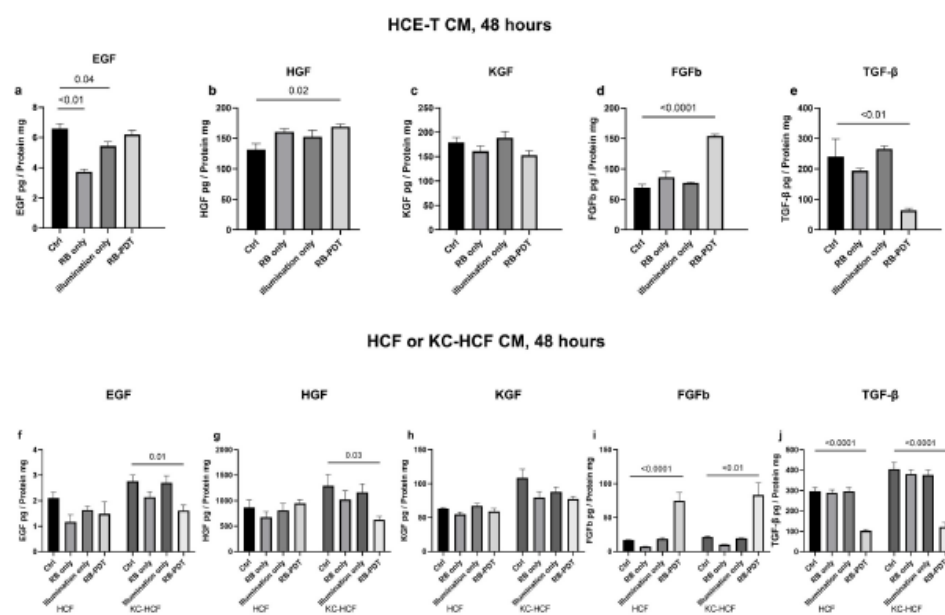

Fig 6. Growth factor concentration in 48 hours conditioned media (CM). Epidermal growth factor (EGF), hepatocyte growth factor (HGF) keratinocyte growth factor (KGF), fibroblast growth factor beta (FGFb) and transforming growth factor beta (TGF-β) concentration in human corneal epithelial cell (HCE-T) (n = 3), human corneal fibroblast (HCF) (n = 5) and human keratoconus fibroblast (KC-HCF) (n = 5) cell culture supernatant 48 hours after treatment, without scratching, were assessed by ELISA. Data are expressed as mean ± SEM. In HCE-T cell culture supernatant, 0.17 J/cm² rose bengal photodynamic therapy (RB-PDT) significantly increased HGF and FGFb concentration (p≤0.02) and significantly decreased TGF-β concentration (p<0.01), compared to controls (Ctrl). In addition, rose bengal or illumination alone also significantly decreased EGF concentration in HCE-T cell culture supernatant, compared to controls (p≤0.04). In HCF cell culture supernatant, 0.17 J/cm² RB-PDT significantly increased FGFb concentration (p<0.0001) and significantly decreased TGF-β concentration (p<0.0001), compared to controls. In KC-HCF cell culture supernatant, 0.17 J/cm² RB-PDT significantly increased FGFb concentration (p<0.01) and significantly decreased EGF, HGF and TGF-β concentration (p≤0.03), compared to controls.

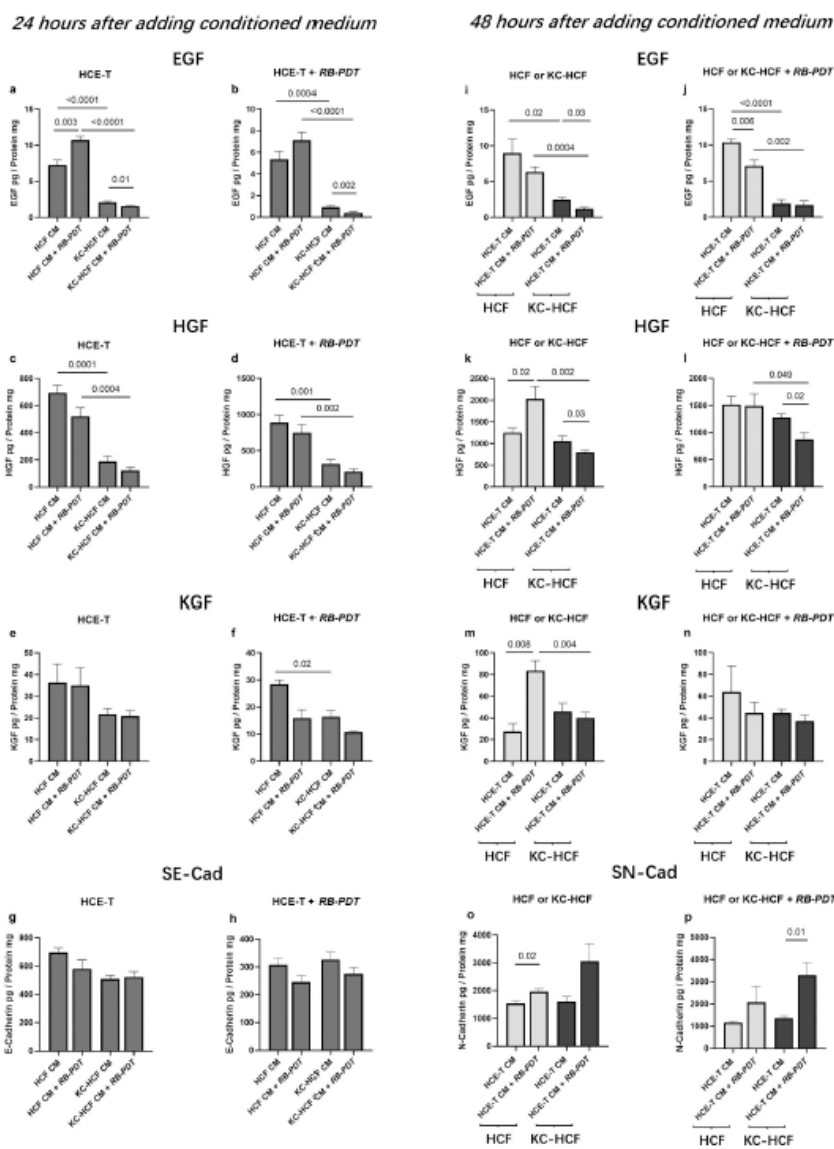https://doi.org/10.1371/journal.pone.0296022.g006

previous RB-PDT (p = 0.003) (Fig 7A). However, both in the supernatant of the scratched HCE-T cultures with or without RB-PDT, EGF concentration was significantly lower using KC-HCF CM with RB-PDT, than with KC-HCF CM without RB-PDT (p = 0.01 and p = 0.002) (Fig 7A and 7B). In addition, both in the supernatant of scratched HCE-T cultures without and with previous RB-PDT, EGF and HGF concentration was significantly lower using KC-HCF CM without RB-PDT, than using HCF CM without RB-PDT (p≤0.001) (Fig 7A–7D). Both in the supernatant of scratched HCE-T cultures without and with previous RB-PDT, EGF and HGF concentration was significantly lower using KC-HCF CM after RB-PDT, than with HCF CM after RB-PDT (p≤0.002) (Fig 7A–7D).

KGF concentration in the supernatant of the scratched HCE-T cultures after RB-PDT, was significantly lower using KC-HCF CM without RB-PDT than using HCF CM without RB-PDT (p = 0.02) (Fig 7F). Nevertheless, KGF concentration in the supernatant did not differ significantly between any of the further scratched HCE-T cultures, using different CM (Fig 7E and 7F).

The **soluble E-Cadherin** (SE-Cad) concentration remained unchanged in the supernatant of the scratched HCE-T cultures, with or without RB-PDT, following the addition of HCF and KC-HCF CM (Fig 7G and 7H).

EGF concentration was significantly lower in the supernatant of the KC-HCF cultures without RB-PDT, than in the supernatant of the HCF cultures without RB-PDT, using HCE-T CM without RB-PDT (p = 0.02) (Fig 7I). Equally, EGF concentration was significantly lower in the supernatant of the KC-HCF cultures with RB-PDT, than in the supernatant of the HCF cultures with RB-PDT, using HCE-T CM, without RB-PDT (p<0.0001) (Fig 7J). In addition, EGF and HGF concentration was significantly lower in the supernatant of the KC-HCF cultures without RB-PDT, than in the supernatant of the HCF cultures without RB-PDT, using HCE-T CM after RB-PDT (p = 0.0004 and p = 0.002) (Fig 7I and 7K). Equally, EGF and HGF concentration was significantly lower in the supernatant of the KC-HCF cultures with RB-PDT, than in the supernatant of the HCF cultures with RB-PDT, using HCE-T CM after RB-PDT (p = 0.002 and p = 0.049) (Fig 7J and 7L).

In the supernatant of the scratched KC-HCF cultures, without RB-PDT, EGF and HGF concentration was significantly lower using HCE-T CM after RB-PDT, than using HCE-T CM without RB-PDT (p = 0.03 for both) (Fig 7I and 7K). In the supernatant of the scratched HCF cultures, with RB-PDT, EGF concentration was significantly lower using HCE-T CM after RB-PDT, than using HCE-T CM without RB-PDT (p = 0.006) (Fig 7J). In the supernatant of the scratched HCF cultures, without RB-PDT, HGF concentration was significantly higher using HCE-T CM after RB-PDT, than using HCE-T CM without RB-PDT (p = 0.02) (Fig 7K). In the supernatant of the scratched KC-HCF cultures, with RB-PDT, HGF concentration was significantly lower using HCE-T CM after RB-PDT, than using HCE-T CM without RB-PDT (p = 0.02) (Fig 7L).

In the supernatant of the scratched HCF cultures, without RB-PDT, KGF concentration was significantly higher using HCE-T CM after RB-PDT, than using HCE-T CM without RB-PDT (p = 0.008) (Fig 7M). KGF concentration was significantly lower in the supernatant of the KC-HCF cultures without RB-PDT, than in the supernatant of the HCF cultures without RB-PDT, using HCE-T CM after RB-PDT (p = 0.004) (Fig 7M).

In the supernatant of the scratched HCF cultures, without RB-PDT, SN-Cad concentration was significantly higher using HCE-T CM after RB-PDT, than using HCE-T CM without

RB-PDT (p = 0.02) (Fig 7O). SN-Cad concentration was significantly higher in the supernatant of the KC-HCF cultures with RB-PDT, using HCE-T CM after RB-PDT, than using HCE-T CM without RB-PDT (p = 0.01) (Fig 7P).

4. Discussion

While RB-PDT has been used as a treatment for corneal pathologies *in vivo*, the effect of RB-PDT on human corneal epithelial cells and human corneal fibroblasts has not been analyzed in detail, yet.

In contrast to riboflavin-UVA-PDT (crosslinking), which is decreasing corneal fibroblast viability with 0.1% riboflavin concentration and 2 J/cm^2 fluence [18], a 0.001% rose bengal concentration already resulted in decreased viability in corneal fibroblasts, using 0.17 J/cm^2 fluence [3]. In a previous study, we further demonstrated that the minimum fluence during RB-PDT that decreases proliferation for HCE-T, HCF, and KC-HCF is 0.14 J/cm^2, 0.17 J/cm^2, and 0.14 J/cm^2, respectively [3]. In this current study, considering the viability data and to maintain consistency in the preparation of conditioned medium, we used 0.17 J/cm^2 fluence for RB-PDT. It is also worth noting that the results of the migration rate reflect the combined actions of migration and proliferation, both crucial for corneal wound healing [19, 20].

In this study, we observed a decrease in HCE-T, HCF, and KC-HCF migration rate 24 hours after 0.001% RB-PDT, with 0.17 J/cm^2 fluence. While there was a decreasing trend, EGF and HGF concentrations in the cell culture supernatant did not change significantly across all cell types. However, KGF concentration significantly decreased in HCF and KC-HCF supernatant, 24 hours after the RB-PDT procedure.

KGF, a well-researched growth factor predominantly produced by corneal fibroblasts, plays a crucial role in epithelial-stromal interactions by regulating the motility and proliferation of corneal epithelial cells in a paracrine manner [21, 22]. However, its impact on corneal fibroblasts is debated [21, 23–25]. Wilson et al. suggested that KGF does not stimulate corneal stromal cell proliferation [22], while another study observed a significant increase in keratocyte density with different KGF concentrations [21]. Recent research by Cai et al. showed that KGF-2 promotes cell migration in rabbit corneal fibroblasts *in vitro* [25]. The decreased KGF level (Fig 4C) after scratching and RB-PDT in corneal fibroblast cultures may partly explain the reduced migration rate of HCF and KC-HCF after treatment.

Interestingly, green light illumination alone also resulted in KGF concentration decrease in HCF and KC-HCF supernatant, after 24 hours. While previous studies have reported damage from UVA and green light to human retinal cells [26], the specific impact of green light alone on corneal cells remains unexplored. Further investigation is needed to understand the mechanisms behind the decreased KGF concentration.

During corneal wound healing, interactions between the epithelium and stroma influence cell proliferation, migration, and differentiation, with various growth factors playing a role in this process [2]. To mimic these *in vivo* interactions, we introduced conditioned medium (CM) from RB-PDT-treated stromal cells into scratched corneal epithelial cell cultures, and *vice versa*.

In HCE-T cultures, using HCF CM after RB-PDT and in HCF cultures, using HCE-T CM after RB-PDT, the migration rate was significantly higher, than using HCF CM or HCE-T CM without RB-PDT (Fig 5A and 5E). Concurrently, the EGF concentration in HCE-T cultures using HCF CM after RB-PDT, and the HGF and KGF concentrations in HCF cultures using HCE-T CM following RB-PDT, were significantly higher, than those using HCF CM or HCE-T CM without RB-PDT (Fig 7A, 7I and 7K).

EGF plays a crucial role in modulating epithelial-stromal interactions, being secreted by either epithelial cells or stromal keratocytes [27, 28]. Within 30 minutes after wounding, the

phosphorylation of EGF receptors in corneal epithelial cells has been observed [29]. Numerous reports suggest that EGF is essential for both epithelial cell proliferation and migration [24, 30]. The elevated EGF level in HCE-T cultures using HCF CM after RB-PDT may partly account for the observed differences in migration rates between groups after 24 hours (Fig 7A).

HGF, like KGF, is secreted by corneal fibroblasts, and both play an important role in facilitating the re-epithelialization process [31, 32]. In the case of an epithelial injury, epithelial cells release tumor necrosis factor-alpha (TNF-α), interleukin-1 (IL-1), and Fas ligand, which, in turn, stimulate the secretion of HGF and KGF by fibroblasts. These factors promote the proliferation and migration of corneal epithelial cells [23], potentially explaining the higher levels of HGF and KGF in HCF cultures after the use of HCE-T CM (Fig 7I and 7K). Furthermore, HGF is recognized as an anti-fibrotic factor in various organs, as it can counteract the TGF-β signaling pathway and promote the apoptosis of myofibroblasts [33].

To gain a better understanding of the composition of growth factors in the used CM, we also assessed EGF, KGF, HGF, FGFb and TGF-β levels in unscratched HCE-T CM, HCF and KC-HCF CM (Fig 6). We observed that growth factor levels in the aforementioned scratched cultures (Fig 7) did not entirely mirror the growth factor levels presented in CM, as there was no change in KGF level in unscratched HCE-T CM, nor EGF change in unscratched HCF CM (Fig 6C and 6F). Therefore, we suspect that other substances in CM may participate in the regulation of these growth factors in the scratched cell cultures, such as IL-1α [34]. It is noteworthy that in CM of all cell types, FGFb levels increased and TGF-β levels decreased following RB-PDT, compared to controls. Both are crucial factors in corneal wound repair. An increase in FGFb facilitates the activation of epithelial cells and initiates cell migration, while a decrease in TGF-β suppresses corneal cell proliferation [34, 35]. Moreover, through the regulation of cell differentiation, TGF-β influences the wound healing outcome.

The process of corneal healing following injury involves the collaborative action of various cell types, including corneal epithelial cells, stromal fibroblasts, bone marrow-derived cells, immune cells, and cytokines [36, 37]. Myofibroblasts, characterized by the presence of α-smooth muscle actin (αSMA), play a crucial role in wound contraction and the secretion of extracellular matrix (ECM) components. Prolonged presence of myofibroblasts can lead to corneal opacity, also known as "haze". Wilson and Singh described that myofibroblasts can arise, both from corneal stromal fibroblasts and bone marrow-derived cells in response to TGF-β and PDGF [38, 39]. In this process, TGF-β can promote the entire developmental process of myofibroblast precursor cells to mature myofibroblasts by facilitating the expression of vimentin and αSMA. Simultaneous presence of TGF-β and PDGF significantly enhances αSMA expression, indicating the maturation of myofibroblast precursors. The blockage of these signals prevents the generation of myofibroblasts after corneal injury [31, 40–43]. Interestingly, a study has suggested that in the presence of heparin, FGFa and FGFb can reverse TGF-β mediated myofibroblast generation, leading to a transformation of myofibroblasts into fibroblasts [44]. In the present study, elevated FGFb levels and decreased TGF-β levels were observed in all types of CM after RB-PDT treatment. This observation may imply a potential beneficial role of RB-PDT in preventing excessive myofibroblast production.

In the healthy cornea, E-Cadherin serves as an adhesive molecule among epithelial cells. Meanwhile, N-Cadherin, functioning as an adhesion molecule for mesenchymal cells, is expressed in corneal fibroblasts and myofibroblasts [45]. Both E- and N-Cadherin belong to the Type I cadherin family, named for their dependence on calcium ions (Ca^{2+}) [45]. During wound healing, Cadherin protein expression is intricately regulated due to cell migration and movement, achieving a dynamic balance [46, 47]. SE-Cad and SN-Cad have different functions compared to the full-length Cadherin. Nevertheless, in different cells types and tissues such as

in endothelial cells, keratinocytes, pulmonary fibrosis, tumor, and inflammatory diseases, both SE-Cad and SN-Cad demonstrate a promoting effect on cell migration [47–52].

In this study, SE-Cad levels in scratched HCE-T cultures did not differ between groups (Fig 7H and 7H). Interestingly, in scratched HCF cultures, without RB-PDT, addition of RB-PDT treated HCE-T CM, increased SN-Cad level of the supernatant (Fig 7O), accompanied by an enhanced migration rate. However, in scratched, RB-PDT treated KC-HCF culture, the addition of RB-PDT treated HCE-T CM also increased SN-Cad concentration (Fig 7H), but it did not coincide with an increased migration rate. This might be related to increased susceptibility of KC-HCF to oxidative stress, which might slow down migration, compared to HCF [53]. In the scratched HCF cultures without the addition of HCE-T CM, we observed decreased SN-Cad concentration after RB-PDT, compared to untreated controls (Fig 4D), which was accompanied by a decreased migration rate (Fig 3B). These findings suggest that RB-PDT influences HCF adhesion and migration behavior by modulating SN-Cad levels, consequently affecting HCF migration rate.

Interestingly, the impact of PDT on migration and growth factor secretion of corneal cells differs depending on the photosensitizer/PDT type. Twenty-four hours-conditioned HCF and KC-HCF supernatant after 0.1% riboflavin CXL increased HCE-T migration [54]. In KC-HCF cultures, 24 hours after 0.1% riboflavin CXL, HGF, KGF, FGFb and TGF-β concentration did not differ significantly from untreated controls [18]. In another study, 24 hours after 100 nM chlorin e6 PDT of normal human fibroblasts, KGF secretion significantly decreased, while HGF, FGFb and TGF-β concentrations remained unchanged in the cell culture supernatant [55].

In conclusion, the migration rate of HCE-T, HCF, and KC-HCF is reduced 24 hours after RB-PDT. However, HCE-T migration is enhanced using HCF CM 24 hours after RB-PDT, and HCF migration rate is increased through HCE-T CM 48 hours following RB-PDT. The modulation of EGF, HGF, FGFb, TGF-β, and N-Cadherin secretion through RB-PDT may play a crucial role in corneal wound healing.

Supporting information

S1 Fig. The diagram of scratches. Three reference lines were drawn at the bottom of the wells of the 6-well plates with 5 mm distance. For each well, 4 different scratch areas have been photographically documented, along the previously drawn reference line.
(TIF)

Author Contributions

Conceptualization: Zhen Li, Nóra Szentmáry.

Formal analysis: Ning Chai.

Methodology: Tanja Stachon, Nóra Szentmáry.

Project administration: Ning Chai, Nóra Szentmáry.

Resources: Achim Langenbucher.

Software: Ning Chai.

Supervision: Tanja Stachon, Nóra Szentmáry.

Writing – original draft: Ning Chai.

Writing – review & editing: Tanja Stachon, Tim Berger, Zhen Li, Berthold Seitz, Achim Langenbucher, Nóra Szentmáry.

References

1. Spoerl E, Huhle M, Seiler T. Induction of cross-links in corneal tissue. Exp Eye Res. 1998; 66: 97–103. https://doi.org/10.1006/exer.1997.0410 PMID: 9533835

2. Kowtharapu BS, Murín R, Jünemann AGM, Stachs O. Role of corneal stromal cells on epithelial cell function during wound healing. Int J Mol Sci. 2018; 19: 464. https://doi.org/10.3390/ijms19020464 PMID: 29401709

3. Chai N, Stachon T, Nastaranpour M, Li Z, Seitz B, Ulrich M, et al. Assessment of Rose Bengal Photodynamic Therapy on Viability and Proliferation of Human Keratolimbal Epithelial and Stromal Cells In Vitro. Klin Monbl Augenheilkd. 2023. https://doi.org/10.1055/a-2038-8899 PMID: 36808578

4. Germann JA, Martínez-Enríquez E, Carmen Martínez-García M, Kochevar IE, Marcos S. Corneal collagen ordering after in vivo Rose Bengal and riboflavin cross-linking. Investig Ophthalmol Vis Sci. 2020; 61: 28. https://doi.org/10.1167/iovs.61.3.28 PMID: 32186674

5. Bazak J, Korytowski W, Girotti AW. Bystander Effects of Nitric Oxide in Cellular Models of Anti-Tumor Photodynamic Therapy. Cancers (Basel). 2019; 11: 1674. https://doi.org/10.3390/cancers11111674 PMID: 31661869

6. Wang J, Stachon T, Eppig T, Langenbucher A, Seitz B, Szentmáry N. Impact of photodynamic inactivation (PDI) using the photosensitizer chlorin e6 on viability, apoptosis, and proliferation of human corneal endothelial cells. Graefe's Arch Clin Exp Ophthalmol. 2013; 251: 1199–1204. https://doi.org/10.1007/s00417-012-2239-6 PMID: 23263624

7. Berger T, Szentmáry N, Latta L, Seitz B, Stachon T. NF-κB, iNOS, IL-6, and collagen 1 and 5 expression in healthy and keratoconus corneal fibroblasts after 0.1% riboflavin UV-A illumination. Graefe's Arch Clin Exp Ophthalmol. 2021; 259: 1225–1234. https://doi.org/10.1007/s00417-020-05058-z PMID: 33443628

8. Martinez JD, Arrieta E, Naranjo A, Monsalve P, Mintz KJ, Peterson J, et al. Rose Bengal Photodynamic Antimicrobial Therapy: A Pilot Safety Study. Cornea. 2021; 40: 1036–1043. https://doi.org/10.1097/ICO.0000000000002717 PMID: 34190718

9. Gallego-Muñoz P, Ibares-Frías L, Lorenzo E, Marcos S, Perêz-Merino P, Bekesi N, et al. Corneal wound repair after rose bengal and green light crosslinking: Clinical and histologic study. Investig Ophthalmol Vis Sci. 2017; 58: 3471–3480. https://doi.org/10.1167/iovs.16-21365 PMID: 28700779

10. Dupps WJ, Wilson SE. Biomechanics and wound healing in the cornea. Exp Eye Res. 2006; 83: 709–720. https://doi.org/10.1016/j.exer.2006.03.015 PMID: 16720023

11. Said DG, Elalfy MS, Gatzioufas Z, El-Zakzouk ES, Hassan MA, Saif MY, et al. Collagen Cross-Linking with Photoactivated Riboflavin (PACK-CXL) for the Treatment of Advanced Infectious Keratitis with Corneal Melting. Ophthalmology. 2014; 121: 1377–1382. https://doi.org/10.1016/j.ophtha.2014.01.011 PMID: 24576886

12. Liu P, Chen H, Yan L, Sun Y. Laminin α5 modulates fibroblast proliferation in epidural fibrosis through the PI3K/AKT/mTOR signaling pathway. Mol Med Rep. 2020; 21: 1491–1500. https://doi.org/10.3892/mmr.2020.10967 PMID: 32016453

13. Angelo L, Gokul Boptom A, McGhee C, Ziaei M. Corneal Crosslinking: Present and Future. Asia-Pacific J Ophthalmol. 2022; 11: 441–452. https://doi.org/10.1097/APO.0000000000000557 PMID: 36094381

14. Cherfan D, Verter EE, Melki S, Gisel TE, Doyle FJ, Scarcelli G, et al. Collagen cross-linking using rose bengal and green light to increase corneal stiffness. Investig Ophthalmol Vis Sci. 2013; 54: 3426–3433. https://doi.org/10.1167/iovs.12-11509 PMID: 23599326

15. Sepulveda-Beltran PA, Levine H, Altamirano DS, Martinez JD, Durkee H, Mintz K, et al. Rose Bengal Photodynamic Antimicrobial Therapy: A Review of the Intermediate-Term Clinical and Surgical Outcomes. Am J Ophthalmol. 2022; 243: 125–134. https://doi.org/10.1016/j.ajo.2022.08.004 PMID: 35952754

16. Lorenzo-Martín E, Gallego-Muñoz P, Ibares-Frías L, Marcos S, Pérez-Merino P, Fernández I, et al. Rose bengal and green light versus riboflavin–UVA cross-linking: Corneal wound repair response. Investig Ophthalmol Vis Sci. 2018; 59: 4821–4830. https://doi.org/10.1167/iovs.18-24881 PMID: 30347076

17. Gao R, Yan M, Chen M, Hayes S, Meek KM, He H, et al. The Impact of Different Rose Bengal Formulations on Corneal Thickness and the Efficacy of Rose Bengal/Green Light Corneal Cross-linking in the Rabbit Eye. J Refract Surg. 2022; 38: 450–458. https://doi.org/10.3928/1081597X-20220601-03 PMID: 35858194

18. Song X, Stachon T, Wang J, Langenbucher A, Seitz B, Szentmáry N. Viability, apoptosis, proliferation, activation, and cytokine secretion of human keratoconus keratocytes after cross-linking. Biomed Res Int. 2015;2015. https://doi.org/10.1155/2015/254237 PMID: 25699261

19. Wilson SE. Corneal wound healing. Exp Eye Res. 2020; 197: 1–21. https://doi.org/10.1016/j.exer.2020.108089 PMID: 32553485

20. Ljubimov A V, Saghizadeh M. Progress in corneal wound healing. Prog Retin Eye Res. 2015; 49: 17–45. https://doi.org/10.1016/j.preteyeres.2015.07.002 PMID: 26197361

21. Carrington LM, Boulton M. Hepatocyte growth factor and keratinocyte growth factor regulation of epithelial and stromal corneal wound healing. J Cataract Refract Surg. 2005; 31: 412–423. https://doi.org/10.1016/j.jcrs.2004.04.072 PMID: 15767167

22. Wilson SE, He Y-G, Weng J, Zieske JD, Jester J V., Schultz GS. Effect of Epidermal Growth Factor, Hepatocyte Growth Factor, and Keratinocyte Growth Factor, on Proliferation, Motility and Differentiation of Human Corneal Epithelial Cells. Exp Eye Res. 1994; 59: 665–678. https://doi.org/10.1006/exer.1994.1152 PMID: 7698260

23. Wilson SE, Liu JJ, Mohan RR. Stromal-epithelial interactions in the cornea. Prog Retin Eye Res. 1999; 18: 293–309. https://doi.org/10.1016/s1350-9462(98)00017-2 PMID: 10192515

24. Imanishi J, Kamiyama K, Iguchi I, Kita M, Sotozono C, Kinoshita S. Growth factors: Importance in wound healing and maintenance of transparency of the cornea. Prog Retin Eye Res. 2000; 19: 113–129. https://doi.org/10.1016/s1350-9462(99)00007-5 PMID: 10614683

25. Cai JQ, Zhou Q, Wang Z, Guo R, Yang R, Yang X, et al. Comparative Analysis of KGF-2 and bFGF in Prevention of Excessive Wound Healing and Scar Formation in a Corneal Alkali Burn Model. Cornea. 2019; 38: 1430–1437. https://doi.org/10.1097/ICO.0000000000002134 PMID: 31490279

26. Rapp LM, Tolman BL, Dhindsa HS. Separate mechanisms for retinal damage by ultraviolet-A and mid-visible light. Investig Ophthalmol Vis Sci. 1990; 31: 1186–1190. PMID: 2354921

27. Wilson SE, Lloyd SA, He YG. EGF, basic FGF, and TGF beta-1 messenger RNA production in rabbit corneal epithelial cells. Investig Ophthalmol Vis Sci. 1992; 33: 1987–1995. PMID: 1582803

28. Jiang Y, Ju Z, Zhang J, Liu X, Tian J, Mu G. Effects of insulin-like growth factor 2 and its receptor expressions on corneal repair. Int J Clin Exp Pathol. 2015; 8: 10185–10191. PMID: 26617727

29. Zieske JD, Takahashi H, Hutcheon AE, Dalbone AC. Activation of epidermal growth factor receptor during corneal epithelial migration. Invest Ophthalmol Vis Sci. 2000; 41: 1346–1355. PMID: 10798649

30. Wilson SE, Lloyd SA. Epidermal growth factor and its receptor, basic fibroblast growth factor, transforming growth factor beta-1, and interleukin-1 alpha messenger RNA production in human corneal endothelial cells. Investig Ophthalmol Vis Sci. 1991; 32: 2747–2756. PMID: 1716619

31. Bukowiecki A, Hos D, Cursiefen C, Eming SA. Wound-healing studies in cornea and skin: Parallels, differences and opportunities. Int J Mol Sci. 2017; 18: 1–24. https://doi.org/10.3390/ijms18061257 PMID: 28604651

32. Sagaradze G, Grigorieva O, Nimiritsky P, Basalova N, Kalinina N, Akopyan Z, et al. Conditioned medium from human mesenchymal stromal cells: Towards the clinical translation. Int J Mol Sci. 2019; 20: 1–16. https://doi.org/10.3390/ijms20071656 PMID: 30987106

33. Miyagi H, Thomasy SM, Russell P, Murphy CJ. The role of hepatocyte growth factor in corneal wound healing. Exp Eye Res. 2018; 166: 49–55. https://doi.org/10.1016/j.exer.2017.10.006 PMID: 29024692

34. Zelenka PS, Arpitha P. Coordinating cell proliferation and migration in the lens and cornea. Semin Cell Dev Biol. 2008; 19: 113–124. https://doi.org/10.1016/j.semcdb.2007.10.001 PMID: 18035561

35. Gallego-Muñoz P, Ibares-Frías L, Garrote JA, Valsero-Blanco MC, Cantalapiedra-Rodríguez R, Merayo-Lloves J, et al. Human corneal fibroblast migration and extracellular matrix synthesis during stromal repair: Role played by platelet-derived growth factor-BB, basic fibroblast growth factor, and transforming growth factor-β1. J Tissue Eng Regen Med. 2018; 12: e737–e746. https://doi.org/10.1002/term.2360 PMID: 27860426

36. Verrecchia F. TGF-beta and TNF-alpha: antagonistic cytokines controlling type I collagen gene expression. Cell Signal. 2004; 16: 873–880. https://doi.org/10.1016/j.cellsig.2004.02.007 PMID: 15157666

37. Wilson SE. Corneal myofibroblasts and fibrosis. Exp Eye Res. 2020; 201: 108272. https://doi.org/10.1016/j.exer.2020.108272 PMID: 33010289

38. Singh V, Jaini R, Torricelli AAM, Santhiago MR, Singh N, Ambati BK, et al. TGFβ and PDGF-B signaling blockade inhibits myofibroblast development from both bone marrow-derived and keratocyte-derived precursor cells in vivo. Exp Eye Res. 2014; 121: 35–40. https://doi.org/10.1016/j.exer.2014.02.013 PMID: 24582892

39. Singh V, Agrawal V, Santhiago MR, Wilson SE. Stromal fibroblast-bone marrow-derived cell interactions: Implications for myofibroblast development in the cornea. Exp Eye Res. 2012; 98: 1–8. https://doi.org/10.1016/j.exer.2012.03.006 PMID: 22465408

40. Singh V, Santhiago MR, Barbosa FL, Agrawal V, Singh N, Ambati BK, et al. Effect of TGFβ and PDGF-B blockade on corneal myofibroblast development in mice. Exp Eye Res. 2011; 93: 810–817. https://doi.org/10.1016/j.exer.2011.09.012 PMID: 21978952

41. Singh V, Barbosa FL, Torricelli AAM, Santhiago MR, Wilson SE. Transforming growth factor β and platelet-derived growth factor modulation of myofibroblast development from corneal fibroblasts in vitro. Exp Eye Res. 2014; 120: 152–160. https://doi.org/10.1016/j.exer.2014.01.003 PMID: 24429028

42. Wilson SE. Bowman's layer in the cornea–structure and function and regeneration. Exp Eye Res. 2020; 195: 108033. https://doi.org/10.1016/j.exer.2020.108033 PMID: 32339517

43. Torricelli AAM, Singh V, Santhiago MR, Wilson SE. The corneal epithelial basement membrane: Structure, function, and disease. Investig Ophthalmol Vis Sci. 2013; 54: 6390–6400. https://doi.org/10.1167/iovs.13-12547 PMID: 24078382

44. Maltseva O, Folger P, Zekaria D, Petridou S, Masur SK. Fibroblast growth factor reversal of the corneal myofibroblast phenotype. Investig Ophthalmol Vis Sci. 2001; 42: 2490–2495. PMID: 11581188

45. Van Aken E, Papeleu P, De Potter P, De Laey JJ, Mareel M. Cadherin expression in the eye. Bull Soc Belge Ophtalmol. 2000; 55–59. PMID: 11761562

46. Brouxhon SM, Kyrkanides S, Teng X, Athar M, Ghazizadeh S, Simon M, et al. Soluble E-cadherin: a critical oncogene modulating receptor tyrosine kinases, MAPK and PI3K/Akt/mTOR signaling. Oncogene. 2014; 33: 225–235. https://doi.org/10.1038/onc.2012.563 PMID: 23318419

47. Derycke L, Morbidelli L, Ziche M, De Wever O, Bracke M, Van Aken E. Soluble N-cadherin fragment promotes angiogenesis. Clin Exp Metastasis. 2006; 23: 187–201. https://doi.org/10.1007/s10585-006-9029-7 PMID: 17028923

48. Tang MKS, Yue PYK, Ip PP, Huang RL, Lai HC, Cheung ANY, et al. Soluble E-cadherin promotes tumor angiogenesis and localizes to exosome surface. Nat Commun. 2018; 9: 1–15. https://doi.org/10.1038/s41467-018-04695-7 PMID: 29891938

49. Deng X, Chen C, Wu F, Qiu L, Ke Q, Sun R, et al. Curcumin Inhibits the Migration and Invasion of Non-Small-Cell Lung Cancer Cells Through Radiation-Induced Suppression of Epithelial-Mesenchymal Transition and Soluble E-Cadherin Expression. Technol Cancer Res Treat. 2020; 19: 1–11. https://doi.org/10.1177/1533033820947485 PMID: 33124505

50. Maretzky T, Reiss K, Ludwig A, Buchholz J, Scholz F, Proksch E, et al. ADAM10 mediates E-cadherin shedding and regulates epithelial cell-cell adhesion, migration, and β-catenin translocation. Proc Natl Acad Sci U S A. 2005; 102: 9182–9187. https://doi.org/10.1073/pnas.0500918102 PMID: 15958533

51. Huang C, Zhong L, Deng J, Chen J. Soluble E-cadherin participates in BLM-induced pulmonary fibrosis by promoting EMT and lung fibroblast migration. 2023; 1–9. https://doi.org/10.1002/tox.23986 PMID: 37792543

52. Bzioueche H, Boniface K, Drullion C, Marchetti S, Chignon-Sicard B, Sormani L, et al. Impact of house dust mite in vitiligo skin: environmental contribution to increased cutaneous immunity and melanocyte detachment. Br J Dermatol. 2023; 189: 312–327. https://doi.org/10.1093/bjd/ljad148 PMID: 37140010

53. Stachon T, Latta L, Seitz B, Szentmáry N. Hypoxic stress increases NF-κB and iNOS mRNA expression in normal, but not in keratoconus corneal fibroblasts. Graefe's Arch Clin Exp Ophthalmol. 2021; 259: 449–458. https://doi.org/10.1007/s00417-020-04900-8 PMID: 32886165

54. Wu MF, Stachon T, Wang J, Song X, Colanesi S, Seitz B, et al. Effect of Keratocyte Supernatant on Epithelial Cell Migration and Proliferation After Corneal Crosslinking (CXL). Curr Eye Res. 2016; 41: 466–473. https://doi.org/10.3109/02713683.2015.1050739 PMID: 26236938

55. Stachon T, Wang J, Eppig T, Langenbucher A, Bischoff M, Seitz B, et al. KGF, FGFb, VEGF, HGF and TGFβ1 secretion of human keratocytes following photodynamic inactivation (PDI) in vitro. Graefe's Arch Clin Exp Ophthalmol. 2013; 251: 1987–1993. https://doi.org/10.1007/s00417-013-2370-z PMID: 23652468

6. Publication 3

Taylor & Francis
Taylor & Francis Group

Check for updates

Short-Term Effect of Rose Bengal Photodynamic Therapy (RB-PDT) on Collagen I, Collagen V, NF-κB, LOX, TGF-β and IL-6 Expression of Human Corneal Fibroblasts, *In Vitro*

Ning Chai[a] , Tanja Stachon[a] , Tim Berger[b], Zhen Li[a], Berthold Seitz[b], Achim Langenbucher[c] , and Nóra Szentmáry[a,d]

[a]Dr. Rolf M. Schwiete Center for Limbal Stem Cell and Aniridia Research, Saarland University, Homburg, Saar, Germany; [b]Department of Ophthalmology, Saarland University Medical Center, Homburg, Saar, Germany; [c]Experimental Ophthalmology, Saarland University, Homburg, Saar, Germany; [d]Department of Ophthalmology, Semmelweis University, Budapest, Hungary

ABSTRACT

Purpose: To investigate collagen I, collagen V, nuclear factor kappa-light-chain-enhancer of activated B cells (NF-κB), lysyl oxidase (LOX), transforming growth factor $\beta1$ (TGF-$\beta1$) and interleukin-6 (IL-6) expression in healthy and keratoconus human corneal fibroblasts (HCFs and KC-HCFs), 24 h after Rose Bengal photodynamic therapy (RB-PDT).

Methods: HCFs were isolated from healthy human corneal donors ($n = 5$) and KC-HCFs from elective penetrating keratoplasties ($n = 5$). Both cell cultures underwent RB-PDT (0.001% RB concentration, 0.17 J/cm^2 fluence) and 24 h later collagen I, collagen V, NF-κB, LOX, TGF-$\beta1$ and IL-6 mRNA and protein expression have been determined using qPCR and Western blot, IL-6 concentration in the cell culture supernatant by ELISA.

Results: TGF-$\beta1$ mRNA expression was significantly lower ($p = 0.02$) and IL-6 mRNA expression was significantly higher in RB-PDT treated HCFs ($p = 0.01$), than in HCF controls. COL1A1, COL5A1 and TGF-$\beta1$ mRNA expression was significantly lower ($p = 0.04$; $p = 0.02$ and $p = 0.003$) and IL-6 mRNA expression was significantly higher ($p = 0.02$) in treated KC-HCFs, than in KC-HCF controls. TGF-$\beta1$ protein expression in treated HCFs was significantly higher than in HCF controls ($p = 0.04$). IL-6 protein concentration in the HCF and KC-HCF culture supernatant after RB-PDT was significantly higher than in controls ($p = 0.02$; $p = 0.01$). No other analyzed mRNA and protein expression differed significantly between the RB-PDT treated and untreated groups.

Conclusions: Our study demonstrates that RB-PDT reduces collagen I, collagen V and TGF-$\beta1$ mRNA expression, while increasing IL-6 mRNA and protein expression in KC-HCFs. In HCFs, RB-PDT increases TGF-$\beta1$ and IL-6 protein level after 24 h.

Introduction

In the last decades, photodynamic therapy (PDT) has been used more and more frequently in the clinical practice. PDT is used as antimicrobial or antitumor therapy, or as crosslinking procedure.[1–3] In ophthalmology, Rose Bengal PDT (RB-PDT) has been used as an alternative of riboflavin–UVA PDT of the cornea.[4–6] In RB-PDT, the used photosensitizer is Rose Bengal (RB), which is activated by green light (wavelength: 500–600 nm). During corneal RB-PDT, as a first step, the epithelium is removed and the Rose Bengal penetrates into the corneal stroma, before green light illumination.[6,7] The result of RB-PDT, similar to other photodynamic treatments is the formation of the biologically active singlet oxygen ($^1O_2$) and formation of covalent bonds between collagen molecules in a non-enzymatic manner.[8] In the corneal stroma, fibroblasts are responsible for maintenance of the stromal homeostasis, through secretion of extracellular matrix (ECM) components, collagens and cytokines, as response to external stimuli.[9,10]

In ophthalmology, literature data are mainly focusing on crosslinking (in ectatic corneal diseases) and antibacterial effect of RB-PDT.[3,11–13]

To maintain a healthy corneal shape and the corneal biomechanical properties, the production of collagen in the corneal stroma (mainly type I and type V collagen) is the first step.[14] The covalent bonding between collagen fibers is important for corneal stiffness and for avoiding the progression of corneal ectasia. These self-generated connections are primarily catalyzed by the enzyme lysyl oxidase (LOX).[15] Transforming growth factor β (TGF-β) regulates the expression of multiple components of the extracellular matrix (ECM). TGF-β levels have been closely linked to fibroblast differentiation into myofibroblasts, characterized by increased expression of α-smooth muscle actin (α-SMA) along with a concurrent decrease in CD34 levels.[16–18]

CONTACT Ning Chai ning.chai@uks.eu Dr. Rolf M. Schwiete Center for Limbal Stem Cell and Congenital Aniridia Research, Saarland University, Kirrberger Str. 100, Homburg, Saar, 66424, Germany.

In case of bacterial keratitis, activation and production of nuclear factor kappa-light-chain-enhancer of activated B cells (NF-κB) and interleukin 6 (IL-6) is essential during corneal inflammatory response against pathogenic microorganism.[19,20]

However, a comprehensive analysis of the impact of RB-PDT on mRNA and protein expression in human corneal fibroblasts has not been conducted, yet.

In the present study, our purpose was to determine collagen I, collagen V, NF-κB p65, LOX, TGF-β1, IL-6, α-SMA and CD34 expression in healthy human corneal fibroblasts (HCFs) and keratoconus fibroblasts (KC-HCFs), 24h after RB-PDT.

Materials and methods

This study was approved by the Ethics Committee of Saarland/Germany (Nr. 217/18). All procedures were performed adhering to the Declaration of Helsinki, an informed consents were obtained from all participants.

Cell isolation and cell culture

Five healthy human corneal buttons (83.2 ± 3.1 (79–86) years; 60% males) were kindly provided by the Klaus Faber Center for Corneal Diseases, including Lions Eye Bank Saar-Lor-Lux, Trier/Westpfalz, in Homburg. Five human keratoconus corneal buttons (48.8 ± 18 (29–72) years; 60% males) were kindly provided by the Department of Ophthalmology of Saarland University Medicinal Center, from elective penetrating keratoplasties.

To isolate keratocytes, healthy and keratoconus corneal buttons were gently rinsed by PBS (Merck, Sigma-Aldrich, Taufkirchen, Germany), then these were cut into 5 mm pieces using a surgical blade. Thereafter, tissue pieces were incubated in a solution containing 1.0 mg/ml collagenase A (Hoffmann-La Roche, Basel, Switzerland) and Dulbecco's modified Eagle's medium (DMEM/F12, Thermo Fisher Scientific, Waltham, MA, USA), which was supplemented by 5% fetal calf serum (FCS, Thermo Fisher Scientific, Waltham, MA, USA), and 1% penicillin–streptomycin (P/S, Sigma-Aldrich, St. Louis, USA) overnight at 37°C. Thereafter, centrifugation has been performed at 1500 rpm for 5 min, and the supernatant was discarded. The cell sediment was seeded into a T75 flask, containing 13 ml of DMEM/F12 with 5% FCS, and 1% P/S (basic medium in the subsequent text). Using FCS containing culture medium, keratocytes differentiated into corneal fibroblasts (as described previously[21–23]) reaching 80% confluence, these cells were passaged into T75 flasks for further experiments.

RB-PDT

RB-PDT has been performed, when cells reached approximately 80% confluence in the T75 flasks. The RB stock powder (C.I. 45440, Carl Roth, Karlsruhe, Germany) was stored in a light-proved bottle until it was dissolved in basic medium at 0.001% concentration (m/v). After a clear solution was obtained, the RB solution was sterilized using a $0.2\,\mu m$ filter, and was stored at 4°C in darkness up to one month.

The illumination box was kindly provided by the Experimental Ophthalmology of Saarland University, Homburg/Saar, Germany. Within the box, cell cultures underwent green-light illumination (wavelength: 565 nm) for 600 s, with $0.17\,J/cm^2$ fluence (LED power: $0.283\,mW/cm^2$). This was the lowest fluence value affecting corneal fibroblast viability, according to our previous experiments.[24]

To perform RB-PDT, the cell culture supernatant was first removed from the T75 flask. Next, 10 ml RB solution was added to the flask, which was then placed in a 37°C incubator for 30 min. After that, the RB solution was removed and the cells were gently rinsed twice with 10 ml PBS. Finally, another 10 ml PBS was added to the flask before proceeding with the illumination step.

Within the control group, cells were gently rinsed with 10 ml PBS three times, without the use of RB or green light illumination.

Following RB-PDT or cell rinsing with PBS within the control group, 13 ml serum free culture medium (SFCM) consisting of DMEM/F12, 1% insulin, transferrin, and selenium (ITS, cat. no. I1884, Sigma-Aldrich, St. Louis, USA) and 1% P/S have been used. Cell culture flasks were stored at 37°C for 24h and thereafter, the cells were harvested using trypsin EDTA (Sigma-Aldrich, St. Louis, USA). At the same time, the supernatant of the cells was collected after a centrifugation step (5000 rpm, 4 min) to remove cell debris. The resulting cell pellet and the supernatant were stored at −80°C before further use.

RNA isolation and cDNA synthesis

RNA isolation has been performed using the RNeasy Plus Mini Kit (cat. no. 74134, QIAGEN, N.V., Venlo, Netherlands), following the manufacturer's protocol. After gDNA removal, total RNA concentration has been determined by a spectrophotometer (Scandrop, Analytik Jena AG, Jena, Germany). Afterwards, One *Taq*® RT-PCR Kit (E5310S, New England Biolabs INC, Frankfurt, Germany) has been used for the reverse transcription process. Thereafter, the cDNA has been stored at −20°C before further measurements.

Quantitative PCR

To detect Collagen 1 (COL1A1), Collagen 5 (COL5A1), NF-κB p65, LOX, TGF-β1 and IL-6 mRNA expression in corneal fibroblasts following RB-PDT, quantitative PCR (qPCR) using the QuantStudio 5 Real-Time PCR System (Thermo Fisher Scientific, Waltham, MA, USA) has been performed. The used primers are listed in Table 1. qPCR has been performed in duplicate using an AceQ SYBR qPCR Master Mix (Vazyme Biotech, Nanjing, China) and $1\,\mu l$ cDNA, following the amplification protocol: 95°C for 10 s, 60°C for 30 s, and 95°C for 15 s (in total 40 cycles). We analyzed the relative expression of genes using the $2^{-\Delta\Delta Ct}$ method, with Tata-

binding protein (TBP) and glyceraldehyde 3-phosphate dehydrogenase (GAPDH) as endogenous controls (using the mean Ct values of two reference genes).

Western blot

As previously described,[25] the collected cell pellet has been lysed using RIPA buffer (R0278, Sigma-Aldrich, St. Louis, USA), and the protein concentration has then been quantified by Pierce™ BCA Protein Assay Kit (cat. no. 23227, Thermo Fisher Scientific, Waltham, MA, USA). The samples were then stored at –20 °C until further use. Before electrophoresis, 15 µg total protein from each sample was boiled at 95 °C for 5 min with loading buffer (Cat. #1610747 Bio-Rad Laboratories, Hercules, USA), and thereafter was loaded to a precast 4–12% NuPage™ Bis–Tris SDS Gel (NP0321BOX, Invitrogen, Waltham, MA, USA). The first lane of the gel was loaded with 5 µl Precision Plus Protein™ Dual Color Standard (1610374EDU, Bio-Rad Laboratories, Hercules, USA) as a marker to indicate the molecular weight of the protein. The proteins were then separated on the gel and blotted on to 0.2 µm nitrocellulose membrane (Cat. #1704158, Bio-Rad Laboratories, Hercules, USA) using the Trans-Blot Turbo Transfer System (Bio-Rad). The membranes were then rinsed three times with 5 ml Western Froxx washing solution (5570ML500, neoFroxx GmbH, Einhausen, Germany) for 5 min, which was followed by incubation with primary antibody at 4 °C. The used antibodies are listed in Table 2. Then, the Western Lightning Plus Chemiluminescence Reagent (NEL103001EA, Perkin Elmer Inc., Waltham, MA, USA) has been used and the signals were captured by the iBright™ FL1500 Imaging System (Invitrogen, Waltham, MA, USA). Protein band intensities were analyzed using the iBright™ Analysis Software 5.0 (Invitrogen Waltham, MA, USA). Finally, the membrane stripping was performed using the Western Froxx stripping solution (1621ML500, neoFroxx GmbH, Einhausen, Germany). Endogenous β-actin was used as reference protein for the normalization process.

Table 1. Primers used for qPCR.

Targeted cDNA	Gene symbol	Qiagen Cat. no.	Amplicon size bp
Collagen 1	COL1A1	QT00037793	118
Collagen 5	COL5A1	QT00044527	105
NF-κB p65	RELA	QT02324308	136
Lysyl oxidase	LOX	QT00017311	68
TGF-β1	TGFB1	QT00000728	108
α-SMA	ACTA2	QT00088102	83
CD34	CD34	QT00056497	106
TATA box binding protein	TBP	QT00000721	132
GUSBP	GUSBP1	QT00085204	104

Enzyme-linked immunosorbent assay

Enzyme-linked immunosorbent assay (ELISA) has been performed to determine IL-6 concentration in the cell culture supernatant. IL-6 DuoSet® ELISA kit (DY206-05) was purchased from R&D Systems (Minneapolis, USA) and measurements have been performed in duplicate according to the manufacturer's protocol. In brief, 100 µl IL-6 capture antibody has been added to 96-well plates, which were incubated overnight at room temperature. After the rinsing and blocking steps, 100 µl cell culture supernatant was added to each well for 2 h, which was followed by the use of the detection antibody for another 2 h. After rinsing, the wells were incubated with 100 µl streptavidin, conjugated to horseradish–peroxidase solution for 20 min, and following addition of the stop solution to the substrate solution, the quantitative IL-6 concentration value has been measured by a Tecan Infinite F50 Absorbance Microplate Reader (Tecan Group AG, Männedorf, Switzerland). The measured IL-6 concentration value has been divided by the corresponding total protein concentration value, and this calculated quotient (IL-6 pg/protein mg) has been used for statistical analysis.

Statistical analysis

The statistical analysis has been performed using GraphPad Prism 9.2 software (GraphPad Software, San Diego, CA). Data are presented as mean ± standard deviation (SD), a paired Student's t test has been used. p values below 0.05 were considered statistically significant.

Results

Collagen I, collagen V, NF-κB p65, LOX, TGF-β1 and IL-6 mRNA expression in HCFs ($n = 5$) and KC-HCFs ($n = 5$) 24 h after 0.17 J/cm^2 RB-PDT is displayed at Figure 1.

TGF-β1 mRNA expression was significantly lower ($p = 0.02$) and IL-6 mRNA expression was significantly higher in HCFs 24 h after RB-PDT ($p = 0.01$), than in HCFs without RB-PDT (e, f). COL1A1, COL5A1, TGF-β1 mRNA expression was significantly lower ($p = 0.04$; $p = 0.02$ and $p = 0.003$) and IL-6 mRNA expression was significantly higher ($p = 0.02$) in KC-HCFs 24 h after RB-PDT, than in KC-HCFs without RB-PDT. NF-κB p65 and LOX mRNA expression did not differ significantly between any of the RB-PDT treated and untreated groups (Figure 1). α-SMA and CD34 mRNA had a very low expression level both in HCFs and KC-HCFs, without and with RB-PDT, compared to the reference genes) (CT values above 30 in all cases).

Table 2. Antibodies used for Western blot.

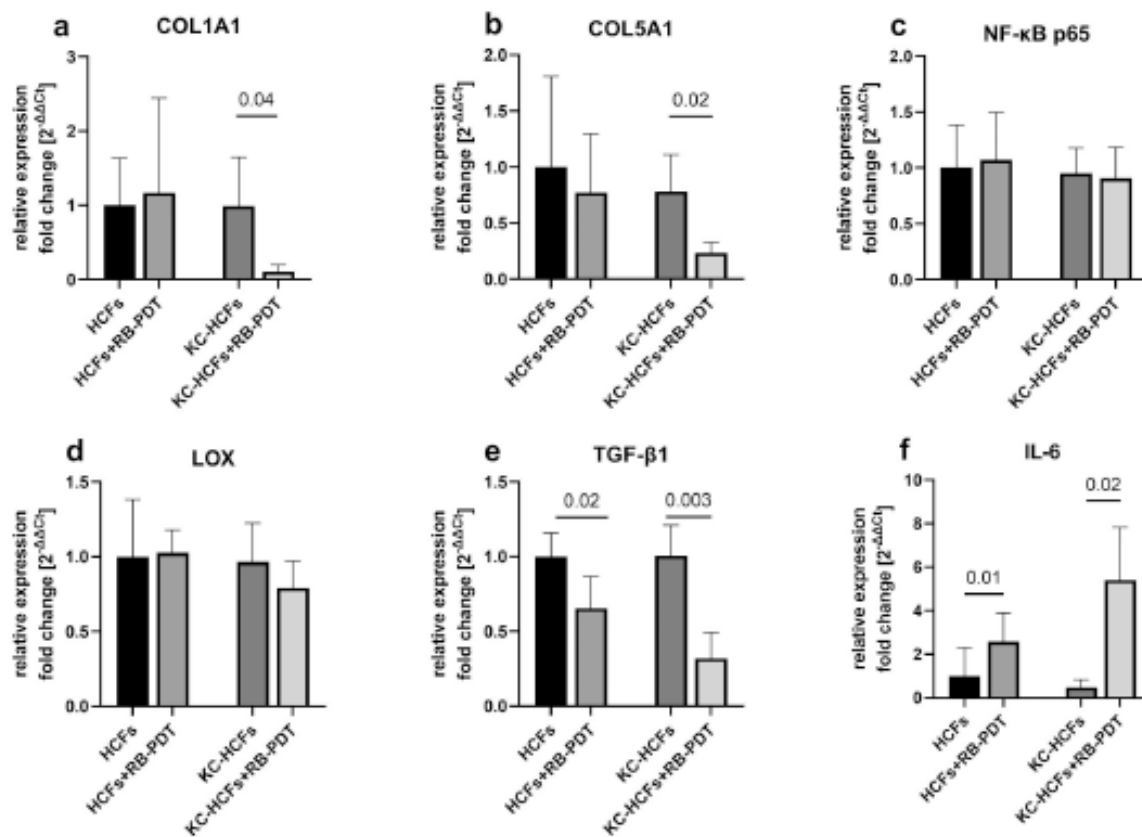| Antibody	Cat. no.	Manufacturer	Dilution	Incubation time (4 °C)
COL1A1	E6A8E	Cell Signaling Technology, MA, USA	1:1000	Overnight
COL5A1	ab7046	Abcam, Cambridge, UK	1:1000	Overnight
NF-κB p65	D14E12	Cell Signaling Technology, MA, USA	1:1000	Overnight
LOX	D8F2K	Cell Signaling Technology, MA, USA	1:1000	Overnight
TGFβ1	ab179695	Abcam, Cambridge, UK	1:2500	Overnight
β-actin	ab8227	Abcam, Cambridge, UK	1:5000	1 hour

Figure 1. Collagen I, collagen V, NF-κB p65, LOX, TGF-β1, IL-6 mRNA expression in human corneal fibroblasts (HCFs; $n = 5$) and human keratoconus fibroblasts (KC-HCFs; $n = 5$) 24 h after 0.17 J/cm² Rose Bengal photodynamic therapy (RB-PDT) (a–h). Measurements have been performed in duplicate. Data are shown as mean ± standard deviation. Paired t tests have been performed, and p values below 0.05 were considered statistically significant. TGF-β1 mRNA expression was significantly lower ($p = 0.02$) and IL-6 mRNA expression was significantly higher ($p = 0.01$) in HCFs 24 h after RB-PDT, than in HCFs without RB-PDT (e, f). COL1A1, COL5A1, TGF-β1 mRNA expression significantly lower ($p = 0.04$; $p = 0.02$ and $p = 0.003$) and IL-6 mRNA expression was significantly higher ($p = 0.02$) in KC-HCFs 24 h after RB-PDT, than in KC-HCFs without RB-PDT (a, b, e, f). LOX and NF-κB p65 mRNA expression did not differ significantly between any of the groups after RB-PDT (c, d).

Collagen I, collagen V, NF-κB p65, LOX, and TGF-β1 protein expression in HCFs ($n = 5$) and KC-HCFs ($n = 5$) and IL-6 protein expression in their cell culture supernatant 24 h after 0.17 J/cm² RB-PDT is displayed at Figure 2.

TGF-β1 protein expression in HCFs was significantly higher 24 h after RB-PDT, than without RB-PDT ($p = 0.04$) (e). IL-6 protein concentration in the HCF and KC-HCF culture supernatant was significantly higher 24 h after RB-PDT, than without RB-PDT ($p = 0.02$; $p = 0.01$) (f). Nevertheless, collagen I, collagen V, NF-κB p65 and LOX protein expression did not differ significantly between any of the RB-PDT treated and untreated groups (Figure 2).

Results are summarized at Table 3.

Discussion

In the past decade, RB-PDT has emerged as a novel therapeutic approach for crosslinking and antimicrobial therapy in corneal diseases.[23] Our aim was to investigate the impact of RB-PDT on several crucial proteins associated with these clinical applications. While some studies have examined the effects of RB-PDT on corneal tissue in animal models,[6,26]

there is limited information available regarding its influence on corneal stromal cells.

The corneal stroma accounts for 80–90% of the corneal thickness and is essential for maintaining corneal transparency.[27] Keratocytes within the corneal stroma primarily produce collagens and proteoglycans, which play a pivotal role in corneal architecture, biomechanics, and wound healing.[28] When activated by external stimuli such as an epithelial defect or inflammation, keratocytes can transform into myofibroblasts and fibroblasts, which are more active in collagen synthesis and cytokine secretion, thereby facilitating the healing process.[29] Specifically, collagen I is a major component of stromal fibrils, while collagen V acts as a regulatory collagen that assembles with collagen I to form properly sized fibrils.[30] In the corneal stroma, collagen fibrils have a smaller diameter ($\sim$25 nm) due to the regulation of collagen V.[31] Collagen V deficient mice exhibit abnormally large stromal fibrils, resulting in disordered fibril structure and ultimately the loss of corneal transparency.[32] Therefore, healthy secretion and organization of collagens are crucial for maintaining corneal transparency, particularly in pathological conditions.
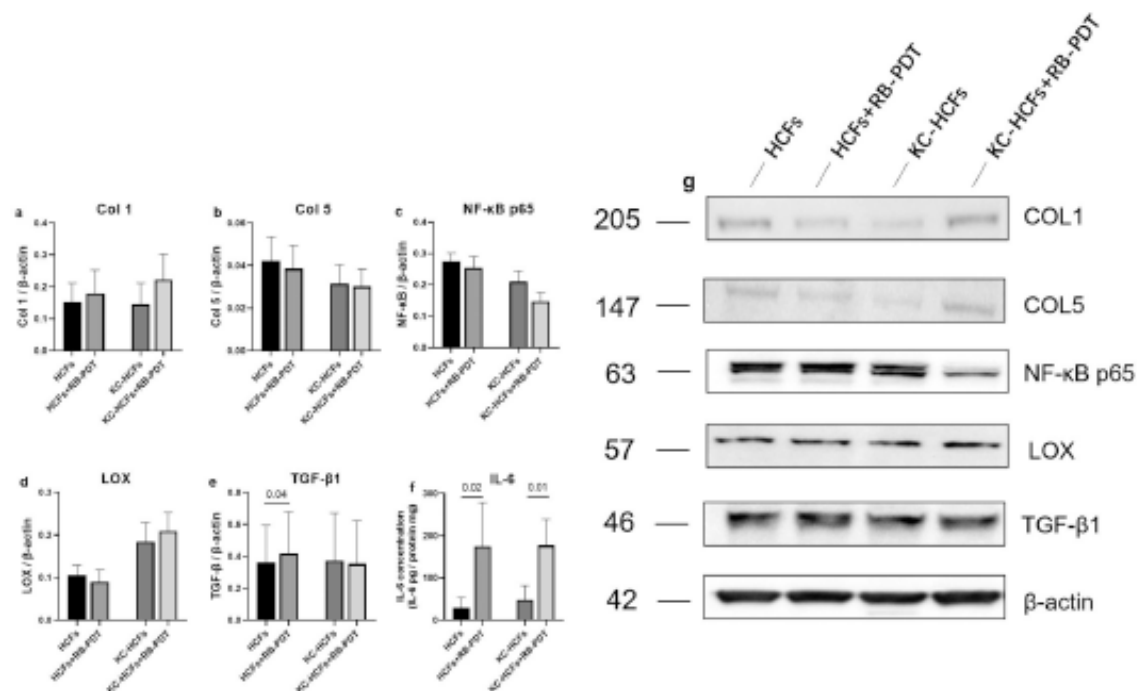
Figure 2. Collagen I, collagen V, NF-κB p65, LOX, and TGF-β1 protein expression in human corneal fibroblasts (HCFs; $n = 5$) and human keratoconus fibroblasts (KC-HCFs; $n = 5$) and IL-6 protein expression in their cell culture supernatant 24 h after 0.17 J/cm² Rose Bengal photodynamic therapy (RB-PDT) (a–g). Data are shown as mean ± standard deviation. Paired t tests have been performed, and p values below 0.05 were considered statistically significant. TGF-β1 protein expression in HCFs was significantly higher 24 h after RB-PDT, than without RB-PDT ($p = 0.04$) (e). IL-6 protein concentration in the HCF and KC-HCF culture supernatant was significantly higher 24 h after RB-PDT, than without RB-PDT ($p = 0.02$; $p = 0.01$) (f). There was no significant difference between any of the other groups.

Table 3. COL1, COL5, NFκB-p65, LOX, TGF-β1 and IL-6 mRNA and protein expression in human corneal fibroblasts (HCFs) and keratoconus HCFs (KC-HCFs) 24 h after Rose Bengal photodynamic therapy (RB-PDT), compared to untreated controls.

	HCFs + RB-PDT		KC-HCFs + RB-PDT	
	mRNA	Protein	mRNA	Protein
COL1	Unchanged	Unchanged	Decreased	Unchanged
COL5	Unchanged	Unchanged	Decreased	Unchanged
NFκB-p65	Unchanged	Unchanged	Unchanged	Unchanged
LOX	Unchanged	Unchanged	Unchanged	Unchanged
TGF-β1	Decreased	Increased	Decreased	Unchanged
IL-6	Increased	Increased	Increased	Increased

Although RB-PDT has been shown to increase corneal stiffness,[3] its impact on collagen synthesis has not been analyzed, yet. In our current study, although RB-PDT did not affect collagen production in cell culture, as collagen I and V protein expression remained unchanged 24 h after treatment, we observed a significant decrease in collagen I and V mRNA levels in KC-HCFs 24 h after RB-PDT. TGF-β, and WNT/β-catenin pathways may be involved in these gene expression changes.[33]

After riboflavin–UVA PDT, although one study reported decreased collagen I, III, and V levels in KC-HCFs 12 h after treatment,[33] the same treatment did not affect collagen I and V protein levels in keratoconus human corneal fibroblast cultures after 48 h.[25] Timely changes in intracellular collagen synthesis and degradation after photodynamic therapy should be further investigated both *in vitro* and *in vivo*.

Our measurements confirmed that the TGF-β mRNA level was downregulated in both HCFs and KC-HCFs, while the TGF-β protein level was upregulated in HCFs 24 h after RB-PDT. Since TGF-β plays a crucial role in regulating collagen synthesis,[34] we suggest that RB-PDT may have a long-term effect on collagen synthesis, although this effect could not be verified in the protein levels of Collagen I and V within 24 h in cell culture. The discordant results between mRNA and protein levels of TGF-β in HCFs and KC-HCFs underscore the complexity of cellular regulatory processes governing transcription and translation.

Proteins serve as the executors of cellular activities; therefore, the processes of transcription and translation are controlled by multiple cellular regulatory mechanisms. There are several potential reasons for the inconsistency between the transcription and translation levels of TGF-β. Firstly, protein levels are influenced not only by mRNA synthesis but also by mRNA stability. After transcription, mRNA must undergo processes such as splicing, editing, and transportation,[35,36] and numerous post-transcriptional regulatory mechanisms are involved in this process. For example, RNA-binding proteins (RBPs) can bind to the 5′ or 3′ untranslated regions (UTR) of mRNA, influencing its stability, subcellular localization, and translation.[37,38] Therefore, even though the level of TGF-β1 mRNA decreased, the protein level may still be maintained if mRNA stability increased after RB-PDT. In addition, from a translation perspective, protein levels may differ from mRNA levels due to

enhanced translation efficiency, which is related to the secondary structure of mRNA, the size of the tRNA pool, and the function of ribosomes.[39] Moreover, protein abundance is determined by both synthesis and degradation, and the increase in protein levels could also be attributed to reduced degradation.[40]

Since TGF-β is critical in the corneal wound healing process, the decrease in TGF-β transcription and the upregulation of its protein level in HCFs may indicate a normal physiological response to RB-PDT as a stimulus. However, this phenomenon is not observed at the same time point in KC-HCFs.

TGF-β regulates not only extracellular matrix synthesis but also influences cell migration and proliferation.[16] Studies have shown that TGF-β supplementation increases the HCF proliferation rate but reduces HCF migration.[41] Song et al. demonstrated that the use of riboflavin–UVA PDT does not influence TGF-β concentration in the culture of human keratoconus keratocytes at both 5 and 24 h after riboflavin–UVA PDT.[42] Similarly, chlorin e6 (Ce6) as a photosensitizer and red light (670 nm) did not have an impact on TGF-β concentration in cultured healthy human keratocytes.[43] In our study, RB-PDT increased TGF-β protein levels after 24 h in HCFs. The elevated TGF-β level can promote fibroblast differentiation into myofibroblasts, which are characterized by α-SMA positive cells.[44,45] This process is beneficial for corneal wound healing due to the increased collagen secretion by these cells in the longer term but may also lead to corneal haze if TGF-β remains at increased levels for an extended period.[29,46] Nevertheless, our results revealed that despite the variations in TGF-β levels, there was no significant change in α-SMA and CD34 mRNA levels in any of the cell types following RB-PDT. CT values for both genes were considerably higher than those for the reference genes, indicating low transcriptional levels. This suggests that in the short term (24 h), RB-PDT does not stimulate the transcription of α-SMA and, thus, does not induce the formation of α-SMA-positive myofibroblasts. One explanation could be that the differentiation of myofibroblasts from their precursor cells may take several days.[47] Due to the low α-SMA and CD34 transcriptional levels, we did not investigate protein expression 24 h after RB-PDT. However, the effect of RB-PDT on human corneal cells in the long term needs further investigation.

RB-PDT can restore corneal stiffness by promoting the formation of covalent bonds between collagens and proteoglycans.[3,48] Under physiological conditions, LOX is an important protein that influences corneal stiffness. It catalyzes the synthesis of bonds between neighboring collagen molecules using lysine or hydroxylysine groups, contributing to corneal cross-links.[15] Sharif et al. demonstrated that the use of riboflavin–UVA PDT could increase LOX protein expression in both human normal and keratoconus fibroblasts 12 h after CXL in a 3D model.[33] In our research, we found that RB-PDT did not affect the expression of LOX at the mRNA or protein level in normal or keratoconus fibroblasts 24 h after RB-PDT. Therefore, it seems that RB-PDT does not interfere with the cornea's intrinsic collagen cross-

linking mechanism, in 2D cultures. Further research is needed to clarify the exact short- and long-term effects of RB-PDT on corneal crosslinks.

p65 (RelA) is one of the subunits of the NF-κB complex, which is widely recognized as a pro-inflammatory factor that regulates various proteins associated with cell survival and senescence, including IL-6, IL-1β, and tumor necrosis factor (TNF).[49] NF-κB activation and its translocation into the nucleus are closely linked to oxidative stress and the production of reactive oxygen species (ROS),[50,51] and UV exposure is a common cause of ROS formation in the cornea.[52,53] Berger et al. proved that riboflavin–UVA PDT triggers a significant increase in NF-κB transcription in human healthy fibroblasts but not in human keratoconus fibroblasts, suggesting that riboflavin–UVA PDT may enhance the inflammatory response within the cornea.[25] However, although RB-PDT can also generate ROS and therefore may induce cellular hypoxia, our study did not verify changes in NF-κB expression, neither at the transcriptional nor at the translational level. Interestingly, the inflammatory cytokine IL-6 showed a significant increase at the transcriptional and translational levels in both HCFs and KC-HCFs, 24 h after RB-PDT. NF-κB serves as a transcription factor located upstream; its presence may not be continuously sustained over time. Nevertheless, IL-6, as an effector molecule, may be synthesized later and may maintain an increased level even 24 h after RB-PDT. A similar phenomenon was observed by Berger et al. as NF-κB protein levels did not increase after riboflavin–UVA PDT. However, a significant increase in IL-6 concentration was observed at the same time point in cell culture.[25] Therefore, similar to riboflavin–UVA PDT, RB-PDT can enhance the inflammatory response in both HCFs and KC-HCFs through IL-6 stimulation. In contrast, Ce6 PDT may have an inhibitory effect on the inflammatory response in the human cornea, as the secretion of IL-6 and IL-8 in keratocytes decreases 5 h after treatment and returns to the same level as the control group after 24 h.[54] Further research is needed to investigate the effect of IL-6 after RB-PDT.

It is important to acknowledge the limitations of our research. Although we collected primary cells from corneal donors and keratoconus subjects, we obtained measurement results 24 h after RB-PDT. Future studies should include long-term observations in cell culture and in corneal tissue after RB-PDT.

In conclusion, our study demonstrates that RB-PDT reduces collagen I, collagen V, and TGF-β1 mRNA expression while increasing IL-6 mRNA and protein expression in KC-HCFs. In HCFs, RB-PDT increases TGF-β and IL-6 protein levels after 24 h. These observations may provide a basis for future research in this field.

Acknowledgments

Disclosure statement

The authors declare that they have no competing interests.

ORCID

Ning Chai http://orcid.org/0000-0001-9689-8887
Tanja Stachon http://orcid.org/0000-0001-7009-7125
Achim Langenbucher http://orcid.org/0000-0001-9175-6177

Data availability statement

The data presented in this study are available on request from the corresponding author.

References

1. Pupkaite J, Ahumada M, Mclaughlin S, Temkit M, Alaziz S, Seymour R, Ruel M, Kochevar I, Griffith M, Suuronen EJ, et al. Collagen-based photoactive agent for tissue bonding. ACS Appl Mater Interfaces. 2017;9(11):9265–9270. doi: 10.1021/acsami. 7b01984.

2. Martinez JD, Naranjo A, Amescua G, Dubovy SR, Arboleda A, Durkee H, Aguilar MC, Flynn HW, Miller D, Parel JM. Human corneal changes after Rose Bengal photodynamic antimicrobial therapy for treatment of fungal keratitis. Cornea. 2018;37(10): e46–8–e48. doi: 10.1097/ICO.0000000000001701.

3. Cherfan D, Verter EE, Melki S, Gisel TE, Doyle FJ, Scarcelli G, Yun SH, Redmond RW, Kochevar IE. Collagen cross-linking using Rose Bengal and green light to increase corneal stiffness. Invest Ophthalmol Vis Sci. 2013;54(5):3426–3433. doi: 10.1167/iovs.12-11509.

4. Redmond RW, Kochevar IE. Medical applications of Rose Bengal- and riboflavin-photosensitized protein crosslinking. Photochem Photobiol. 2019;95(5):1097–1115. doi: 10.1111/php. 13126.

5. Germann JA, Martínez-Enríquez E, Carmen Martínez-García M, Kochevar IE, Marcos S. Corneal collagen ordering after in vivo Rose Bengal and riboflavin cross-linking. Invest Ophthalmol Vis Sci. 2020;61(3):28. doi: 10.1167/iovs.61.3.28.

6. Naranjo A, Pelaez D, Arrieta E, Salero-Coca E, Martinez JD, Sabater AL, Amescua G, Parel JM. Cellular and molecular assessment of Rose Bengal photodynamic antimicrobial therapy on keratocytes, corneal endothelium and limbal stem cell niche. Exp Eye Res. 2019;188(May):107808. doi: 10.1016/j.exer.2019.107808.

7. Wollensak G, Spoerl E, Seiler T. Riboflavin/ultraviolet-A-induced collagen crosslinking for the treatment of keratoconus. Am J Ophthalmol. 2003;May 135(5):620–627. doi: 10.1016/s0002-9394(02)02220-1.

8. Alarcon EI, Poblete H, Roh HG, Couture JF, Comer J, Kochevar IE. Rose Bengal binding to collagen and tissue photobonding. ACS Omega. 2017;2(10):6646–6657. doi: 10.1021/acsomega. 7b00675.

9. Kowtharapu BS, Murin R, Jünemann AGM, Stachs O. Role of corneal stromal cells on epithelial cell function during wound healing. Int J Mol Sci. 2018;19(2):464. doi: 10.3390/ijms19020464.

10. Ljubimov AV, Saghizadeh M. Progress in corneal wound healing. Prog Retin Eye Res. 2015;Nov49(310):17–45. doi: 10.1016/j.preteyeres.2015.07.002.

11. Arboleda A, Miller D, Cabot F, Taneja M, Aguilar MC, Alawa K, Amescua G, Yoo SH, Parel JM. Assessment of Rose Bengal versus riboflavin photodynamic therapy for inhibition of fungal keratitis isolates. Am J Ophthalmol. 2014;Jul158(1):64–70.e2. doi: 10.1016/j.ajo.2014.04.007.

12. Amescua G, Arboleda A, Nikpoor N, Durkee H, Relhan N, Aguilar MC, Flynn HW, Miller D, Parel JM. Rose Bengal photodynamic antimicrobial therapy: a novel treatment for resistant fusarium keratitis. Cornea. 2017;36(9):1141–1144. doi: 10.1097/ICO.0000000000001265.

13. Gumus K. A new alternative to riboflavin/ultraviolet-a: Collagen cross-linking with Rose Bengal/green light. Invest Ophthalmol Vis Sci. 2016;57(3):1002. doi: 10.1167/iovs.16-19319.

14. Karamichos D, Guo XQ, Hutcheon AEK, Zieske JD. Human corneal fibrosis: An in vitro model. Invest Ophthalmol Vis Sci. 2010;51(3):1382–1388. doi: 10.1167/iovs.09-3860.

15. McKay TB, Priyadarsini S, Karamichos D. Mechanisms of collagen crosslinking in diabetes and keratoconus. Cells. 2019;8(10): 1239. doi: 10.3390/cells8101239.

16. Terai K, Call MK, Liu H, Saika S, Liu CY, Hayashi Y, Chikama TI, Zhang J, Terai N, Kao CWC, et al. Crosstalk between TGF-β and MAPK signaling during corneal wound healing. Invest Ophthalmol Vis Sci. 2011;52(11):8208–8215. doi: 10.1167/iovs. 11-8017.

17. Guo X, Hutcheon AEK, Zieske JD. Molecular insights on the effect of TGF-$\beta1$/-$\beta3$ in human corneal fibroblasts. Exp Eye Res. 2016;May 146(12):233–241. doi: 10.1016/j.exer.2016.03.011.

18. Espana EM, Kawakita T, Liu CY, Tseng SCG. CD-34 expression by cultured human keratocytes is downregulated during myofibroblast differentiation induced by TGF-$\beta1$. Invest Ophthalmol Vis Sci. 2004;45(9):2985–2991. doi: 10.1167/iovs.04-0201.

19. Ghasemi H. Roles of IL-6 in ocular inflammation: a review. Ocul Immunol Inflamm. 2018;26(1):37–50. doi: 10.1080/09273948. 2016.1277247.

20. Johannessen M, Askarian F, Sangvik M, Sollid JE. Bacterial interference with canonical NFκB signalling. Microbiology (Reading)). 2013;159(Pt 10):2001–2013. doi: 10.1099/mic.0. 069369-0.

21. Berryhill BL, Kader R, Kane B, Birk DE, Feng J, Hassell JR. Partial restoration of the keratocyte phenotype to bovine keratocytes made fibroblastic by serum. Investig Ophthalmol Vis Sci. 2002;43(11):3416–3421.

22. Foster JW, Gouveia RM, Connon CJ. Low-glucose enhances keratocyte-characteristic phenotype from corneal stromal cells in serum-free conditions. Sci Rep. 2015;5(1):10839. doi: 10.1038/srep10839.

23. Berger T, Szentmáry N, Chai N, Flockerzi E, Daas L, Stachon T, Seitz B. In vitro expression analysis of cytokines and ROS-related genes in human corneal fibroblasts and keratocytes of healthy and keratoconus corneas. Ocul Immunol Inflamm. 2023;17:1–10. doi: 10.1080/09273948.2023.2176325.

24. Chai N, Stachon T, Nastaranpour M, Li Z, Seitz B, Ulrich M, Langenbucher A, Szentmáry N. Assessment of Rose Bengal photodynamic therapy on viability and proliferation of human keratolimbal epithelial and stromal cells in vitro. Klin Monbl Augenheilkd. 2023;20. doi: 10.1055/a-2038-8899.

25. Berger T, Szentmáry N, Latta L, Seitz B, Stachon T. NF-κB, iNOS, IL-6, and collagen 1 and 5 expression in healthy and keratoconus corneal fibroblasts after 0.1% riboflavin UV-A illumination. Graefes Arch Clin Exp Ophthalmol. 2021;259(5):1225–1234. doi: 10.1007/s00417-020-05058-z.

26. Martinez JD, Arrieta E, Naranjo A, Monsalve P, Mintz KJ, Peterson J, Arboleda A, Durkee H, Aguilar MC, Pelaez D, et al. Rose Bengal photodynamic antimicrobial therapy: a pilot safety study. Cornea. 2021;40(8):1036–1043. doi: 10.1097/ICO. 0000000000002717.

27. Bukowiecki A, Hos D, Cursiefen C, Eming SA. Wound-healing studies in cornea and skin: parallels, differences and opportunities. Int J Mol Sci. 2017;18(6):1257. doi: 10.3390/ijms18061257.

28. Meek KM, Knupp C. Corneal structure and transparency. Prog Retin Eye Res. 2015;49:1–16. doi: 10.1016/j.preteyeres.2015.07. 001.

29. de Oliveira RC, Wilson SE. Fibrocytes, wound healing, and corneal fibrosis. Invest Ophthalmol Vis Sci. 2020;61(2):28. doi: 10. 1167/iovs.61.2.28.

30. Miyagi H, Thomasy SM, Russell P, Murphy CJ. The role of hepatocyte growth factor in corneal wound healing. Exp Eye Res. 2018;166(3):49–55. doi: 10.1016/j.exer.2017.10.006.

31. Espana EM, Birk DE. Composition, structure and function of the corneal stroma. Exp Eye Res. 2020;198:108137. doi: 10.1016/j.exer.2020.108137.

32. Sun M, Chen S, Adams SM, Florer JB, Liu H, Kao WWY, Wenstrup RJ, Birk DE. Collagen V is a dominant regulator of collagen fibrillogenesis: dysfunctional regulation of structure and function in a corneal-stroma-specific Col5a1-null mouse model. J Cell Sci. 2011;124(Pt 23):4096–4105. doi: 10.1242/jcs.091363.

33. Sharif R, Hjortdal J, Sejersen H, Frank G, Karamichos D. Human in vitro model reveals the effects of collagen cross-linking on keratoconus pathogenesis. Sci Rep. 2017;7(1):12517. doi: 10.1038/s41598-017-12598-8.

34. Lichtman MK, Otero-Vinas M, Falanga V. Transforming growth factor beta (TGF-β) isoforms in wound healing and fibrosis. Wound Repair Regen. 2016;24(2):215–222. doi: 10.1111/wrr.12398.

35. Shi H, Chai P, Jia R, Fan X. Novel insight into the regulatory roles of diverse RNA modifications: re-defining the bridge between transcription and translation. Mol Cancer. 2020;19(1):78. doi: 10.1186/s12943-020-01194-6.

36. Kumari P, Sarovar Bhavesh N. Birth and death view of DNA, RNA, and proteins. Gene. 2023;883:147672. doi: 10.1016/j.gene.2023.147672.

37. Kang D, Lee Y, Lee JS. RNA-binding proteins in cancer: functional and therapeutic perspectives. Cancers (Basel). 2020;12(9):2699. doi: 10.3390/cancers12092699.

38. Ma J, Sun L, Gao W, Li Y, Dong D. RNA binding protein: coordinated expression between the nuclear and mitochondrial genomes in tumors. J Transl Med. 2023;21(1):512. doi: 10.1186/s12967-023-04373-3.

39. Gingold H, Pilpel Y. Determinants of translation efficiency and accuracy. Mol Syst Biol. 2011;7(1):481. doi: 10.1038/msb.2011.14.

40. Hanna J, Guerra-Moreno A, Ang J, Micoogullari Y. Protein degradation and the pathologic basis of disease. Am J Pathol. 2019;189(1):94–103. doi: 10.1016/j.ajpath.2018.09.004.

41. Gallego-Muñoz P, Ibares-Frías L, Garrote JA, Valsero-Blanco MC, Cantalapiedra-Rodríguez R, Merayo-Lloves J, Carmen Martínez-García M. Human corneal fibroblast migration and extracellular matrix synthesis during stromal repair: role played by platelet-derived growth factor-BB, basic fibroblast growth factor, and transforming growth factor-β1. J Tissue Eng Regen Med. 2018;12(2):e737–46–e746. doi: 10.1002/term.2360.

42. Song X, Stachon T, Wang J, Langenbucher A, Seitz B, Szentmáry N. Viability, apoptosis, proliferation, activation, and cytokine secretion of human keratoconus keratocytes after cross-linking. Biomed Res Int. 2015;2015:254237–11. doi: 10.1155/2015/254237.

43. Stachon T, Wang J, Eppig T, Langenbucher A, Bischoff M, Seitz B, Szentmáry N. KGF, FGFb, VEGF, HGF and TGFβ1 secretion of human keratocytes following photodynamic inactivation (PDI) in vitro. Graefes Arch Clin Exp Ophthalmol. 2013;251(8):1987–1993. doi: 10.1007/s00417-013-2370-z.

44. Szentmáry N, Wang J, Stachon T, Goebels S, Seitz B. CD34 und alpha-smooth-muscle-actin-keratozyten-expression nach photodynamischer inaktivierung (PDI). Klin Monbl Augenheilkd. 2013;230(6):570–574. doi: 10.1055/s-0032-1328639.

45. Menko AS, Walker JL, Stepp MA. Fibrosis: shared lessons from the lens and cornea. Anat Rec (Hoboken). 2020;303(6):1689–1702. doi: 10.1002/ar.24088.

46. Wilson SE. Coordinated modulation of corneal scarring by the epithelial basement membrane and Descemet's basement membrane. J Refract Surg. 2019;35(8):506–516. doi: 10.3928/1081597X-20190625-02.

47. Corneal myofibroblasts and fibrosis. Exp Eye Res. 2020;201:108272. doi: 10.1016/j.exer.2020.108272.

48. Brummer G, Littlechild S, McCall S, Zhang Y, Conrad GW. The role of nonenzymatic glycation and carbonyls in collagen cross-linking for the treatment of keratoconus. Invest Ophthalmol Vis Sci. 2011;52(9):6363–6369. doi: 10.1167/iovs.11-7585.

49. Yu Q, Biswas S, Ma G, Zhao P, Li B, Li J. Canonical nf-kb signaling maintains corneal epithelial integrity and prevents corneal aging via retinoic acid. Elife. 2021;10:1–26. doi: 10.7554/eLife.67315.

50. Podskochy A, Fagerholm P. Repeated UVR exposures cause keratocyte resistance to apoptosis and hyaluronan accumulation in the rabbit cornea. Acta Ophthalmol Scand. 2001;79(6):603–608. doi: 10.1034/j.1600-0420.2001.790611.x.

51. Kase S, Aoki K, Harada T, Harada C, Ohgami K, Shiratori K, Nishi S, Ohno S, Yoshida K. Activation of nuclear factor-kappa B in the conjunctiva with the epithelial scraping of the mouse cornea and human epidemic keratoconjunctivitis. Br J Ophthalmol. 2004;88(7):947–949. doi: 10.1136/bjo.2003.024646.

52. O'Dea EL, Kearns JD, Hoffmann A. UV as an amplifier rather than inducer of NF-κB activity. Mol Cell. 2008;30(5):632–641. doi: 10.1016/j.molcel.2008.03.017.

53. Lee DH, Jung KK, Joo CK. Translocation of nuclear factor-κB on corneal epithelial cells induced by ultraviolet B irradiation. Ophthalmol Res. 2005;37(2):83–88. doi: 10.1159/000084249.

54. Stachon T, Wang J, Langenbucher A, Eppig T, Bischoff M, Seitz B, Szentmáry N. IL-1α, IL-1β, IL-6, and IL-8 secretion of human keratocytes following photodynamic inactivation (PDI) in vitro. Graefes Arch Clin Exp Ophthalmol. 2013;251(11):2585–2590. doi: 10.1007/s00417-013-2465-6.

7. References

1. Alarcon EI, Poblete H, Roh HG, Couture JF, Comer J, Kochevar IE (2017) Rose Bengal binding to collagen and tissue photobonding. ACS Omega 2:6646–6657

2. Amescua G, Arboleda A, Nikpoor N, Durkee H, Relhan N, Aguilar MC, Flynn HW, Miller D, Parel J-M (2017) Rose Bengal Photodynamic Antimicrobial Therapy: A Novel Treatment for Resistant Fusarium Keratitis. Cornea 36:1141–1144

3. Bagga B, Pahuja S, Murthy S, Sangwan VS (2012) Endothelial Failure After Collagen Cross-Linking With Riboflavin and UV-A. Cornea 31:1197–1200

4. Baldea I, Giurgiu L, Teacoe ID, Olteanu DE, Olteanu FC, Clichici S, Filip GA (2017) Photodynamic Therapy in Melanoma - Where do we Stand? Curr Med Chem 25:5540–5563

5. Balmus I-M, Alexa AI, Ciuntu R-E, Danielescu C, Stoica B, Cojocaru SI, Ciobica A, Cantemir A (2020) Oxidative stress markers dynamics in keratoconus patients' tears before and after corneal collagen crosslinking procedure. Exp Eye Res 190:107897

6. Bischoff M, Stachon T, Seitz B, Huber M, Zawada M, Langenbucher A, Szentmáry N (2017) Growth Factor and Interleukin Concentrations in Amniotic Membrane-Conditioned Medium. Curr Eye Res 42:174–180

7. Blaser F, Zweifel S, Wiest MRJ, Bajka A, Said S, Barthelmes D, Muth DR (2022) Severe Complications after Corneal Collagen Cross-Linking (CXL). Klin Monbl Augenheilkd 240:369–378

8. Bonanno JA (2012) Molecular mechanisms underlying the corneal endothelial pump. Exp Eye Res 95:2–7

9. Chai N, Stachon T, Nastaranpour M, Li Z, Seitz B, Ulrich M, Langenbucher A, Szentmáry N (2023) Assessment of Rose Bengal Photodynamic Therapy on Viability

and Proliferation of Human Keratolimbal Epithelial and Stromal Cells In Vitro. Klin Monbl Augenheilkd

10. Chai N, Stachon T, Berger T, Li Z, Seitz B, Langenbucher A, Szentmáry N (2023) Human corneal epithelial cell and fibroblast migration and growth factor secretion after rose bengal photodynamic therapy (RB-PDT) and the effect of conditioned medium. PLoS One 18:e0296022

11. Chai N, Stachon T, Berger T, Li Z, Seitz B, Langenbucher A, Szentmáry N (2023) Short-Term Effect of Rose Bengal Photodynamic Therapy (RB-PDT) on Collagen I, Collagen V, NF-κB, LOX, TGF-β and IL-6 Expression of Human Corneal Fibroblasts, In Vitro. Curr Eye Res 1–8

12. Cherfan D, Verter EE, Melki S, Gisel TE, Doyle FJ, Scarcelli G, Yun SH, Redmond RW, Kochevar IE (2013) Collagen cross-linking using rose bengal and green light to increase corneal stiffness. Investig Ophthalmol Vis Sci 54:3426–3433

13. Collin J, Queen R, Zerti D, Bojic S, Dorgau B, Moyse N, Molina MM, Yang C, Dey S, Reynolds G, Hussain R, Coxhead JM, Lisgo S, Henderson D, Joseph A, Rooney P, Ghosh S, Clarke L, Connon C, Haniffa M, Figueiredo F, Armstrong L, Lako M (2021) A single cell atlas of human cornea that defines its development, limbal progenitor cells and their interactions with the immune cells. Ocul Surf 21:279–298

14. Covre JL, Cristovam PC, Loureiro RR, Hazarbassanov RM, Campos M, Sato ÉH, Gomes JÁP (2016) The effects of riboflavin and ultraviolet light on keratocytes cultured in vitro. Arq Bras Oftalmol 79:180–185

15. Davis SA, Bovelle R, Han G, Kwagyan J (2020) Corneal collagen cross-linking for bacterial infectious keratitis. Cochrane Database Syst Rev 2020:

16. Delic NC, Lyons JG, Di Girolamo N, Halliday GM (2017) Damaging Effects of

Ultraviolet Radiation on the Cornea. Photochem Photobiol 93:920–929

17. Derycke L, Morbidelli L, Ziche M, De Wever O, Bracke M, Van Aken E (2006) Soluble N-cadherin fragment promotes angiogenesis. Clin Exp Metastasis 23:187–201

18. Durkee H, Arboleda A, Aguilar MC, Martinez JD, Alawa KA, Relhan N, Maestre-Mesa J, Amescua G, Miller D, Parel J-M (2020) Rose bengal photodynamic antimicrobial therapy to inhibit Pseudomonas aeruginosa keratitis isolates. Lasers Med Sci 35:861–866

19. Fujii J, Soma Y, Matsuda Y (2023) Biological Action of Singlet Molecular Oxygen from the Standpoint of Cell Signaling, Injury and Death. Molecules 28:

20. Gallego-Muñoz P, Ibares-Frías L, Lorenzo E, Marcos S, Perèz-Merino P, Bekesi N, Kochevar IE, Martínez-García MC (2017) Corneal wound repair after rose bengal and green light crosslinking: Clinical and histologic study. Investig Ophthalmol Vis Sci 58:3471–3480

21. Gao J, Chen Z, Li X, Yang M, Lv J, Li H, Yuan Z (2022) Chemiluminescence in Combination with Organic Photosensitizers: Beyond the Light Penetration Depth Limit of Photodynamic Therapy. Int J Mol Sci 23:

22. Germann JA, Martínez-Enríquez E, Carmen Martínez-García M, Kochevar IE, Marcos S (2020) Corneal collagen ordering after in vivo Rose Bengal and riboflavin cross-linking. Investig Ophthalmol Vis Sci 61:28

23. Ghosh A, Singh VK, Singh V, Basu S, Pati F (2022) Recent Advancements in Molecular Therapeutics for Corneal Scar Treatment. Cells 11:3310

24. Gumus K (2014) Acute Idiopathic Endotheliitis Early After Corneal Cross-linking With Riboflavin and Ultraviolet-A. Cornea 33:630–633

25. Gumus K (2016) A new alternative to riboflavin/ultraviolet-a: Collagen cross-linking

with Rose Bengal/green light. Investig Ophthalmol Vis Sci 57:1002

26.   Imanishi J, Kamiyama K, Iguchi I, Kita M, Sotozono C, Kinoshita S (2000) Growth

        factors: Importance in wound healing and maintenance of transparency of the cornea.

        Prog Retin Eye Res 19:113–129

27.   Juarranz Á, Jaén P, Sanz-Rodríguez F, Cuevas J, González S (2008) Photodynamic

        therapy of cancer. Basic principles and applications. Clin Transl Oncol 10:148–154

28.   Kowtharapu BS, Murín R, Jünemann AGM, Stachs O (2018) Role of corneal stromal

        cells on epithelial cell function during wound healing. Int J Mol Sci 19:464

29.   Kurosu M, Mitachi K, Yang J, Pershing E V., Horowitz BD, Wachter EA, Lacey JW,

        Ji Y, Rodrigues DJ (2022) Antibacterial Activity of Pharmaceutical-Grade Rose

        Bengal: An Application of a Synthetic Dye in Antibacterial Therapies. Molecules 27:

30.   Ljubimov A V., Saghizadeh M (2015) Progress in corneal wound healing. Prog Retin

        Eye Res 49:17–45

31.   Ljubimov A V, Saghizadeh M (2015) Progress in corneal wound healing. Prog Retin

        Eye Res 49:17–45

32.   Lorenzo-Martín E, Gallego-Muñoz P, Ibares-Frías L, Marcos S, Pérez-Merino P,

        Fernández I, Kochevar IE, Martínez-García MC (2018) Rose bengal and green light

        versus riboflavin–UVA cross-linking: Corneal wound repair response. Investig

        Ophthalmol Vis Sci 59:4821–4830

33.   Lorenzo-Martín E, Gallego-Muñoz P, Ibares-Frías L, Marcos S, Pérez-Merino P,

        Fernández I, Kochevar IE, Martínez-García MC (2018) Rose bengal and green light

        versus riboflavin–UVA cross-linking: Corneal wound repair response. Investig

        Ophthalmol Vis Sci 59:4821–4830

34.   Martinez JD, Naranjo A, Amescua G, Dubovy SR, Arboleda A, Durkee H, Aguilar

MC, Flynn HW, Miller D, Parel JM (2018) Human Corneal Changes After Rose Bengal Photodynamic Antimicrobial Therapy for Treatment of Fungal Keratitis. Cornea 37:e46–e48

35. Martinez JD, Arrieta E, Naranjo A, Monsalve P, Mintz KJ, Peterson J, Arboleda A, Durkee H, Aguilar MC, Pelaez D, Dubovy SR, Miller D, Leblanc R, Amescua G, Parel JM (2021) Rose Bengal Photodynamic Antimicrobial Therapy: A Pilot Safety Study. Cornea 40:1036–1043

36. McKay TB, Priyadarsini S, Karamichos D (2019) Mechanisms of collagen crosslinking in diabetes and keratoconus. Cells 8:1–28

37. Medeiros CS, Marino GK, Santhiago MR, Wilson SE (2018) The corneal basement membranes and stromal fibrosis. Investig Ophthalmol Vis Sci 59:4044–4053

38. Müller PL, Loeffler KU, Messmer E, Holz FG, Perdikakis G, Kohlhaas M, Herwig-Carl MC (2020) Histological Corneal Alterations in Keratoconus After Crosslinking-Expansion of Findings. Cornea 39:333–341

39. Panzarini E, Inguscio V, Dini L (2011) Overview of Cell Death Mechanisms Induced by Rose Bengal Acetate-Photodynamic Therapy. Int J Photoenergy 2011:1–11

40. Parsa S, Rodriguez A, Robertson DM, Bowman RW, Petroll WM (2022) Temporal and Spatial Assessment of the Corneal Response to UV Cross-Linking Using 3-Dimensional In Vivo Confocal Microscopy. Eye Contact Lens 48:308–312

41. Qin J, Kunda N, Qiao G, Calata JF, Pardiwala K, Prabhakar BS, Maker A V. (2017) Colon cancer cell treatment with rose bengal generates a protective immune response via immunogenic cell death. Cell Death Dis 8:1–9

42. Raiskup F, Spoerl E (2013) Corneal Crosslinking with Riboflavin and Ultraviolet A. I. Principles. Ocul Surf 11:65–74

43. Redmond RW, Kochevar IE (2019) Medical Applications of Rose Bengal- and Riboflavin-Photosensitized Protein Crosslinking. Photochem Photobiol 95:1097–1115

44. Richoz O, Tabibian D, Hammer A, Majo F, Nicolas M, Hafezi F (2014) The Effect of Standard and High-Fluence Corneal Cross-Linking (CXL) on Cornea and Limbus. Investig Opthalmology Vis Sci 55:5783

45. Sagaradze G, Grigorieva O, Nimiritsky P, Basalova N, Kalinina N, Akopyan Z, Efimenko A (2019) Conditioned medium from human mesenchymal stromal cells: Towards the clinical translation. Int J Mol Sci 20:1–16

46. Santhiago MR, Randleman JB (2021) The biology of corneal cross-linking derived from ultraviolet light and riboflavin. Exp Eye Res 202:108355

47. Singh M, Li J, Han Z, Vantipalli S, Liu CH, Wu C, Raghunathan R, Aglyamov SR, Twa MD, Larin K V. (2016) Evaluating the effects of riboflavin/UV-a and rose-bengal/green light cross-linking of the rabbit cornea by noncontact optical coherence elastography. Investig Ophthalmol Vis Sci 57:OCT112–OCT120

48. Sliney DH (2011) Intraocular and Crystalline Lens Protection From Ultraviolet Damage. Eye Contact Lens Sci Clin Pract 37:250–258

49. Spoerl E, Huhle M, Seiler T (1998) Induction of cross-links in corneal tissue. Exp Eye Res 66:97–103

50. Tavakkoli Yaraki M, Liu B, Tan YN (2022) Emerging Strategies in Enhancing Singlet Oxygen Generation of Nano-Photosensitizers Toward Advanced Phototherapy. Springer Nature Singapore

51. Wilson SE (2020) Corneal wound healing. Exp Eye Res 197:1–21

52. Wilson SE (2020) Corneal myofibroblasts and fibrosis. Exp Eye Res 201:108272

53. Xu L, Yang K, Fan Q, Zhao D, Pang C, Ren S (2021) Whole mitochondrial genome

analysis in Chinese patients with keratoconus. Mol Vis 27:270–282

54.   Yu Q, Biswas S, Ma G, Zhao P, Li B, Li J (2021) Canonical nf-kb signaling maintains

corneal epithelial integrity and prevents corneal aging via retinoic acid. Elife 10:1–26

8. Publication list

Original articles

First authorships

1. Yan L, <u>Chai N</u>, Bao Y, Ge Y, Cheng Q (2020) Enhanced computed tomography-based radiomics signature combined with clinical features in evaluating nuclear grading of renal clear cell carcinoma. J Comput Assist Tomogr 44:730–736

2. <u>Chai N</u>, Lang Z, Wang M, Chu Y (2020) Oculodentodigital dysplasia: plastic treatments and self-esteem estimation. Eur J Plast Surg 43:657–660

3. <u>Chai N</u>, Stachon T, Nastaranpour M, Li Z, Seitz B, Ulrich M, Langenbucher A, Szentmáry N (2023) Assessment of Rose Bengal Photodynamic Therapy on Viability and Proliferation of Human Keratolimbal Epithelial and Stromal Cells In Vitro. Klin Monbl Augenheilkd

4. <u>Chai N</u>, Stachon T, Berger T, Li Z, Seitz B, Langenbucher A, Szentmáry N (2023) Short-Term Effect of Rose Bengal Photodynamic Therapy (RB-PDT) on Collagen I, Collagen V, NF-κB, LOX, TGF-β and IL-6 Expression of Human Corneal Fibroblasts, *in vitro*. Curr Eye Res 1–8

5. <u>Chai, N,</u> Stachon, T, Berger, T, Li, Z, Seitz, B, Langenbucher, A, & Szentmáry, N (2023). Human corneal epithelial cell and fibroblast migration and growth factor secretion after rose bengal photodynamic therapy (RB-PDT) and the effect of conditioned medium. PLoS One 18:e0296022.

Co-authorships

1. Muthukumar V, Shi L, <u>Chai N</u>, Langenbucher A, Becker SL, Seitz B, Orosz E, Stachon T, Kiderlen AF, Bischoff M, Szentmáry N (2022) Efficacy of Off-Label Anti-Amoebic Agents to Suppress Trophozoite Formation of Acanthamoeba spp. on Non-Nutrient Agar Escherichia Coli Plates. Microorganisms 10:

2. Berger T, Szentmáry N, <u>Chai N</u>, Flockerzi E, Daas L, Stachon T, Seitz B (2023) In Vitro Expression Analysis of Cytokines and ROS-Related Genes in Human Corneal Fibroblasts and Keratocytes of Healthy and Keratoconus Corneas. Ocul Immunol Inflamm 1–10

Posters

1. <u>Chai N</u>, Stachon T, Nastaranpour M, Li Z, Seitz B, Ulrich M, Langenbucher A, Szentmáry N (2023) Assessment of Rose Bengal Photodynamic Therapy on Viability and Proliferation of Human Keratolimbal Epithelial and Stromal Cells In Vitro. September 2022, Jahrestagung der Deutschen Ophthalmologischen Gesellschaft, Berlin, Deutschland

2. <u>Chai, N,</u> Stachon, T, Berger, T, Li, Z, Seitz, B, Langenbucher, A, & Szentmáry, N (2023). Human corneal epithelial cell and fibroblast migration and growth factor secretion after rose bengal photodynamic therapy (RB-PDT) and the effect of conditioned medium. September 2023, Jahrestagung der Deutschen Ophthalmologischen Gesellschaft, Berlin, Deutschland.

3. <u>Chai N</u>, Stachon T, Berger T, Li Z, Seitz B, Langenbucher A, Szentmáry N (2023) Short-Term Effect of Rose Bengal Photodynamic Therapy (RB-PDT) on Collagen I, Collagen V, NF-κB, LOX, TGF-β and IL-6 Expression of Human Corneal Fibroblasts, *in vitro*. October 2023, Jahrestagung der European Society for Vision and Eye Research, Valencia, Spain.

.

9. Acknowledgements

I would like to express my heartfelt gratitude to my doctoral mother, Professor Nóra Szentmáry, for her invaluable guidance throughout my academic journey. Her patience and insightful suggestions have been instrumental in shaping both my academic and personal development. I am also thankful to all the members of the laboratory. Facing challenging scientific problems, my teachers and colleagues in the lab provided me with invaluable advice and assistance. I want to extend special thanks to Dr. Tanja Stachon, who patiently taught me every technique, step by step.

I would like to convey my gratitude to my family and friends for their selfless love. Your unwavering support has been my anchor throughout the entire research period, and without you, every step would have been daunting.

Finally, I want to express my love and admiration for my grandfather, Prof. Dr. Zhong-Pei Chai. You are the star in my heart.

10. Curriculum Vitae

The curriculum vitae was removed from the electronic version of the doctoral thesis for reasons of data protection.